personal buildup for

Force Motors Ltd.

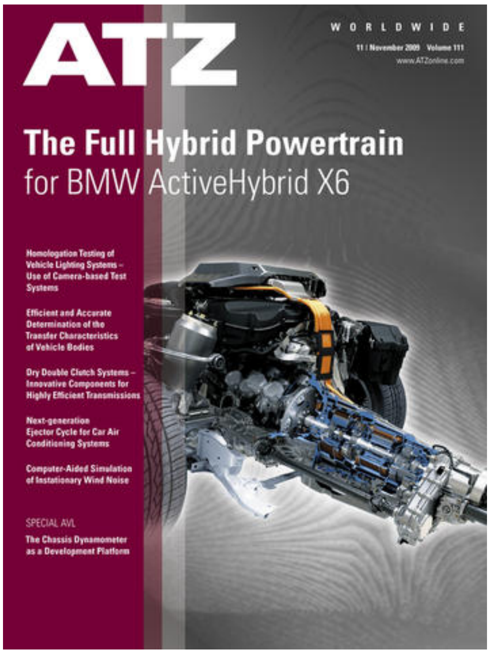

ATZ .worldwide 11/2009, as epaper released on 30.10.2009
http://www.atz-worldwide.com

content:

page 60: Susanne Krampol, Matthias Riegel, Jochen Wiedemann: Computer-Aided Simulation of Instationary Wind Noise. p.60-65

ATZ

WORLDWIDE

11 | November 2009 Volume 111

www.ATZonline.com

The Full Hybrid Powertrain for BMW ActiveHybrid X6

Homologation Testing of Vehicle Lighting Systems – Use of Camera-based Test Systems

Efficient and Accurate Determination of the Transfer Characteristics of Vehicle Bodies

Dry Double Clutch Systems – Innovative Components for Highly Efficient Transmissions

Next-generation Ejector Cycle for Car Air Conditioning Systems

Computer-Aided Simulation of Instationary Wind Noise

SPECIAL AVL

The Chassis Dynamometer as a Development Platform

For more information visit:
www.ATZonline.com

COVER STORY

The Full Hybrid Powertrain for BMW ActiveHybrid X6

4
In 2008, the BMW Group launched the new SUV X6 XDrive. In line with the BMW EfficientDynamics Strategy, the BMW Group developed a **Full Hybrid Powertrain** for the X6 to complement the highly efficient gasoline and diesel powertrains.

COVER STORY

DEVELOPMENT

SPECIAL AVL

RESEARCH

RUBRICS

Turning Heat into Electricity

Dear Reader,

Generating electricity directly from heat, isn‘t that something reserved only for space probes? The answer is no. At its latest „Innovation Days“, BMW demonstrated that this space technology has more to offer. BMW and DLR have been carrying out research in this field since 2004 and showcased it as an underfloor solution as part of the exhaust system in 2008 (see MTZ 4|2009). Now, they have presented a new development stage in which the thermoelectric generator (TEG) has been integrated into the EGR cooler of an internal combustion engine.

Even a very efficient internal combustion engine uses only one third of the energy contained in the fuel to actually propel the vehicle. The remaining two thirds are lost in the form of heat, which is dissipated to the surroundings through the exhaust gas and the radiator. It is this wasted energy that BMW is now focusing on.

The number of electrical components in modern vehicles, the level of equipment and consequently their overall power consumption are constantly increasing. Today — depending on the vehicle model, equipment level and driving profile — electric power generation is responsible for between three and eight percent of the total fuel consumption in customer operation.

What is so special about the new development stage is the elegant integration of the TEG into the already existing structure of the exhaust gas recirculation cooler. This makes the system very compact and, without the need for major modifications, will be ready for series production in three to five years. As the TEG has undergone practically no further development since the 1960s, BMW is expecting to achieve major advances in this technology. Whereas last year‘s TEG system produced 200 W, the EGR cooler solution now generates 250 W. A further underfloor solution offers as much as 500 W. The Munich-based company even considers 1000 W to be possible soon. As a 5-Series BMW currently has an electric power consumption of 500 W, worries about power generation may soon be a thing of the past.

Michael Reichenbach

Dipl.-Ing. Michael Reichenbach
Munich, 9 October 2009

Dipl.-Ing. Michael Reichenbach
Vice-Editor-in-Chief

ATZ WORLDWIDE
11|2009

Organ of the VDI-Gesellschaft Fahrzeug- und Verkehrstechnik (FVT)

Organ of the Forschungsvereinigung Automobiltechnik e. V. (FAT) and of the Normenausschuss Kraftfahrzeuge (FAKRA) in the DIN Deutsches Institut für Normung e. V.

Organ of the Wissenschaftliche Gesellschaft für Kraftfahrzeug- und Motorentechnik e. V. (WKM)

The Full Hybrid Powertrain for BMW ActiveHybrid X6

In 2008, the BMW Group launched the new BMW X6 XDrive. In line with the BMW EfficientDynamics Strategy, the BMW Group developed a full hybrid powertrain for the X6 to complement the highly efficient gasoline and diesel powertrains. In this paper the authors discuss the technical targets, the implementation, and the achieved results. Accentuating the BMW "Sheer Driving Pleasure" was the goal behind the selection of the operating strategies in both the electrical and conventional drive modes. Despite the additional weight of the hybrid components the BMW typical dynamics were maintained and even improved. The CO_2 emissions were significantly reduced at the same time.

1 Introduction

„Sheer Driving Pleasure through Efficient Dynamics“ – once again BMW highlighted this credo by developing a high-performance hybrid car based on the platform of the X6. In 2008, the BMW Group launched the new BMW X6 XDrive. In line with the BMW EfficientDynamics Strategy, the BMW Group developed a full hybrid powertrain for the X6 to complement the highly efficient gasoline and diesel powertrains. In this paper the authors discuss the technical targets, the implementation, and the achieved results.

2 Target Definition and Result

In 2006 BMW made the decision to introduce full and mild hybrid concepts to the SUV and large cars segment. The realization of these concepts significantly expands BMWs EfficientDynamics strategy in terms of the involved technology. As part of the BMW hybrid strategy of the near future full and mild hybrid technology will be introduced to the more cost-intensive medium cars and small cars segments.

The elementary product characteristics of the first BMW hybrid vehicle are outstanding dynamics and convincing efficiency. The high-performance V8 engine and the brand-specific design of the full hybrid system result in a unique selling point with regard to the competitors. The BMW ActiveHybrid X6 is the most efficient and sportiest vehicle of its class.

Due to its maximum level of complexity the full hybrid drive electrification also served as a pilot project with a high learning potential for the entire BMW Group. In 2006, the year of project launch, the challenges were quite demanding and the experience gathered over the last years in the fields of development, manufacturing and service lead to hybrid-specific adaptations on various BMW-internal standards and processes.

The cooperation with Daimler, Chrysler and GM at the development of the hybrid transmission and the hybrid software contributed significantly to the realization of the first BMW full hybrid in a short period. Compared to the time required for the BMW series process the development process for the ActiveHybrid could be reduced significantly.

Using and adapting the jointly developed components and software BMW has exploited the “degree of freedom” involved in the system to establish higher efficiency as well as driving dynamics and a driving behavior of a characteristic that is typical for the BMW brand. The objective of the respective operating strategy is to convey the BMW motto „Sheer Driving Pleasure“ also to the electric drive concept. The BMW full hybrid design with two-mode system realized in the X6 offers the driver the highly comfortable „eDrive“ experience up to medium urban speeds.

When the vehicle is driven in combustion mode the specifically adapted software contributes to a driving characteristic that is typical for a BMW vehicle by adding virtual gears. When accelerating the eCVT transmission, on which the design is based in principle, realizes a sporty character that is typical for a seven-gear automatic transmission. The additional boost and the use of the electric motors to enable quick gearshifts convey a high dynamic character and the precision and emotion that distinguish BMW vehicles.

3 Hybrid Aggregates in the Vehicle

The essential components are the new V8 TwinPower Turbo combustion engine, its hybrid-specific adaptations, the two-mode hybrid transmission and the high-voltage batteries in the rear end of the vehicle, **Titel Figure**.

3.1 V8 TwinPower Turbo Engine for Hybrid Drive

Due to the efficiency-oriented V8 TwinPower technology it was possible to adopt the engine of the X6-series model without need for major modifications. The engine compartment package is already optimized to suit the V8 engine. Despite the deletion of the starter, alternator and hydraulic drive for the power steering pump the engineering measures required to generate installation space for the electronic box, the electric cooling pumps and cooling hoses and the HV cables was still quite a challenge. Eventually a package free of conflicts could be realized however. The central power electronics box that contains the master controller and the power electronics for the e-machines is located above the engine, **Figure 1**.

The Authors

Dipl.-Ing.
Hans Stefan Braun
is Head of Department Powertrain Functions In-Line Engines & V-Engines in Powertrain Development at BMW in Munich (Germany).

Dipl.-Ing.
Michael Krauß
is Project Manager Hybrid Powertrains in Powertrain Development at BMW in Munich (Germany).

Dr.-Ing.
Fabian Rattei
is Team Leader Electrics/Electronics in Powertrain and Driving Dynamic Systems Department at BMW in Munich (Germany).

Dipl.-Ing.
Wolfram Bohne
is Team Leader Development Drive Management Functions inclusive Driving and Operating Strategy in Powertrain Development at BMW in Munich (Germany).

Dipl.-Ing.
Martin Engelmann
is Team Leader Hybrid Powertrain Calibration in Powertrain Development at BMW in Munich (Germany).

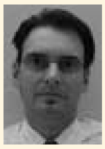

Dipl.-Ing. Uwe Deuke
is Team Leader Hybrid Transmission Development in Powertrain Development at BMW in Munich (Germany).

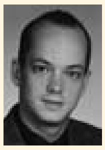

Dr.-Ing.
Marco Di Pierro
is Team Leader Software Developement & E/E Integration in Powertrain Development at BMW in Munich (Germany).

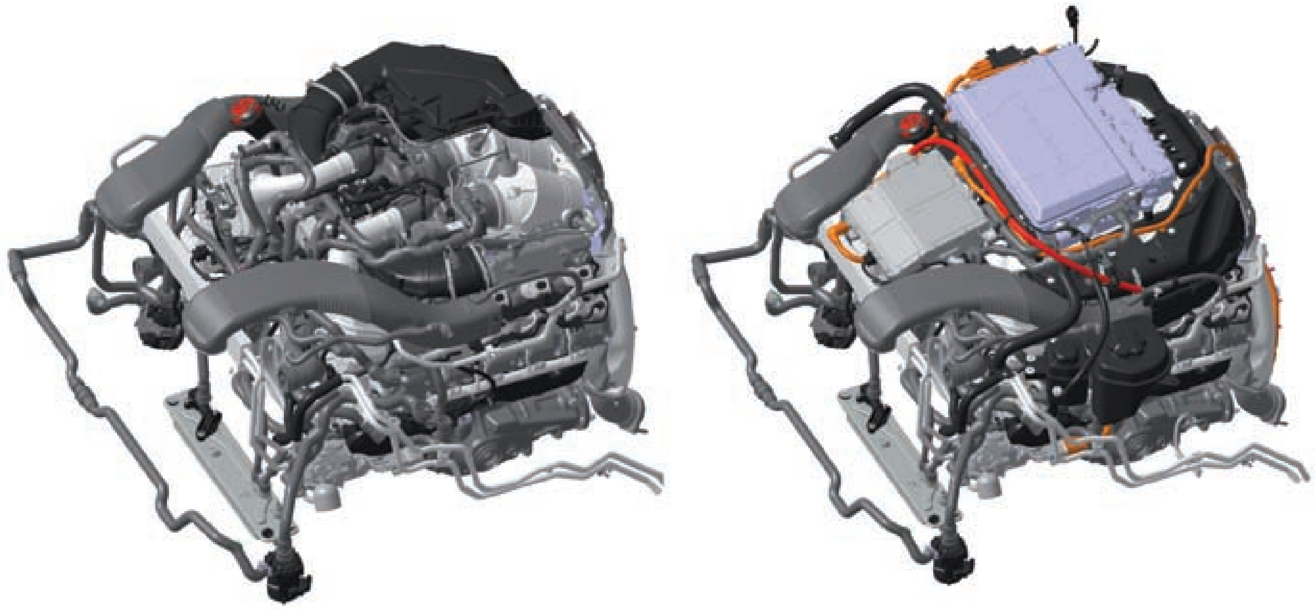

Figure 1: V8 TwinPower Turbo engine in conventional design (left) and with full hybrid power electronics and ECUs (right)

The temperature load on the power electronics and the HV cables due to heat dissipated by the neighboring turbochargers and catalytic converters was limited by fitment of an additional heat shield. By making use of the existing low-temperature charge-air cooling for water cooling of the power electronics no additional cooling system had to be developed.

3.2 AHS Transmission System

The AHS transmission (Advanced Hybrid System) optimized for use in the Active Hybrid X6 has been developed within the frame of the cooperation with companies Daimler, Chrysler and GM. The particular challenge was to design this core component of the so-called two-mode hybrid system to suit the requirements of the 600 Nm V8 TwinPower turbo combustion engine without compromises in terms of compactness. A maximum degree of common scopes was achieved towards the system fitted in the Mercedes Benz ML 450 Hybrid. Significant differences exist only with regard to the design of the flange to the engine and to the transfer box and the geometry of the oil pan. All components of the transmission that transfer torque are identical for both vehicle applications, Figure 2.

The AHS transmission technology is based on a special combination of three planetary gear sets, two integrated compact e-motors and four clutch elements. The power output branches into a mechanical and an electrical power path. This topology allows to realize two continuously variable eCVT operating modes. Four additional fixed gear ratios are realized by use of shift elements. A separate drive off element is not required since the two e-machines are used as electric variator. Here, the two-mode technology allows for the fitment of relatively small e-machines with an output of maximal 67 kW and torque of 280 Nm, Figure 3.

The two eCVT operating modes (Mode1/Mode2) cover two transmission ratios. Mode 1 covers high ratios from drive off to fixed gear 2, resulting in high drive torques. Mode2 covers ratios above the 2nd fixed gear up to the high overdrive ratio beyond the 4th fixed gear. In Mode2 the portion of power that is transmitted electrically is reduced to a maximum of 20 %, resulting in an efficiency factor that is considerably higher than the factor for single-mode systems. In addition, the use of fixed gears avoids the

Figure 2: AHS-C hybrid transmission with HV cables

losses that occur in the electric power path when driving in eCVT mode.

The high variability the AHS system offers with regard to setting of torque values and transmission ratios allows to tailor the operating strategy to the application purpose. In this way a clear differentiation could be achieved despite the common parts strategy.

3.3 High-voltage Battery

The design of the high-voltage (HV) battery was determined in particular by the requirements on the electric drive system in terms of power output and energy throughput the different operating modes. Further boundary conditions like available space in the vehicle, battery cells available on the market or currently being developed and other influencing parameters additionally limit the range of suitable batteries.

The best solution proved to be a HV battery in NiMH technology with 260 cells arranged in series and bundled in two cassettes that lie on top of each other and consist of 13 modules each that in turn comprise ten cells each, **Figure 4**.

This results in a nominal voltage of 312 V. The total capacity amounts to 2.4 kWh, of which 1.4 kWh are used in accordance with service-life requirements. The weight amounts to approximately 85 kg. The battery pack is fitted in the trunk below the load floor without limiting the variability of the vehicle, **Figure 5**. The battery housing also contains the battery control unit, a coolant unit, fuse, pre-charge circuit and contactors.

The requirements on the power output and the energy throughput necessitate a high-performance cooling concept. Simulations of various driving cycles indicate that an air-cooled variant dissipates the heat loss only insufficiently and hence clearly limits the reproducibility of the behavior. In order to achieve reliable dissipation of the heat liquid cooling with a water pump that is integrated into the housing was realized.

The energy required for cooling of the battery is dissipated mainly via an air-to-water heat exchanger circuit. In order to provide sufficient cooling capacity even under conditions that prevail in countries with hot climates the cooling circuit is coupled to the cooling circuit of the air conditioning compressor via a heat ex-

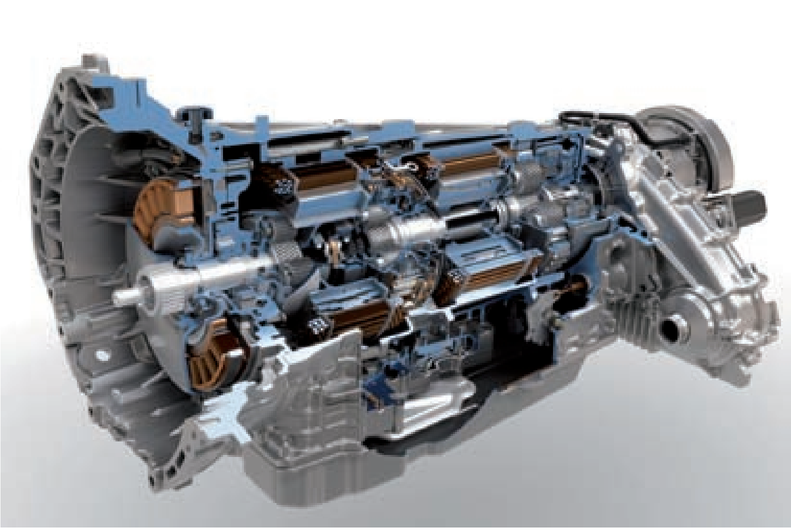

Figure 3: AHS-C hybrid transmission with two integrated e-machines, three planetary gear sets, for multiple-disk clutches and electric oil pump drive

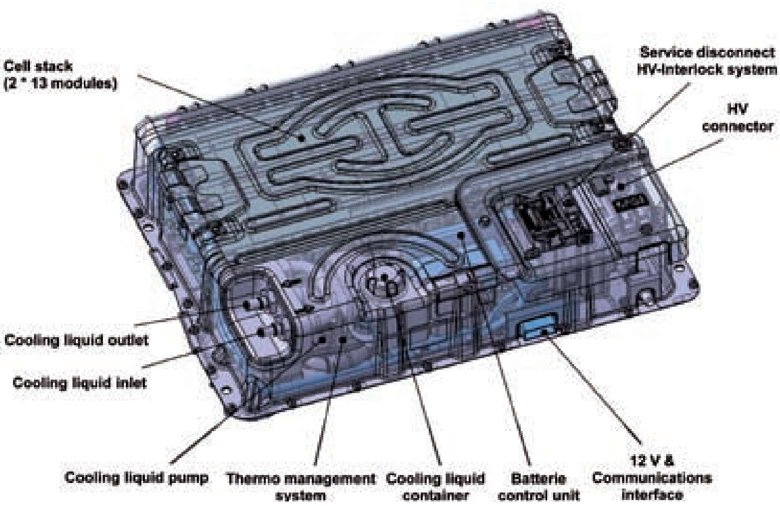

Figure 4: Interfaces and components of HV battery in NiMH technology

Figure 5: NiMH HV battery fitted above rear axle carrier, in trunk below load floor

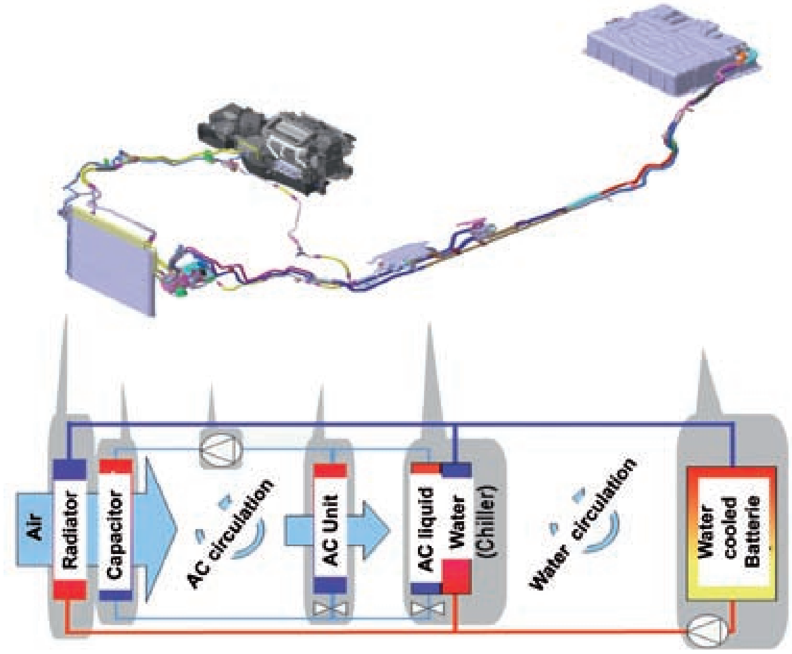

Figure 6: Battery cooling circuit coupled to air conditioning circuit of the vehicle

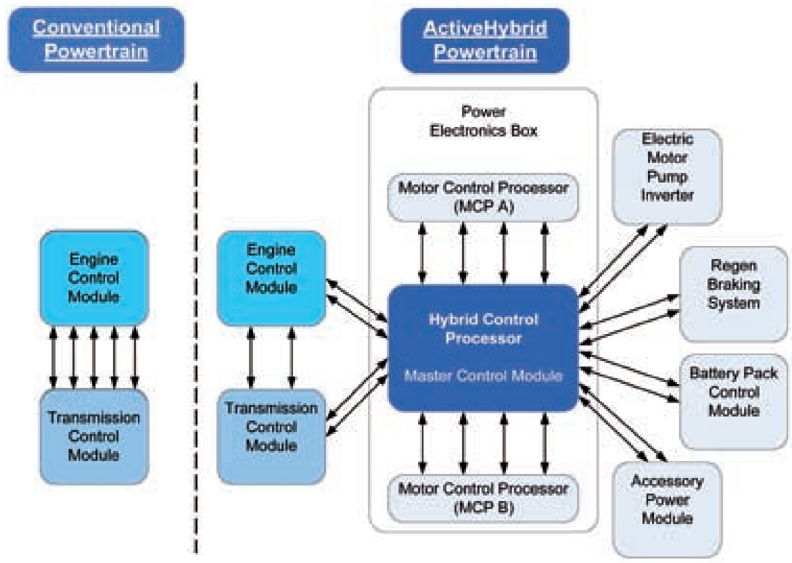

Figure 7: Extension of the drivetrain control module network by seven hybrid-specific controllers

changer, also referred to as chiller. These measures establish the prerequisites that are essential to achieve high recuperation outputs, high boost power, adequate mileage in eDrive mode and the necessary reproducibility of the behavior, **Figure 6**.

The battery condition detection integrated into the battery control unit analysis the state of charge (SOC) and the state of health (SOH) of the cells while driving. Depending on these parameters and the temperature corresponding power output values are defined and transferred to the hybrid master control unit. Additional voltage monitoring ensures the absolute compliance with these operating limits. The operating strategy in the hybrid master control unit adapts to the pre-defined limitations and ensures that the battery is operated in the optimal SOC range. The mean energy throughput at mixed driving cycle lies clearly below the intended limit values. The mean energy throughput for the BMW-specific cycle that was realized based on the operating strategy lets expect a mileage of about 300.000 kilometers.

4 System Design and Software

The development scope of the cooperation comprises the hybrid transmission, the associated ECUs and the software (SW). The challenge for BMW was to develop a BMW-specific differentiation by implementing unique software functions beyond the common software platform. Based on the existing basic functions (like operating system or HW-IO) the BMW solution required re-partitioning of BMW drive functions with regard to the different ECUs. A gateway was introduced that enables a communication between the hybrid system and the BMW ECUs in order to keep the changes on the onboard data net to the lowest possible level.

The hybrid system comprises a total of seven additional controllers. The master controller contains the hybrid intelligence with approximately 150 software modules. The overall system including engine control is made up of approximately 25000 application parameters and approximately 500 new hybrid-specific diagnosis functions, **Figure 7**.

Mastering of this networked complexity requires the application of systematic and structured processes. In the case of the hybrid drive the engineering effort for software functions, application and validation absorbs more than 50 % of the overall effort.

5 Driving Characteristic and Dynamics

As compared to conventional drive concepts the X6 ActiveHybrid uses for the first time a changed accelerator pedal interpretation which no longer interprets the driver´s request as a clutch torque of a single-source drive but reflects a model-based speed-dependent traction force potential on the accelerator pedal. Compared to a pure combustion engine the torque limits are clearly expanded due to the e-machines and the battery, **Figure 8**.

As a result the continuous realization of the driver´s request can be maintained over a clearly extended range. The traction force potential is variable and depends on the state of charge (SOC) of the battery, the battery temperature, transmission ratio and other factors. Here, the additional logics „traction force approach“ complements the approach of the best possible

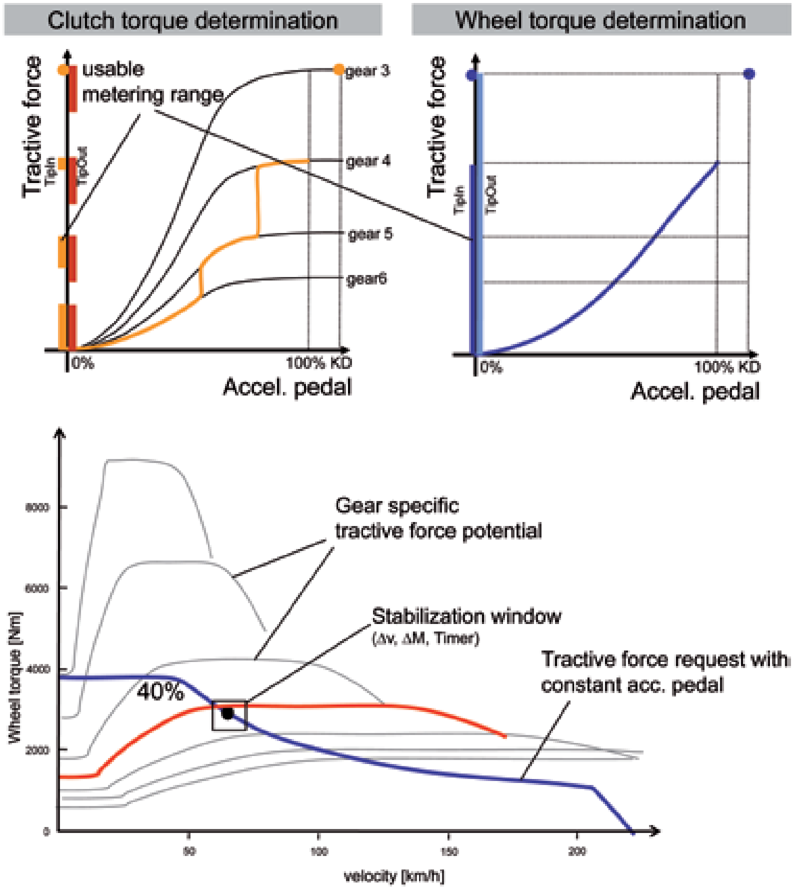

Figure 8: Discrete versus continuous position of wheel torque (top), traction force approach hits always the „adequate gear“ (bottom)

„gear selection“. Depending on the load and the speed the current gear is no longer generated from a set of characteristic shift curves but the best possible gear is selected on the basis of the driving resistance and strategic aspects like curve driving, hill climbing and others.

Although the AHS transmission represents an eCVT (electrical Continuously Variable Transmission) with four additional fixed gears a transmission with discrete ratio steps must be used in the ActiveHybrid X6 in order to maintain the BMW-typical driving characteristic. Beyond the drive off range a familiar characteristic where the engine speed (rpm) increases proportional to the driving speed is offered by seven additional gears. Taking into account a mostly optimal harmonization of the ratio steps, three virtual gears are emulated between the four fixed gears by speed control through the e-machines, **Figure 9**.

In order to increase the potential for brake energy recuperation an overdrive is used that reduces the speed of the combustion engine again up to 900/min when the vehicle runs in coast mode.

The gearshifts in the partial-load range are performed without influence of the traction force and hence with maximum comfort. This is achieved by the short-term use of battery power which keeps the transmission output on a constant level and by the e-machines which adapt the speed of the combustion engine to the target speed. When accelerating at full load an additional clutch, **Figure 10**, is used to boost the dynamic behavior.

The vehicle speed range below 65 km/h is of particular importance. Provided that the battery is adequately charged, here the most extreme shift of the load level towards the dormant combustion engine takes place. When an acceleration request is made that can no longer be answered by pure electrical power the combustion engine is “seamlessly” reset to the target speed and comfortably re-integrated into the drive network. This leads to a comfortable shift between predominantly combustion mode outside built-up areas and silent and comfortable electric cruising within urban zones with speed limits.

In order to ensure that the battery is always sufficiently charged the coast and brake recuperation plays an important role in addition to strategy “load level increase”. The drive system provides the brake system continuously with information about the braking torques and outputs that can be delivered by the e-machines in a particular situation. Depending on the current driving situation a brake-by-wire system splits the brake re-

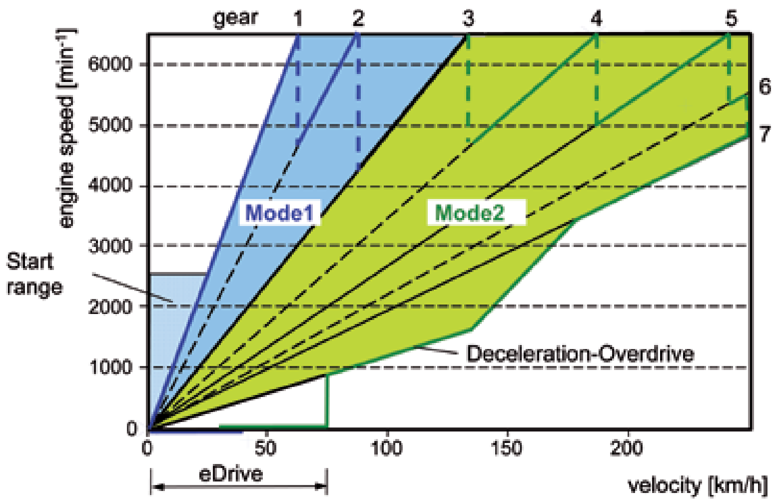

Figure 9: Gear ratio ranges with fixed and virtual gears, eDrive and coast-mode overdrive

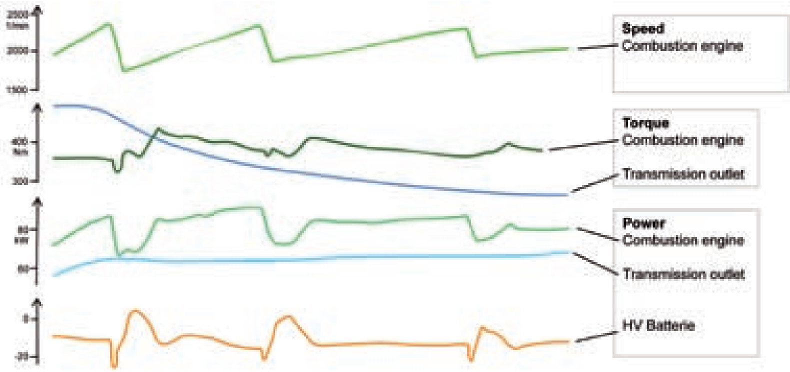

Figure 10: Improved shifting by electric motors and battery

quest into an electrical and a hydraulic brake portion that consumes as much from the offered recuperation capacity as possible. The total braking torque requested by the driver is then complemented by the hydraulically provided portion of the operating brake. Drive train oscillations related to longitudinal dynamics are minimized by an observer-based control concept in the e-machines.

6 Operating Strategy and Hybrid Functions

In addition to excellent driving behavior the development of the BMW ActiveHybrid X6 focused on the battery charging strategy and the electric drive strategy with the objective to achieve a significant reduction in consumption and to make electric driving an emotional experience. The use of these hybrid functions on the basis of a precisely harmonized operating strategy leads to good fuel consumption values not only in the low-dynamic homologation cycles but offers consumption advantages also to the dynamic driver. This can be experienced in particular at the interplay between e.g. dynamic driving on country roads and subsequent electric cruising through towns or villages with dormant combustion engine.

Up to speeds of approximately 60 km/h the driver may operate the vehicle in pure electric mode and accelerate the vehicle as to float with the traffic. A display in the instrument panel, the so-called "eDrive Reserve", supports the driver in deliberately setting this condition at the accelerator pedal. It also facilitates electric drive-off. Furthermore, the combustion engine is switched off in deceleration phases and at standstill.

The decision to connect the eDrive is governed by many parameters and corresponding efficiency maps of all sub systems are available in the software. In order to supply the required output a software module continuously compares the efficiency of the combustion mode with the electric mode. By superimposition of further criteria like state of charge, driving situation or component condition it is defined whether the combustion engine should be switched off.

The energy for the electric operation is delivered, on the one hand, by brake energy recuperation and, on the other hand, by the load point increase where the torque of the combustion engine is increased beyond the torque required to cover the demand of the electrical system and of the drive system.

Consumption advantages are not only achieved by the use of stored energy for electric driving but also by use of the so-called "assist function" which lowers the load point of the combustion engine as required. Then the electric motors engage and supply a portion of the drive torque. The assist function is particularly efficient when recuperated energy is used and is applied in situations where the combustion engine is not switched off, e.g. at higher speeds.

Figure 11 shows the application of the hybrid function as a function of the state of charge (SOC) of the HV battery. The wide eDrive and Motor-Start/Stop (MSA) ranges are clearly visible. At high SOC levels the recuperation is not active, at low SOC levels the combustion engine is started and the battery recharged by a higher load point increase rate. After having reached the SOC target range, which depends on the driving speed and other conditions, neither load point increase nor assisting takes place.

As second essential factor of the operating strategy, the charging strategy differentiates a variety of situations like engine heat-up phase, transmission program or hill drive and sets an adequate strategic charging output and a target SOC. In this way the charging strategy ensures the best possible adaptation to the driving requirements and operation of the engine at a high efficiency level.

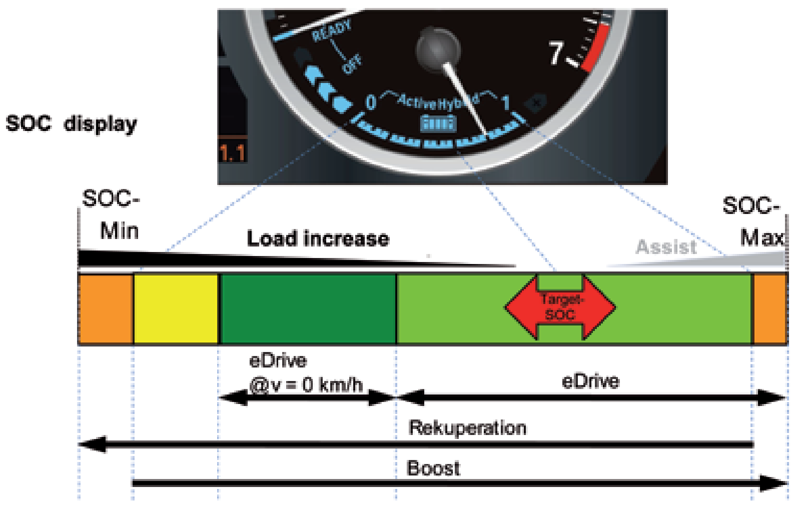

Figure 11: Hybrid operation as a function of the state of charge (SOC) of the HV battery

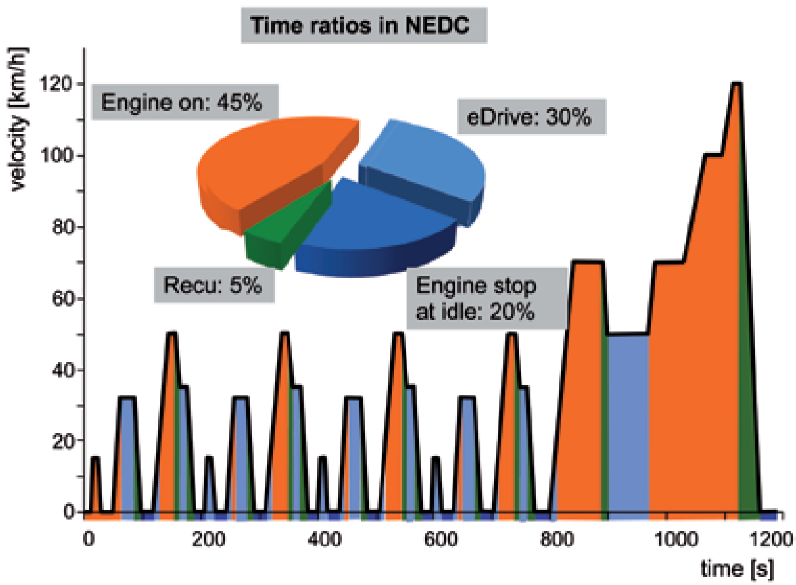

Figure 12: Operating strategy in NEDC cycle

Table: Technical data of BMW ActiveHybrid X6

Engine / number of cylinders / valves	–	V / 8 / 4
Engine / number of cylinders / valves	–	MSD85
Displacement effective	cm^3	4395
Stroke / bore	mm	88.3 / 89.0
Nominal output of combustion engine/ at rev/min	kW/min^{-1}	300 / 5500-6400
Nominal torque of combustion engine/ at rev/min	Nm/min^{-1}	600 / 1750-4500
Nominal output of E-machine A	kW	67
Nominal torque of E-machine A	Nm	260
Nominal output of E-machine B	kW	63
Nominal torque of E-machine B	Nm	280
Nominal output (System)	kW	357
Nominal torque (System)	Nm	780
Compression ratio / fuel type	–	10.0 / ROZ 91-98
Transmission type	–	AHS-C
Ratio 1^{st} / 2^{nd} / 3^{rd} / 4^{th} gear	–	3.889 / 2.619 / 1.800 / 1.300
Ratio 5^{th} / 6^{th} / 7^{th} / 8^{th} Gang	–	1.000 / 0.825 / 0.723 / –
Ratio reverse gear	–	variabel
Axle ratio	–	3.640
Top speed	km/h	236
max. speed in E-mode	km/h	60 (traction) / 65 (traction)
Acceleration 0-100 km/h	s	5.6
1000 m, start from standstill	s	24.9
Elasticity 80-120 km/h 4^{th} / 5^{th} gear	s	– / –
Consumption EC urban (EU5)	l/100km	10.8
Consumption EC extra urban (EU5)	l/100km	9.4
Consumption EC combined / mileage (EU5)	l/100km/km	9.9 / 860
CO_2 emission combined	g/Km	231
Exhaust standard	–	EU5 / ULEV II

Figure 12 shows the operating strategy by example of a low-dynamic driving cycle (NEDC). For emission reasons the engine is first started and switched off for the first time after approximately 70 s. All urban constant drives below a speed of 50 km/h and all decelerations and standstill phases are performed without combustion engine. The combustion engine is activated at accelerations from a speed of approximately 15 km/h. In the extra urban cycle the 50 km/h constant drive is performed in electric mode.

The consumption advantages of the BMW ActiveHybrid X6, compared to the basic vehicle with identical engine, depend strongly on the driving profile. In the low-dynamic cycles (similar to NEDC) the X6 ActiveHybrid consumes up to 25 % less fuel, in the medium-dynamic combined US cycle approximately 15 % less fuel and in the European driving cycle with higher highway portions about 12 % less than the basic vehicle.

7 Driving Performance and Functional Properties

The combustion engine has an output of 300 kW and a torque of 600 Nm and the electric synchronous motors have an output of 67 kW or 63 kW, respectively. In connection with the battery power this yields a maximum system output of 357 kW and a torque of maximal 780 Nm.

The relation between driving performance and the fuel consumption achieved by the BMW ActiveHybrid X6 establishes a new benchmark in the hybrid vehicle segment as well as in the competitor environment of the BMW X models. The acceleration from 0 to 100 km/h is 5.6 s and the top speed is 236 km/h (regulated). The average consumption in the EC cycle is 9.9 l, the CO_2 values 231 g/km, **Table**.

Driving characteristic and comfort of the BMW ActiveHybrid X6 meet the standards set by the current BMW models of the X-series. In this regard the driver experiences no differences between the electric mode and the combustion mode. The intelligent four-wheel system xDrive with permanent variable force distribution between the front and the rear wheels also contributes to a driving dynamics that is unparalleled by the competitors.

IMPRINT

ATZ WORLDWIDE

www.ATZonline.com

11|2009 · November 2009 · Volume 111
Springer Automotive Media | GWV Fachverlage GmbH
P. O. Box 15 46 · 65173 Wiesbaden · Germany
Abraham-Lincoln-Straße 46 · 65189 Wiesbaden · Germany

Managing Directors Dr. Ralf Birkelbach, Albrecht Schirmacher
Senior Advertising Thomas Werner
Senior Production Christian Staral
Senior Sales Gabriel Göttlinger

EDITORS-IN-CHARGE

Dr.-Ing. E. h. Richard van Basshuysen
Wolfgang Siebenpfeiffer

EDITORIAL STAFF

Editor-in-Chief
Johannes Winterhagen (win)
Phone +49 611 7878-342 · Fax +49 611 7878-462
E-Mail: johannes.winterhagen@springer.com

Vice-Editor-in-Chief
Dipl.-Ing. Michael Reichenbach (rei)
Phone +49 611 7878-341 · Fax +49 611 7878-462
E-Mail: michael.reichenbach@springer.com

Chief-on-Duty
Kirsten Beckmann M. A. (kb)
Phone +49 611 7878-343 · Fax +49 611 7878-462
E-Mail: kirsten.beckmann@springer.com

Sections
Body, Safety
Dipl.-Ing. Ulrich Knorra (kno)
Phone +49 611 7878-314 · Fax +49 611 7878-462
E-Mail: ulrich.knorra@springer.com

Chassis
Roland Schedel (rs)
Phone +49 6128 85 37 58 · Fax +49 6128 85 37 59
E-Mail: ATZautotechnology@text-com.de

Electrics, Electronics
Markus Schöttle (scho)
Phone +49 611 7878-257 · Fax +49 611 7878-462
E-Mail: markus.schoettle@springer.com

Engine
Dipl.-Ing. (FH) Moritz-York von Hohenthal (mvh)
Tel. +49 611 7878-278 · +49 611 7878-462
E-Mail: moritz.von.hohenthal@springer.com

Heavy Duty Techniques
Ruben Danisch (rd)
Phone +49 611 7878-393 · Fax +49 611 7878-462
E-Mail: ruben.danisch@springer.com

Online
Dipl.-Ing. (FH) Caterina Schröder (cs)
Phone +49 611 7878-190 · Fax +49 611 7878-462
E-Mail: caterina.schroeder@springer.com

Production, Materials
Stefan Schlott (hlo)
Phone +49 8191 70845 · Fax +49 8191 66002
E-Mail: Redaktion_Schlott@gmx.net

Service, Event Calendar
Martina Schraad
Phone +49 212 64 235 16
E-Mail: martina.schraad@springer.com

Transmission, Research
Dipl.-Ing. Michael Reichenbach (rei)
Phone +49 611 7878-341 · Fax +49 611 7878-462
E-Mail: michael.reichenbach@springer.com

English Language Consultant
Paul Willin (pw)

Permanent Contributors
Richard Backhaus (rb), Christian Bartsch (cb), Prof. Dr.-Ing. Peter Boy (bo), Prof. Dr.-Ing. Stefan Breuer (sb), Jörg Christoffel (jc), Jürgen Grandel (gl), Prof. Dr.-Ing. Fred Schäfer (fs), Bettina Seehawer (bs)

Address
P.O. Box 15 46, 65173 Wiesbaden, Germany
E-Mail: redaktion@ATZonline.de

MARKETING | OFFPRINTS

Product Management Automotive Media
Sabrina Brokopp
Phone +49 611 7878-192 · Fax +49 611 7878-407
E-Mail: sabrina.brokopp@springer.com

Offprints
Martin Leopold
Phone +49 2642 9075-96 · Fax +49 2642 9075-97
E-Mail: leopold@medien-kontor.de

ADVERTISING | GWV MEDIA

Ad Manager
Britta Dolch
Phone +49 611 7878-323 · Fax +49 611 7878-140
E-Mail: britta.dolch@gwv-media.de

Key Account Manager
Elisabeth Maßfeller
Phone +49 611 7878-399 · Fax +49 611 7878-140
E-Mail: elisabeth.massfeller@gwv-media.de

Ad Sales Manager
Sabine Röck
Phone +49 611 7878-269 · Fax +49 611 7878-140
E-Mail: sabine.roeck@gwv-media.de

Ad Sales
Heinrich X. Prinz Reuß
Phone +49 611 7878-229 · Fax +49 611 7878-140
E-Mail: heinrich.reuss@gwv-media.de

Display Ad Manager
Susanne Bretschneider
Phone +49 611 7878-153 · Fax +49 611 7878-443
E-Mail: susanne.bretschneider@gwv-media.de

Ad Prices
Price List No. 53 (10/2009)

SUBSCRIPTIONS

VVA-Zeitschriftenservice, Abt. D6 F6, ATZ
P. O. Box 77 77, 33310 Gütersloh, Germany
Renate Vies
Phone +49 5241 80-1692 · Fax +49 5241 80-9620
E-Mail: SpringerAutomotive@abo-service.info

SUBSCRIPTION CONDITIONS

The eMagazine appears 11 times a year at an annual subscription rate of 269 €. Special rate for students on proof of status in the form of current registration certificate 124 €. Special rate for VDI/ÖVK/VKS members on proof of status in the form of current member certificate 208 €. Special rate for studying VDI members on proof of status in the form of current registration and member certificate 89 €. The subscribtion can be cancelled in written form at any time with effect from the next available issue.

PRODUCTION | LAYOUT

Kerstin Brüderlin
Phone +49 611 7878-173 · Fax +49 611 7878-464
E-Mail: kerstin.bruederlin@gwv-fachverlage.de

HINTS FOR AUTHORS

All manuscripts should be sent directly to the editors. By submitting photographs and drawings the sender releases the publishers from claims by third parties. Only works not yet published in Germany or abroad can generally be accepted for publication. The manuscripts must not be offered for publication to other journals simultaneously. In accepting the manuscript the publisher acquires the right to produce royalty-free offprints. The journal and all articles and figures are protected by copyright. Any utilisation beyond the strict limits of the copyright law without permission of the publisher is illegal. This applies particularly to duplications, translations, microfilming and storage and processing in electronic systems.

Springer Automotive Media is part of the specialist publishing group Springer Science+Business Media.

8 Summary and Outlook

The BMW ActiveHybrid X6 is world-wide the first Sport Activity Coupé with full hybrid drive and offers technology on the highest level as regards the combustion engine as well as the components of the electrified drive.

The BMW ActiveHybrid X6 offers a driving experience that is unique compared to the competitor environment of the BMW X-series models and with regard to hybrid vehicles offered by other brands. The combination V8 gasoline engine with electric drive results in a clearly noticeable gain in dynamics and, at the same time, in a reduction of the consumption and emission values by up to 25 %. The parallel increase of driving pleasure and efficiency identifies the BMW ActiveHybrid X6 as a typical BMW in the segment of hybrid vehicles.

The BMW ActiveHybrid Technology allows the driver to operate the vehicle in either pure electric mode, in combustion mode or in a mode that combines both drive concepts.

CO_2 free driving in electric mode is possible up to a speed of 60 km/h. The combustion engine is activated when required by the driving situation and switched off when coasting at a speed below 65 km/h.

The drive system of the BMW ActiveHybrid X6 consists of a V8 engine with an output of 300 kW and BMW TwinPower Turbo technology, supplemented by two electric motors that generate 67 kW and 63 kW, respectively. The maxim deliverable system output is 357kW and the maximum achievable torque is 780 Nm. These impressive data render the BMW ActiveHybrid X6 the most powerful hybrid vehicle of its segment.

The relation between driving performance and the fuel consumption achieved by the BMW ActiveHybrid X6 establishes a new benchmark in the hybrid vehicle segment as well as in the competitor environment of the BMW X models. The acceleration from o to 100 km/h is 5.6 s and the top speed is 236 km/h (regulated). The average consumption in the EC cycle is 9.9 l/100 km, the CO_2 values 231 g/km. BMW ActiveHybrid X6 – an innovative vehicle that will further strengthen the BMW EfficientDynamics strategy. ■

Homologation Testing of Vehicle Lighting Systems

Use of Camera-based Test Systems

At night, obstacles are very often recognized too late. Safety can be enhanced by improving vehicle lighting. IAV uses camera-based test procedures for homologation testing to evaluate head lamps with quality demands going over and beyond the legal requirements.

1 Introduction

New technologies enable flexible lighting functions such as dynamic high beam, adaptive brake lights or variable luminance distribution on the road, referring to town lights or motorway lights at the vehicle, for example. At the moment, these systems are only available for top-of-the-line vehicles, but not for vehicles in the lower price segment. Uniform evaluation standards can make such safety-relevant equipment available for all vehicles. New evaluation standards of this type are being discussed in the rule CIE TC 4-45, where thought has been given to an New Car Assessment Program (NCAP) for active vehicle safety [1].

However, this results in new challenges for photometric metrology. This article of IAV shows how camera-based spatial luminance measurements can take up these challenges. We used the LDK 98-4 color spatial luminance measuring camera by TechnoTeam. The test field consisted of a hall measuring 40 m × 16 m and 8 m in height, together with IAV's test track for outdoor testing.

2 Evaluation of Vehicle Lighting

In physiological terms, luminance is the photometric variable that comes closest to the human sense of brightness [2]. For a road user, it is the luminance of the signal lamps on the car ahead that plays a crucial role, and not the absolute value of luminous intensity [1]. For an obstacle to be recognized, its contrast to the surroundings must be greater than the threshold contrast of the eye. These contrasts are calculated from luminances. In fact, the detection distance can be determined by measuring the luminance as seen by the driver. This uses targets placed on the road at certain distances in the field of vision [3]. The homogeneity of near-field luminance on the road is also included as evaluation parameter [4].

Consideration also has to be given to the glare effect; this can be ascertained with luminance measurements. A suitable set-up is described later. A luminance camera can be used to capture the whole scene in one picture; luminances and contrasts can be defined at any point. The various states of adaptive lamps can be measured quickly in succession. Lamps fitted in the vehicle can be tested, which is not the case when using goniometric measurement. Camera-based measurement also takes account of the installation position and shading from other components, together with the interplay of two or more lamps operating at the same time.

3 Testing in a Hall

Closed room testing can be carried out under reproducible, comparable conditions. However, light from a head lamp, for example, is reflected from the walls and ceiling onto the floor, distorting illuminance distribution on the ground. This is also a problem in light tunnels, which are usually long but often narrow. Ideally [1], the hall should have no supports and offer an area of 50 m × 150 m, but this is practically not available.

IAV compromises therefore with a hall measuring 40 m × 16 m × 8 m (height). The width of this hall causes interfering light to fizzle out. As part of a bachelor's assignment [5], the materials were defined for the walls and floor to eliminate the remaining interfering light and permit precise measurement. This is shown in [6].

The hall is large enough to evaluate the homogeneity of luminance distribution on the road in the driver's near-field of vision. The test set-up is shown in **Figure 1**: The unprepared hall with road markings is shown at the top. The reflections from the wall can be clearly seen (arrow b). They distort the luminance picture with corrected perspective (in the middle). The reflections are supressed by covering the wall (arrow a, top and bottom). The anisotropic reflection properties are clearly visible, which is just one of the reasons why the bird´s eye view is then preferred. After preparing the floor, it is possible to carry out homogeneity evaluation, for example. Homogeneity is then defined by forming the gradients of luminance in certain zones [4]. The floor in question must be very flat with easily defined optical properties, resilient and easy to clean. A floor covering made of special plastic tiles proved to be the best compromise.

The Authors

Dr.-Ing.
Peter Schintag
is Head of Lighting and Vision Department at IAV in Gifhorn (Germany).

Dr. rer. nat.
Michael Marutzky
is Development Engineer with main focus in optical metrology at IAV in Gifhorn (Germany).

Dipl.-Ing. (FH)
Torsten Rehberg
is Development Engineer with main focus in photometry and light simulation at IAV in Gifhorn (Germany).

Dipl.-Ing. (FH)
Simon Lansmann
is Development Engineer with main focus in photometry and light simulation at IAV in Gifhorn (Germany).

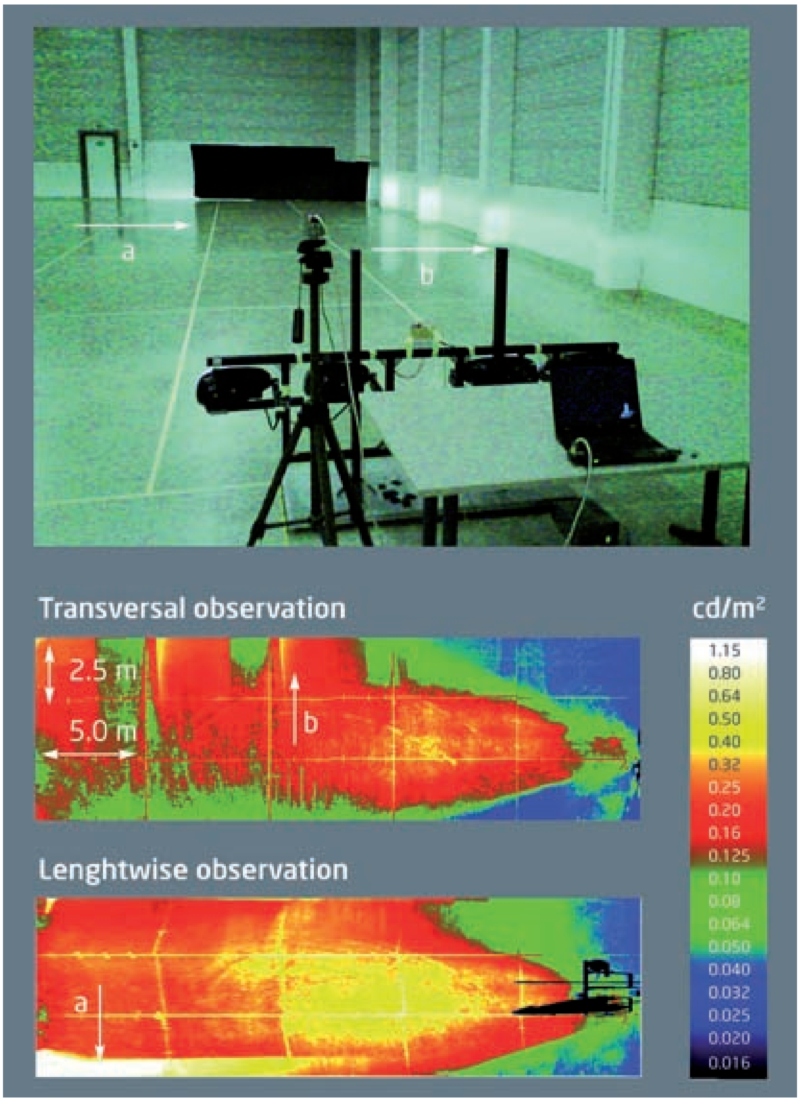

Figure 1: Test set-up for the detection distance by measuring the luminance as seen by the driver

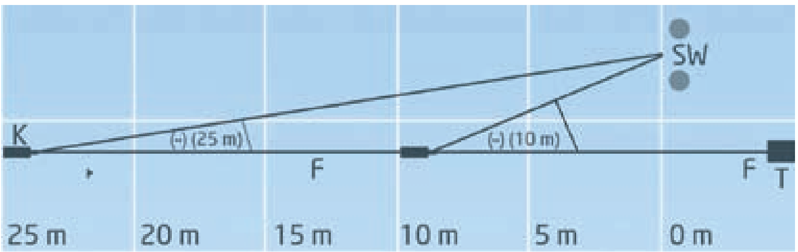

Figure 2: Set-up for examining the glare effect of head lamps on the driver when vehicles pass (SW: head lamp; K: camera mounted in driver's position; F: fixation axis of the simulated driver; T: target)

The set-up shown in **Figure 2** was developed to examine glare. It simulates the passing of an oncoming vehicle on the left-hand lane with its light switched on and evaluates the glare effect [7]. The contrast K_{BL}:

$$K_{BL} = L_O - L_U/L_U + L_S \qquad \text{Eq. (1)}$$

between an object fixed with the eye with its inherent luminance L_O and the surrounding luminance L_U is reduced by the disability glare L_S:

$$L_S = kE_B/\Theta^2 \qquad \text{Eq. (2)}$$

In Eq. (2), the age-dependent factor k is defined as:

$$k = 9.05\,[1 + (age/66.4)^4] \qquad \text{Eq. (3)}$$

The value E_B is the illuminance at the glared eye (here at the luminance camera) and Θ is the angle between glare source and the fixation axis. The glare caused by signal lamps and by interior lighting can be determined in the same way. As glare depends on the surrounding luminance, light simulation is to be installed in the hall to quantify glare at night, during the day and in twilight.

Measurement of the cut-off line on a screen 25 m away from the head lamp presents a challenge to metrology. The illuminance at the screen decreases from some 10 lux to a few tenth of a lux within a few centimeters and has to be measured accurately in all ranges. The test set-up is similar to the measurement system shown in [8]. There was a detailed error analysis for the measurement field using a series-production head lamp. [6] describes how interfering light can be reduced to a level of about 0.06 lux, which is sufficient for verifying the ECE requirement of E < 0.7 lux above the cut-off line.

A screen measurement can also be used for indirect measurement of the luminous flux distribution of signal lamps, day-time running lights or rear lamps. The advantage of this measurement compared to goniometric measurement is that it is completed with just one high-resolution shot. This can be used for fast consecutive testing of the various states of an adaptive lamp.

4 Measurements in the Open Air

Measurements in the open air know no space problems, but conditions here are not reproducible. For example, night brightness depends on the weather, time of day and the season etc. Starting at sunset, every 5 min luminance pictures were taken of the dipped head lamps on the road as seen by the driver, deducting the luminance picture of the background with the head lamps switched off as reference, **Figure 3**. After about 45 min, the measurements correspond to each other down to the 0.01-cd/m² range although the surrounding brightness is still decreasing considerably [6]. This permits reproducible tests such as defining the detection distance via targets.

Road wetness poses another problem with reflection and luminance differing drastically between the road in wet condition and in dry condition. The bi-directional luminance coefficient breaks down into one part for specular reflection and one part for diffuse reflection. The first is less manageable as it includes glancing angles with very high reflections. The diffuse part is easier to handle since scattering is the causing effect. To measure just this part, we measured the luminance on the road of the dipped head lamps in a mass-produced vehicle as seen from a bird's-eye view. The luminance coefficient required to calculate illuminance then only depends on the shallow angle of incidence, has a smooth progression and is quickly defined, **Figure 4**. This trivializes the actually difficult conversion. The bird's-eye view, **Figure 5**, is composed of 4 m × 8 m sections. As the camera's pixel resolution is roughly 1000 × 1000, the effective angle resolution at a distance of 50 m to the head lamp is better than 0.001°.

It takes about one hour for the complete measurement of a head lamp, **Figure 6** and **Figure 7**. Exactly one reference measurement of illuminance is carried out for each camera picture to eliminate the problem of time-variant properties of the road surface (drying out, dew, frost).

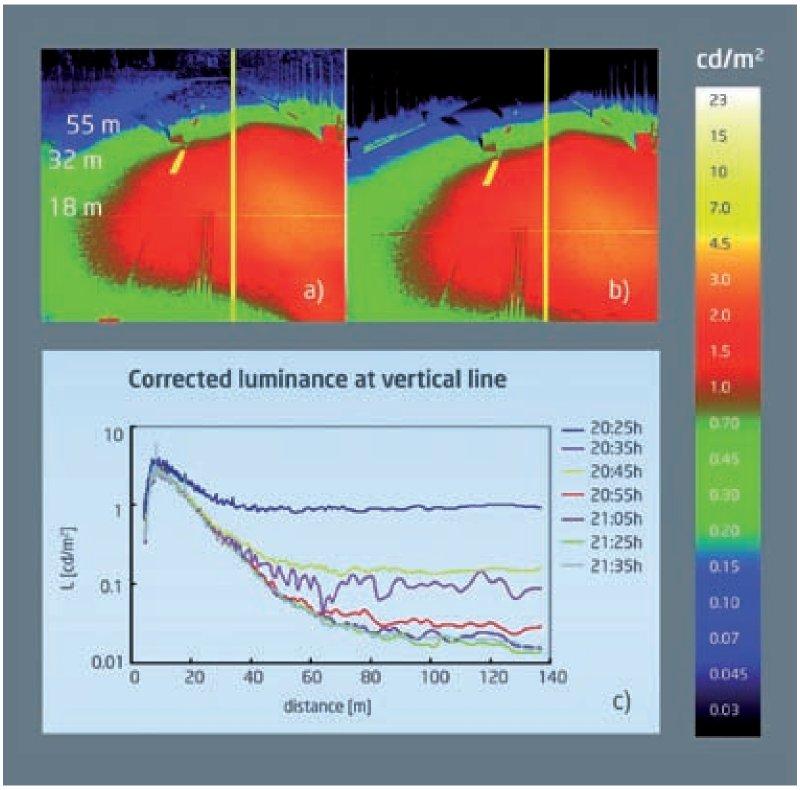

Figure 3: Luminance pictures of the dipped head lamps on the road as seen by the driver – the luminance picture of the background with the head lamps switched off as reference (a: corrected luminance picture at 8.35 p. m.; b: at 9.10 p. m.; c: luminance sheet along the yellow line in Figure 3a and Figure 3b depending on the distance to the head lamp)

5 Summary and Outlook

In this article IAV presented concepts for camera-based testing of head lamps with a suitable measuring environment. The tests can be carried out quickly and with sufficient accuracy. The physiological impact on the driver can be evaluated. It is possible to mitigate the difficulties of open-air testing caused by changing ambient conditions. The bird's-eye view concept is an interesting possibility for visualizing illuminance distribution on the road in reality, while avoiding the complicated angle dependencies of the luminance coefficient. Such visualizations are normal procedure for evaluating head lamps, but have only been used in the form of simulation results up to now.

The test methods described in this article are part of the process chain applied at IAV to develop vehicle lighting. It was used, for example, for developing the exterior lights on the new small car Trabant nT, Figure 6 and Figure 7, presented at IAA 2009 Frankfurt Motor Show. The luminance images of beam patterns as well

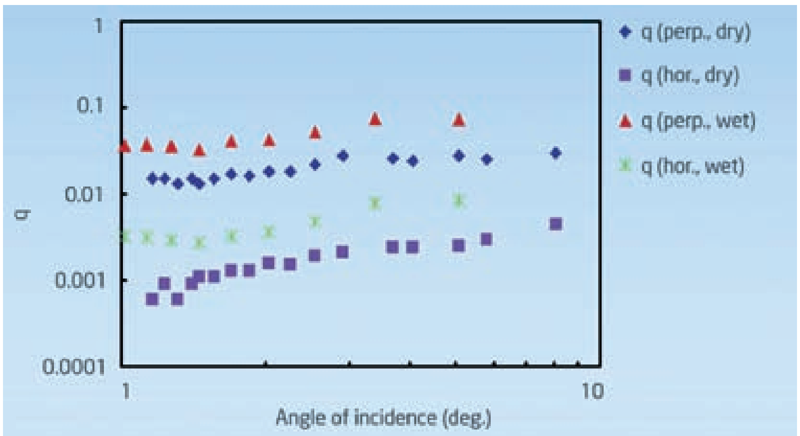

Figure 4: Measuring of the luminance coefficient in wet and in dry condition (luminance coefficients $q = L/E$ in perpendicular observation direction; illuminance was measured horizontally and vertically to the road in dry and wet state)

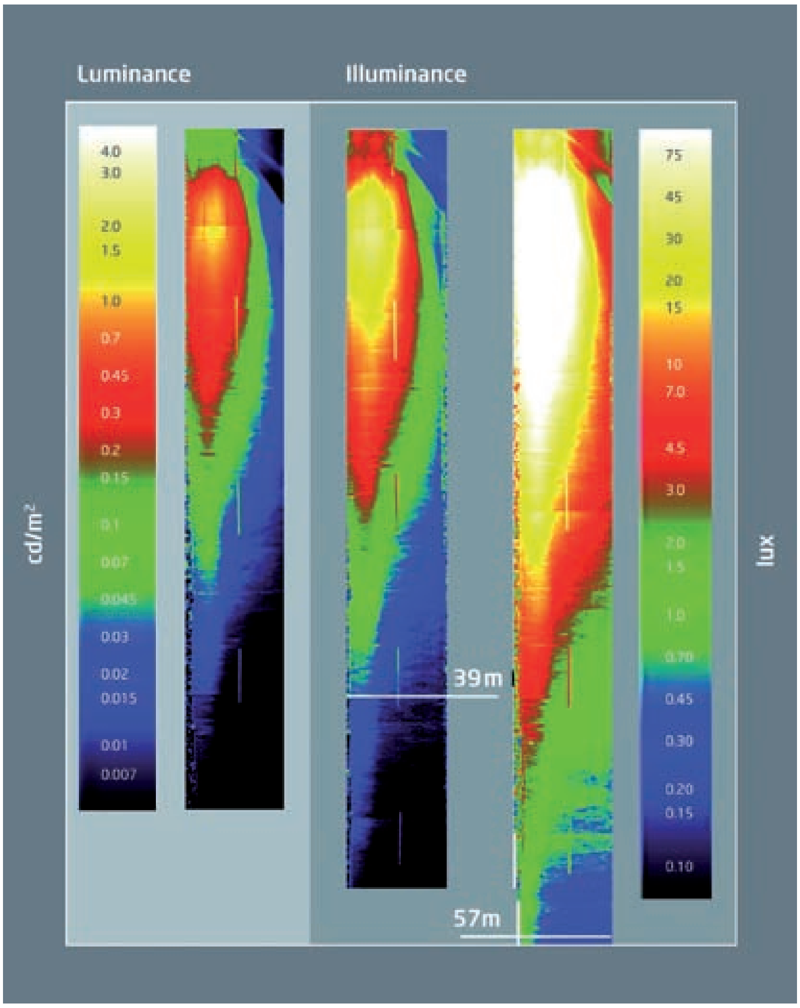

Figure 5: Measuring of the luminance on the road from the bird's-eye view (luminance on the road measured from the bird's-eye view (left); one luminance coefficient was defined for each picture for converting into illuminance (compare with. Figure 4); the vertical component is shown in the middle and the horizontal component on the right; intersections of the 1-lux isoline with the roadside shown in m)

as comparison with the simulated distribution of light provided important information for optimizing the layout of light and document the level of performance attained in comparison to headlamps available on the market.

References

[1] Manz, K.; Kooß, D.; Klinger, K.; Schellinger, S.: Entwicklung von Kriterien zur Bewertung der Fahrzeugbeleuchtung im Hinblick auf ein NCAP für aktive Fahrzeugsicherheit. BAST, Heft F65, Bergisch Gladbach, 2007

[2] Völker, S.: Hell- und Kontrastempfindung – ein Beitrag zur Entwicklung von Zielfunktionen für die Auslegung von Kfz-Scheinwerfern. Habilitationsschrift, Universität Paderborn, 2006

[3] Kliebisch, D.; Völker, S.: Measurement and Calculation of Detection Distances of Headlamp Distributions. In: Proceedings of 7th ISAL, P8.2, Darmstadt, Germany, 2007

[4] Kleinkes, M.: Objektivierte Bewertung des Gütemerkmals Homogenität für Scheinwerfer-Lichtverteilungen. Dissertation, Universität Bielefeld, 2003

[5] Letzin, R.: Kamerabasierte Untersuchungen des Reflexions- und Streuverhaltens von Oberflächen. Bachelorarbeit, Fachhochschule Jena, 2008

[6] Marutzky, M.; Lansmann, S.; Rehberg, T.; Schintag P.: Feasibility Study on Spatial Luminance Camera Based Measurements in a Large Hall. In: Proceedings for 8th ISAL, P18 (accepted), Darmstadt, Germany, 2009

[7] Adrian, W.: Change of Visual Acuity with Age. In: 40 Jahre Lichttechnik. S. 19–33, Darmstadt, 1996

[8] Schwanengel, C.; Krüger, U.; Schmidt, F.; Rodenkirchen, J.: Spatially Resolved Luminance Measuring Methods Compared with Illuminance Measurements of Automotive Headlamps. In: Proceedings for 6th ISAL, C8, Darmstadt, Germany, 2006

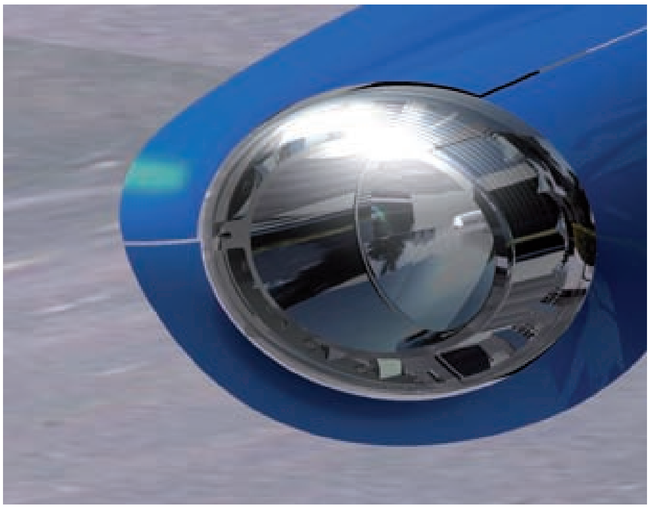

Figure 6: Headlamp, presented with the visualization tool Icem-Surf

Figure 7: Photograph of the new small car Trabant nT light pattern presented at IAA 2009

The new dimension of information: eMagazines!

One click – all the latest news! Experience our electronic magazines in English. You simply flip through the pages via mouse click. But there is far more to the new electronic magazine:

- **No distribution cost:**
  Every issue delivered directly on to your screen.
- **Keyword search:**
  Find contents by simply entering a keyword.
- **Online-archive:**
  As a subscriber, you will have full access to our online publication database containing all articles from 2000 up to the present.
- **6 issues ATZautotechnology for free:**
  You will also receive 6 issues/year of the FISITA magazine ATZautotechnology in printed form – at no extra cost!

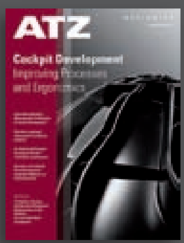

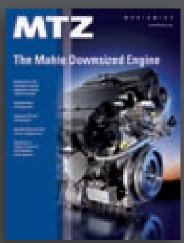

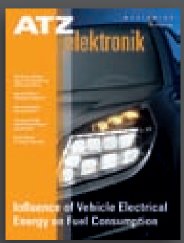

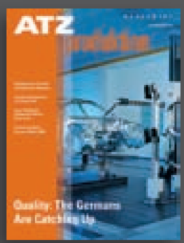

Experience the new dimension of information. Check out your test issue online at: **emagazine.ATZonline.com**

Please send my subscription to:

☐ **ATZ** (11 issues / 269,- Euro)*
☐ **ATZelektronik** (6 issues / 131,- Euro)*
☐ **MTZ** (11 issues / 269,- Euro)*
☐ **ATZproduktion** (6 issues / 131,- Euro)*

to the following e-mail address:

E-mail

Date/signature

* annual subscription rate

Please send the print version of ATZautotechnology to the following address:
(this is automatically included in the price of my subscription)

Name	Company	311 08 009
Department	Position	
Address	Postal code	
City	Country	

Springer Automotive Media subscription service | Abraham-Lincoln-Str. 46 | D-65189 Wiesbaden | Phone: +49 611.7878-151 | Fax: +49 611.7878-423 | SpringerAutomotive@abo-service.info | www.ATZonline.com

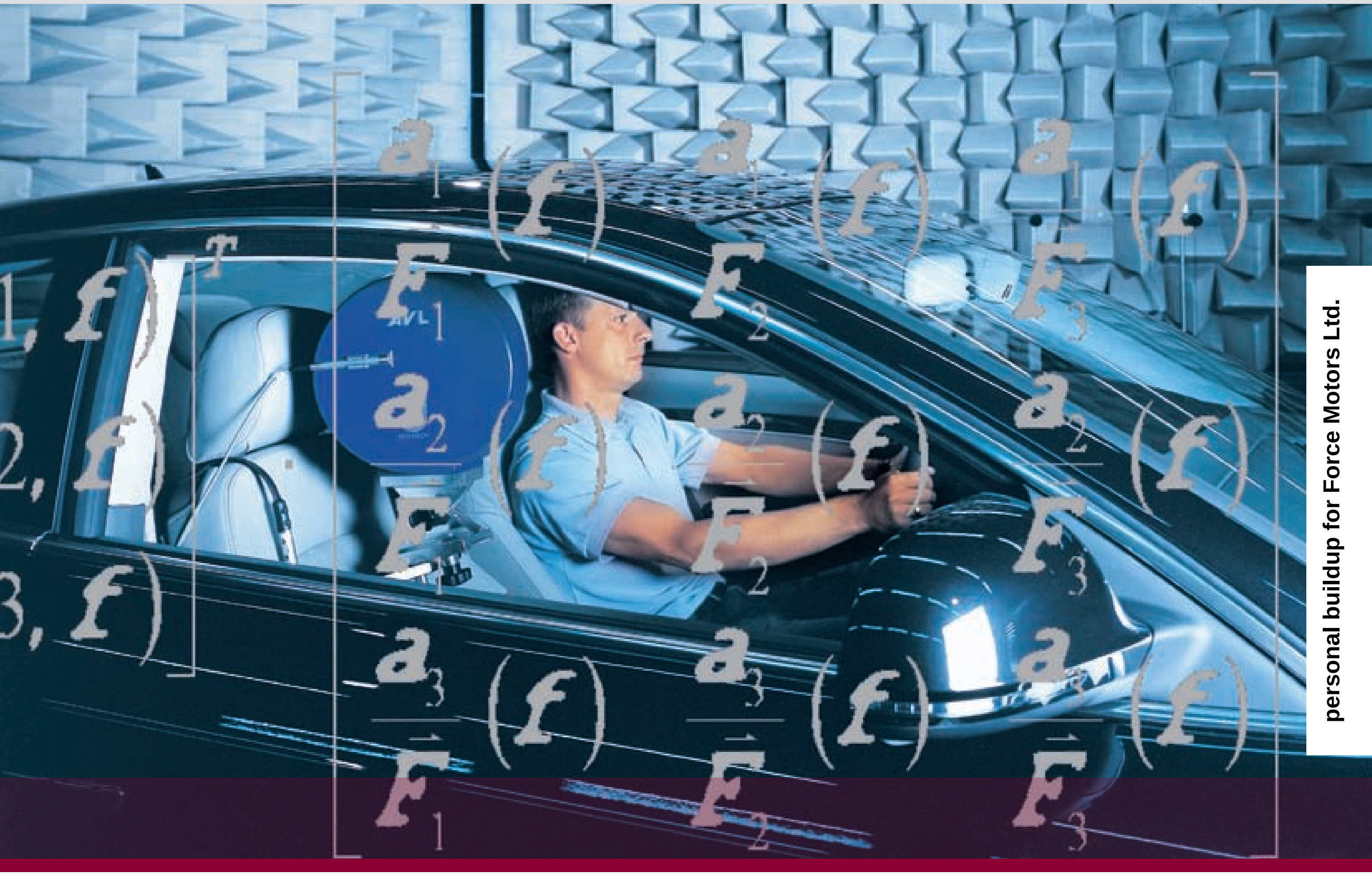

Efficient and Accurate Determination of the Transfer Characteristics of Vehicle Bodies

An evaluation of the complex properties of the NVH transfer of a vehicle body is done by transfer path analysis (TPA). Result quality is mainly depending on measurement technology and the applied mathematical models. AVL List GmbH developed a new promising approach during a research project and presents the simulation tool TPA-Form, which allows a remarkable increase in efficiency and result quality.

1 Introduction

A common tool to determine contributions of different noise sources to vehicle interior noise is the Transfer Path Analysis (TPA). As the information about contribution of different sources to the overall sound at target positions is highly necessary during an interior noise optimisation process, the quality of results out of TPA analyses is crucial for interior noise improvements.

In the first part of this paper valuable results concerning drawbacks in TPA analysis procedures are discussed. Afterwards promising approaches for enhancements of TPA methods are presented. Finally a completely new, fast and efficient TPA method is introduced and verification results are shown.

2 Commercially Available TPA Methodologies

On a C-class passenger car, which was used as the test object of this R&D project, three different commercially available TPA methodologies were tested and evaluated. For all TPA methodologies the same time signals were used as inputs. As a result different source contributions were obtained for each system.

Additionally the overall measured interior noise level did not fit to the TPA calculation result. Based on a detailed analysis a specification of possible errors that might influence the results of a TPA was developed [1].

Figure 1 shows a classification of the most important measurement and mathematically based errors of an inertance based TPA [2], which occur by force excitations of the vehicle structure. To measure the inertances (ratio of acceleration and acting force) and frequency response functions (FRFs) an artificial excitation like an impact hammer or shaker has to be used.

Due to severe limitation in space, especially within engine compartments of nowadays passenger cars, deviations in excitation direction and excitation position can easily occur. To analyse the influences of these deviations, a substantial sensitivity analysis was performed. Representative examples of influences of the deviations in excitation position with 35 mm and excitation direction of 15° are plotted in **Figure 2** as a difference of 10 dB. Also the influence of temperature of the vehicle body leads to differences between ambient temperature (20 °C) and operational measurements (60 °C) and results in 5 dB. Beside errors that are based on measurement problems, errors based on numerical reasons contribute to the overall error of inertance-based TPA calculations.

In order to quantify those numerically based errors a special verification measurement setup and a substantial crosstalk influence analysis has been accomplished. The combination of both errors (measurement and mathematics) leads to important differences in the results. Aim of this verification measurement was the comparison of different TPA methodologies in the face of numerical correctness. Therefore the elimination of all measurement based errors had to be accomplished by the verification measurement setup.

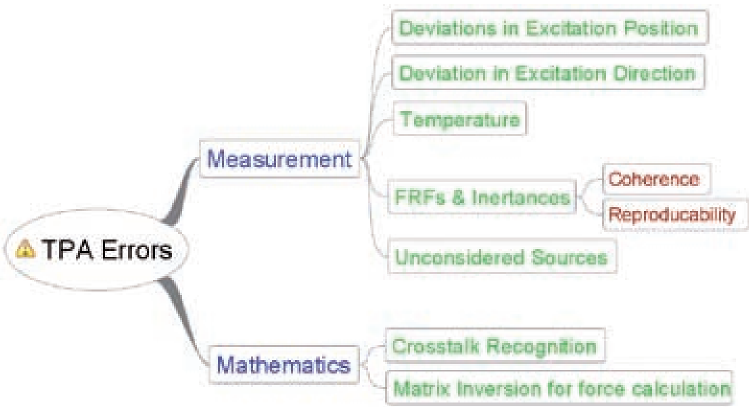

Figure 1: Overview of measurement and mathematics error possibilities that influence TPA results

The Authors

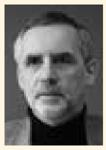

Dr. techn.
Franz K. Brandl
is Manager of Vehicle and Powertrain Acoustics Department at AVL List GmbH in Graz (Austria).

Dr. techn.
Stephan Brandl
is Project Manager at Vehicle and Powertrain Acoustics Department at AVL List GmbH in Graz (Austria).

Prof. Dr.
Robert Höldrich
is Full Professor at the Institute of Electronic Music and Acoustics of University of Music and Performing Arts Graz (Austria).

Dr. Alois Sontacchi
is Senior Researcher at the Institute of Electronic Music and Acoustics of University of Music and Performing Arts Graz (Austria).

Prof. Dr.
Hans H. Priebsch
is Scientific Head of Area Area NVH & Friction Kompetenzzentrum "Das Virtuelle Fahrzeug Forschungsgesellschaft mbH" (ViF) in Graz (Austria).

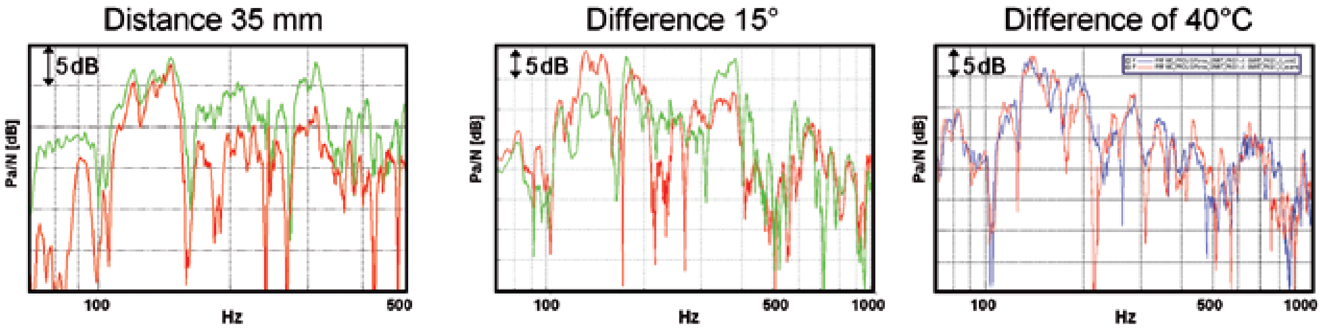

Figure 2: Comparison of measured FRFs at one engine mount with deviations in excitation position (left), excitation direction (centre) and excitation temperature (right)

In this setup mini shakers have been used to generate 'operational conditions' by exciting the chassis as under a engine run-up in third gear. To prevent deviation in excitation direction and excitation position all shakers have been fixed to the chassis. By utilizing Mini Shakers for excitation, additionally measurement based error caused by temperature differences is eliminated. Finally problems based on reproducibility, coherence of the transfer functions and unconsidered sources are eliminated due to the fixation of the shakers.

Utilizing the generated operational data, TPA's using different TPA methodologies have been performed. Due to the used methodology the tools have been separated into acceleration based [3] and force (inertance) based [2] methodologies. For verification purposes the exact knowledge of induced forces at all excitation positions is necessary. Therefore force transducers have been placed between the Mini Shakers and the chassis. Additionally the overall target sound pressure has been measured during this operational condition. **Figure 3** shows one example for an excitation position setup including one of six mini shaker, force transducer and accelerometers.

Figure 3: Measurement setup for fixing of one of six mini shakers, force transducer and accelerometers in the area of included force position

Beside the well known force (inertance) based approach [2] a TPA procedure based on operational acceleration measurements on a large number of chassis position was introduced lately [3]. In this acceleration based approach a regression analysis is used to determine the contribution of different excitation positions to interior noise. However no forces at the mount positions can be obtained, which eliminates the possibility of a target oriented power train excitation based optimisation.

One main reason for the bad agreement obtained between measurement and calculation [4] is the consideration of influences of different excitations on the measured accelerations. In such a complex environment as a passenger car accelerations are influenced by different sound sources.

In the frame of TPA these interactions are defined as crosstalk (XT). In this investigation XT for each source is defined as the ratio of the sum of energies transmitted through all side paths divided by the energy transmitted through the main path of the excitation. The XT for one power train mount direction is plotted based on the results of the sensitivity analysis. It is calculated by dividing the energy, which is transferred through the two other directions of the mount, through the energy transferred in excitation direction. 0 dB therefore indicates that the same amount of energy is transferred through the main and the two auxiliary paths. A positive dB number indicates that more energy is transmitted through the auxiliary paths and a negative dB number indicates that more energy is transmitted through the main path.

Based on this XT definition the induced error in force calculation by omitting the XT can be estimated. This estimation is plotted on the right ordinate in **Figure 4** and **Figure 5**. As plotted in Figure 4 errors up to 8 dB in force calculation can arise by omitting XT within the engine mounts.

Beside the XT within mounts the XT between different mounts can be considered too. For that purpose the summed energy transmitted through all other mounts is divided by the energy transmitted through the main excitation path. Comparison of calculated XT leads to the conclusion that on the specific test vehicle XT within the engine mounts is substantial and would lead to estimated errors up to 10 dB when omitted.

3 Possibilities for TPA Optimisation

To reduce numerically based errors, crosstalk recognition and error amplification have been investigated to optimize the inertance-based TPA. Usually an increase in crosstalk recognition leads to an increase in "condition number" of the inertance matrix. As the condition number is an indicator for the upper bound of the error amplification, in-

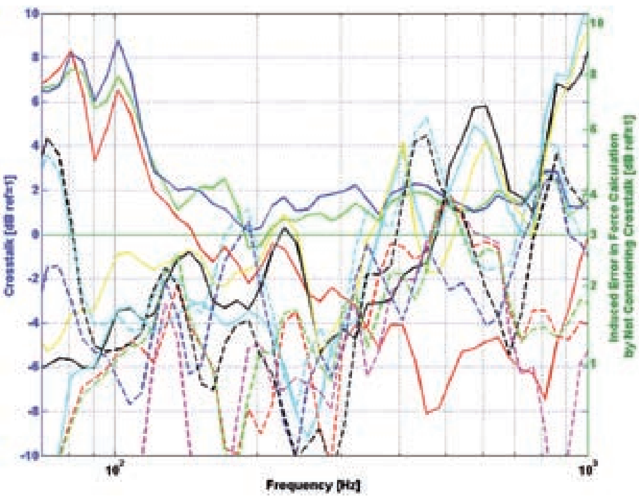

Figure 4: Possible error for force measurement if crosstalk is not considered inside each engine mount

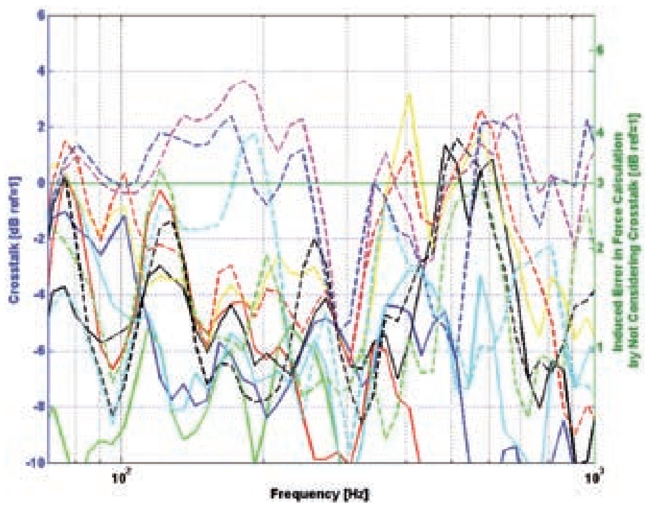

Figure 5: Possible error for force measurement if crosstalk is not considered between several engine mounts

creased crosstalk recognition might lead to increased error amplification. Using more inertances for apparent mass calculation to increase crosstalk recognition usually leads to a higher condition number of the inertance matrix. Very low eigenvalues will give excessive values after inversion of the inertance matrix to calculate the different contributions under operational conditions.

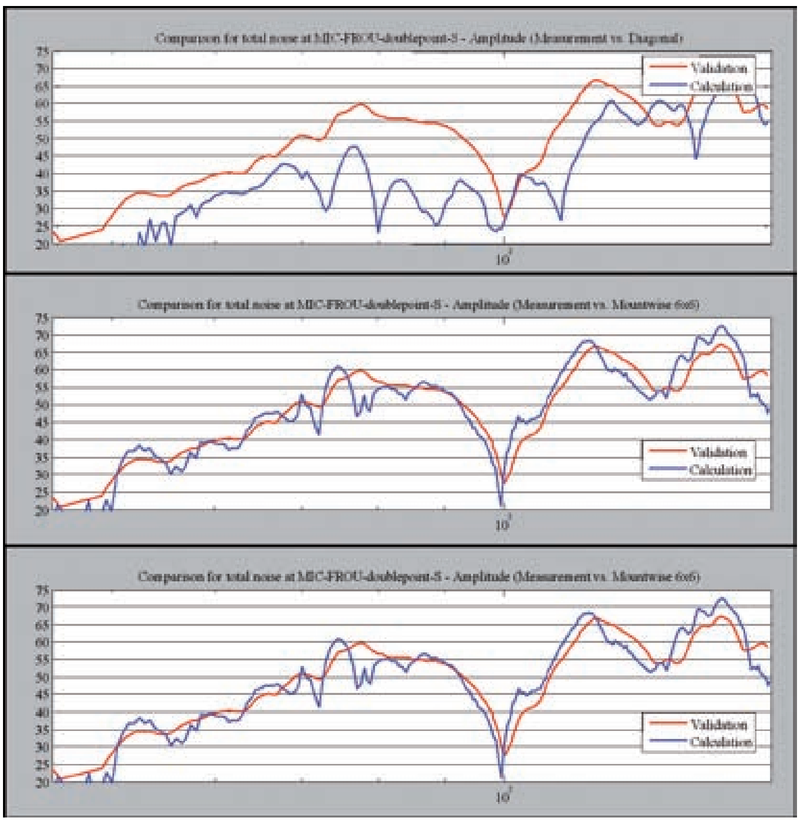

Figure 6: Comparison of measured (red) and calculated (blue) single part of a powertrain component for three variants of matrix version: without crosstalk (top), with crosstalk inside (center) and between (bottom) the mount

For the verification of the mount wise approach (only XT within mounts are considered), data from the verification measurement described before were utilized. As no measurement based errors occur in the verification setup deviations between measurement and calculation are only caused by numerical problems of the applied approaches.

As can be seen in **Figure 6** the calculation using the main diagonal of the inertance matrix shows very little agreement with the measured sound pressure level at the considered target microphone. Utilizing the mount wise approach agreement between measured and calculated sound pressure level increases strongly. Through application of the full matrix approach further improvements in the agreement between measured and calculated sound pressure level can be achieved. Since the amount of XT strongly differs in magnitude between different vehicles and over frequency no general rule can be given, by which extend XT between mounts has to be considered.

4 Innovative Methodology TPA-Form

The innovative methodology TPA-Form assumes that the excitation of all main sources is covered by measuring the accelerations or sound pressures close to all defined excitation positions [5]. Addi-

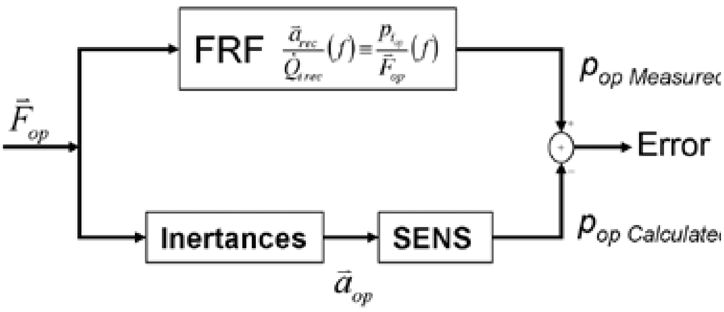

Figure 7: Block diagram showing relations between sensitivities and inertances

tionally it is assumed that acceleration to sound pressure sensitivity functions are constant for all measurements in operational condition. This means that the structure (chassis in case of application on cars) temperature while measuring in operational conditions has to be as constant as possible.

The new approach allows the computation of inertances from measurements in operational condition and reciprocally measured source to target FRFs. The advantages of this new method are its time saving approach and the elimination of common errors in inertance and FRF measurements. While the time saving aspect of this method is obvious, the increase in result quality has to be described in detail.

Using reciprocally measured FRFs the deviation in excitation direction is eliminated because directions of forces of measured FRFs are identical to the accelerometer axis. Additionally it is easier to place an accelerometer close to the origin of the exciting sources as to use a shaker or an impact hammer as excitation at these positions to measure the inertances and FRFs. Furthermore the error based on temperature differences is negligible by the reciprocal measurement if it will be accomplished directly after the operational measurement.

5 Theory Basics of TPA-Form

To compute inertances from operational and reciprocal measurement two steps are necessary. In Step 1 operational mount acceleration to interior sound pressure sensitivities are obtained. They are needed in Step 2 to compute the inertances. For defined timeslots interior sound pressure and acceleration spectra at engine mount positions in an adequate number are calculated from time data. In TPA FRFs, acceleration to sound pressure sensitivities and inertances are assumed to be constant for all operational conditions. Therefore, the system of equations given in Eq. (1) can be solved to compute the required acceleration to sound pressure sensitivities.

Based on the reciprocity principle, reciprocally measured FRFs and FRFs in operational condition are equal in Step 2. For determination of inertances reciprocally measured FRFs are compared to FRFs computed from the operational measurement.

As shown in Eq. (2) the FRFs in operational condition can be computed by utilizing a least squares approach. As the inertances are the only unknowns in this system of equations in Eq. (3), they can be computed by utilizing appropriate mathematical methods. In order to compute all inertances, multiple, sufficiently independent, target positions have to be used. To obtain this independence, a minimum distance between the target positions has to be kept.

Following the presented TPA-Form approach all inertances can be computed with the consideration of crosstalk effects. Having determined all inertances from operational measurement and reciprocally measured FRFs, the required forces and source contributions can be obtained.

6 Verification of TPA-Form

To verify the results of TPA-Form a similar test concept was defined as for the verification of the conventional TPA in a test car. Therefore, two mini shakers were attached at two mounting positions of the body and were operated under engine operation conditions in a engine ramp-up. Between each mini shaker and body a force transducer was placed and a 3D accelerometer was placed next. With the help of the delivered data the following verifications could be done:

- verification of calculated sensitivities
- verification of calculated inertances
- verification of induced forces.

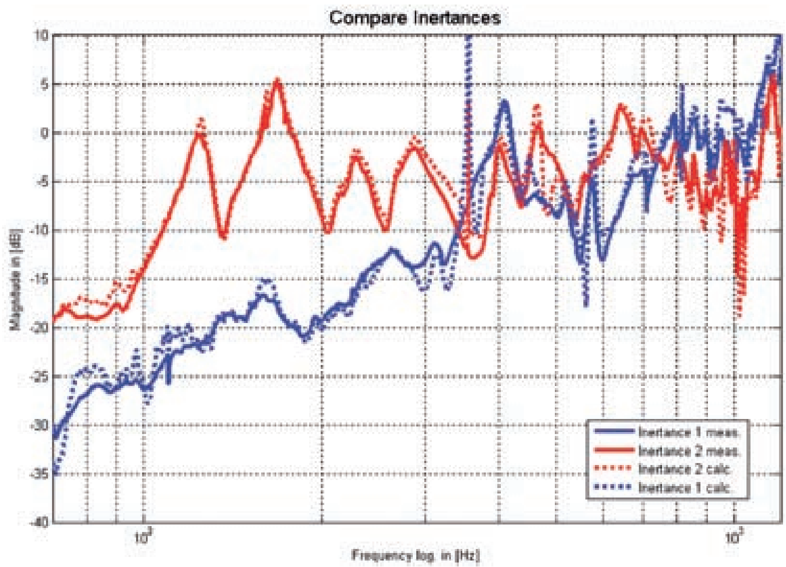

Figure 8: Comparison between two via TPA-Form measured and calculated inertances

6.1 Verification of Calculated Sensitivities

In order to verify the calculated sensitivities a comparison was made of the measured and calculated values (accelerations in the case of verification measurement) at the response points for the entire ramp-up, **Figure 7**. Therefore, the accelerations were defined on the one hand by using the measured transfer functions and were investigated on the other hand with the help of the calculated sensitivities and measured inertances. Via the high correlation between both values the conclusion is possible that the determination of the sensitivities is correct and the statement of constancy of sensitivities over all operation points is given.

For verification of all values a block diagram is given in Figure 7. The block diagram shows the relations between sensitivities, inertances and (reciprocally measured) FRFs. This diagram was used to design appropriate verification procedures for all values computed in TPA-Form.

6.2 Verification of Calculated Inertances

Verification of the inertances computed by TPA-Form is done by comparing them to conventionally measured inertances. For the conventional inertance measurement it is crucial that the error made in inertance measurement is minimal. Therefore the excitation direction of the inertance measurement has to be equal to the direction of the accelerometer that has been used in TPA-Form. Additionally the location of the excitation position for the conventional inertance measurement has to be as close as possible to the real excitation position of the shaker. Finally the temperature in operational condition has to be equal to the temperature when the conventional inertance measurement is performed.

In case of the verification measurement setup the conventional determination of inertances should fulfil all requirements. Therefore the error in measured inertance is assumed to be neglectible. **Figure 8** shows a comparison between conventionally measured inertances (full) and inertances that were calculated using TPA-Form. The difference between measured and calculated inertances is less than 3 dB for the considered frequency area.

$$P_{SB\,i}(t) = \square\square\square\square\square\square\square\square\square\square\square\square\square\square\square\square\square\square\cdots\square\square\square\square\square\square\square\square\square$$

$$\begin{bmatrix} \boxed{p_{SB\,i}(f,t_1)} \\ \vdots \\ \vdots \\ \vdots \\ \boxed{p_{SB\,i}(f,t_m)} \end{bmatrix} = \begin{bmatrix} a_1(f,t_1) & \cdots & a_n(f,t_1) & p_{S1}(f,t_1) & & p_{S1}(f,t_1) \\ \vdots & & \vdots & & & \\ a_1(f,t_m) & \cdots & a_n(f,t_m) & p_{S1}(f,t_m) & & p_{S1}(f,t_m) \end{bmatrix} \cdot \begin{bmatrix} S(i,l,f) \\ \vdots \\ S(i,n,f) \\ D(i,l,f) \\ \\ D(i,l,f) \end{bmatrix}$$

i … target microphone position
f … considered frequency
t_l … t_m … considered timeslots
a_l … a_n … considered accelerations
$S(i,j,f)$ … acceleration to pressure sensitivity for target mircrophone i and acceleration j for frequency f

Eq. (1)

$$\frac{\vec{a}_{rec}}{\dot{Q}_{i\ rec}}(f) \equiv \frac{p_{i_{op}}}{\vec{a}_{op}}(f) \cdot \frac{\vec{a}_{op}}{\vec{F}_{op}} = S(f) \cdot \frac{\vec{a}_{op}}{\vec{F}_{op}}(f) = S(f) \cdot I(f)$$

$\vec{a}_{rec}$ … acceleration in reciprocal measurement in direction of $\vec{F}_{op}$

$\dot{Q}_{i\ rec}$ … volume acceleration in reciprocal measurement at target microphone i

$p_{i_{op}}$ … sound pressure level at microphone i in operational condition

$\vec{a}_{op}$ … acceleration in operational condition

$\vec{F}_{op}$ … vector of applied forces in operational measurement

Eq. (2)

$$\begin{bmatrix} \frac{a_{1\,rec}}{\dot{Q}_{1\,rec}}(f) \\ \frac{a_{2\,rec}}{\dot{Q}_{1\,rec}}(f) \\ \frac{a_{3\,rec}}{\dot{Q}_{1\,rec}}(f) \\ \frac{a_{1\,rec}}{\dot{Q}_{2\,rec}}(f) \\ \frac{a_{2\,rec}}{\dot{Q}_{2\,rec}}(f) \\ \frac{a_{3\,rec}}{\dot{Q}_{2\,rec}}(f) \\ \frac{a_{1\,rec}}{\dot{Q}_{3\,rec}}(f) \\ \frac{a_{2\,rec}}{\dot{Q}_{3rec}}(f) \\ \frac{a_{3\,rec}}{\dot{Q}_{3\,rec}}(f) \end{bmatrix} = \begin{bmatrix} I_{11}(f) \\ I_{12}(f) \\ I_{13}(f) \\ I_{21}(f) \\ I_{22}(f) \\ I_{23}(f) \\ I_{31}(f) \\ I_{32}(f) \\ I_{33}(f) \end{bmatrix}^T \cdot \begin{bmatrix} S(1,1,f) & 0 & 0 & S(2,1,f) & 0 & 0 & S(3,1,f) & 0 & 0 \\ 0 & S(1,1,f) & 0 & 0 & S(2,1,f) & 0 & 0 & S(3,1,f) & 0 \\ 0 & 0 & S(1,1,f) & 0 & 0 & S(2,1,f) & 0 & 0 & S(3,1,f) \\ S(1,2,f) & 0 & 0 & S(2,2,f) & 0 & 0 & S(3,2,f) & 0 & 0 \\ 0 & S(1,2,f) & 0 & 0 & S(2,2,f) & 0 & 0 & S(3,2,f) & 0 \\ 0 & 0 & S(1,2,f) & 0 & 0 & S(2,2,f) & 0 & 0 & S(3,2,f) \\ S(1,3,f) & 0 & 0 & S(2,3,f) & 0 & 0 & S(3,3,f) & 0 & 0 \\ 0 & S(1,3,f) & 0 & 0 & S(2,3,f) & 0 & 0 & S(3,3,f) & 0 \\ 0 & 0 & S(1,3,f) & 0 & 0 & S(2,3,f) & 0 & 0 & S(3,3,f) \end{bmatrix}$$

Eq. (3)

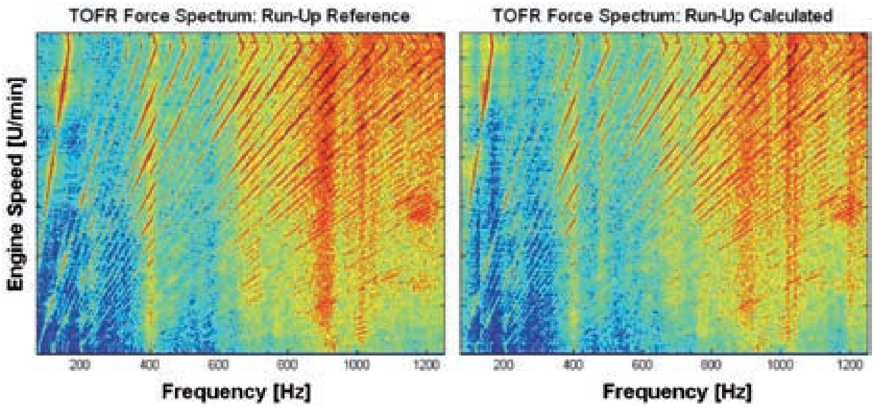

Figure 9: Comparison between measured forces (left) and forces computed by using a full inertance matrix TPA-Form method (right)

6.3 Verification of Induced Forces

In order to quantify the overall influence of deviations between measured and calculated inertances on force calculation, the full inertance matrix method was used to compute forces induced by the shakers in operational condition as a last step. For verification Campbell plots of the force measured in operational condition and the force computed by a full matrix TPA using inertances calculated by TPA-Form are compared in **Figure 9**. It is a comparison between measured forces (left) and forces computed by using a full matrix method (right) containing inertances calculated by TPA-Form.

As can be seen, both diagrams show a very good agreement of measured and computed forces. The TPA-Form method, which was used for determination of the inertances, could be verified with the described experimental set-up and a very positive result.

7 Summary and Outlook

The methodology with TPA-Form described here by AVL allows a significant better description of the transfer behaviour in vehicles as similar methods. Up to now TPA is used in the optimisation of vehicles available in hardware. This not only leads to advantages in common TPA applications but is also a requirement to integrate the TPA into the vehicle development process earlier as before.

For a use of TPA before first prototypes are available, a connection to CAE data has to be accomplished. Thus the advantages of CAE based calculations (simple variant calculation, early use in the development process, no prototype needed, etc.) can be combined with these of TPA (no upper frequency restriction, measurement data verified in hardware, etc.).

The integration of this data leads essentially to two challenges: First, the data transfer has to be realised between the different programs. Second out of theoretical view, the possibly most accurate accordance of induced forces position and induced forces direction between calculation model and measurement is of much higher importance.

This would allow again obtaining important advantages in early development steps. The big benefit of TPA-Form in this frame is an exact matching of force positions and directions acting on the chassis structure. TPA data from previous vehicles can be used in connection with CAE data of a new power train.

First applications in this direction have been performed at AVL and are reported in [6]. With such an approach reliable TPA data can help to predict vehicle interior noise in early development stages where still no hardware is available.

References

[1] Biermayer, W.; Brandl, F.; Höldrich, R.; Sontacchi, A.; Brandl, S.; Fliesser, W.: Sound Engineering based on Source Contributions and Transfer Path Results. JSAE Paper 318 / 20075399, Japan, 2007

[2] Genuit, K.; Sottek, R.; Vorländer, M.; Behler, G.; Kellert, T.: Binaurale Transferpfadanalyse und -synthese. Abschlussbericht, FVV-Vorhaben, Nr. 806, Frankfurt/Main, 2005

[3] Noumura, K.; Yoshida, J.: Method of Transfer Path Analysis for Interior Vehicle Sound by Actual Measurement. JSAE Paper 268 / 20065041, Japan, 2006

[4] Brandl, S.; Priebsch, H.; Brandl, F.; Biermayer, W.; Höldrich, R.; Sontacchi, A.: Challenges and New Solutions for Transfer Path Analysis. ISMA, Leuven, September 15th to 17th 2008

[5] AVL Patent Application: No. 55625 "TPA-Form"

[6] Brandl, S.; Brandl, F.; Pramberger, H.; Zieher, F.: Necessities for CAE Supported Transfer Path Analysis for Vehicle Interior Noise Prediction. JSAE Paper 201 / 20095052, Japan, 2009

Dry Double Clutch Systems

Innovative Components for Highly Efficient Transmissions

Modern double clutch transmissions by Volkswagen are distinguished by high dynamics and low fuel consumption. Transmissions with a dry double clutch are particularly efficient. LuK shows here how to minimize both the drag torque and the power requirement for clutch and transmission operation via an electromotive actuation system.

1 Introduction

Despite the incredible development and investment costs required to launch a new automatic transmission, it is the unit in the powertrain that has gone through the most design innovations in recent years. An important aim was to significantly reduce fuel consumption in automatic vehicles. In addition, innovative transmission designs were intended to win over new customers in the markets and vehicle classes where the share of automatic transmissions was still low. The transmission technology that has most crucially influenced this development is the double clutch transmission (DCT). The first series production, introduced in 2003, was the six-speed transmission as "Direktschaltgetriebe" (DSG), DQ250, by Volkswagen, which was based on an oil-cooled, "wet" double clutch. The potential of this transmission concept in terms of fuel consumption and spontaneity allowed Volkswagen to acquire new market shares and, through the use of the DSG's excellent characteristics, become the driving force for innovations that have been made subsequently in the field of classic automatic transmissions.

It is simply a logical consequence that Volkswagen has implemented a further development of this transmission concept in the form of the seven-speed DCT, which aims to achieve further significant reductions in consumption and extend the possible applications, in particular to engines less than 250 Nm. The core component of the seven-speed DCT DQ200, launched in spring 2008, is the dry double clutch by LuK. It is connected to the combustion engine via a dual mass flywheel and is operated via an engagement system with levers by an electrohydraulic actuation mechanism.

As described in [1], the use of the dry double clutch can improve gearbox efficiency by 6 % in comparison to a wet double clutch transmission. The resulting advantage in fuel consumption is shown in **Figure 1**. One main reason for the improved efficiency is the method of clutch cooling. While dry clutches are cooled by free air convection, a wet clutch requires oil flow adapted to the respective power loss, which is approximately 30 l/min at high outputs, depending on the design. A reduction in the maximum oil volume would lead to a corresponding reduction in cooling losses, but is not permissible from the perspective of robustness. Even when using special clutch facings, the additives in the oil were damaged to such an extent by high temperatures that the requirements in terms of frictional properties could no longer be achieved.

The Authors

Dipl.-Ing.
Uwe Wagner
is Vice President of the Business Unit Transmission Technologies at LuK GmbH & Co. oHG in Bühl (Germany).

Dr.-Ing.
Peter Bührle
is Director of the Product Line XSG in the Business Unit Transmission Technologies at LuK GmbH & Co. oHG in Bühl (Germany).

Dipl.-Ing.
Bruno Müller
is Head of the Department Automation/Actuator in the Product Line XSG at LuK GmbH & Co. oHG in Bühl (Germany).

Dipl.-Ing.
Karl-Ludwig Kimmig
is Head of the Double Clutch Development in the Product Line XSG at LuK GmbH & Co. oHG in Bühl (Germany).

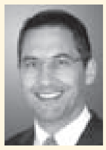

Dipl.-Ing.
Markus Kneissler
is Senior Project Manager in the Product Line XSG at LuK GmbH & Co. oHG in Bühl (Germany).

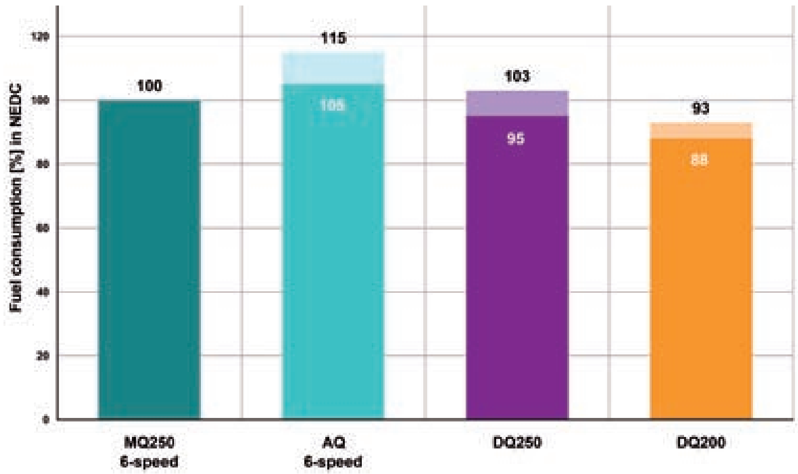

Figure 1: Fuel consumption of the seven-speed DSG (DQ200) in comparison to a manual transmission (MQ250), an automatic transmission (AQ250) and a six-speed DSG (DQ250) by Volkswagen in % (source: Volkswagen AG [1])

2 Requirements of a Double Clutch System

The requirements, in terms of function quality and robustness, in a dry double clutch are disproportionately higher than those of a single clutch in a manual transmission. New safety requirements, greater demands for comfort and operating conditions with higher power, such as power shifts, are the primary reasons for the high demand and lead to the following requirements:

1. self-opening behaviour in the event of transmission control failure
2. high thermal robustness with low weight and limited packaging space
3. high resistance to wear of the friction system and stability of the clutch system characteristic curve
4. compensation of axial and angular offset between the engine and transmission
5. very good isolation against the torsional irregularity coming from the engine
6. powerful and efficient actuation mechanisms for clutches and gears.

Based on experience in the field of single clutches for manual transmissions and automated manual transmissions (AMT), different versions of dry double clutches have been developed at LuK to meet the demanding requirements. **Figure 2** shows the dry double clutch system with arc spring damper and engagement system for the seven-speed DSG by Volkswagen.

2.1 Self-opening Behaviour

The basic design of the double clutch system is driven by the safety requirement that at least one of the two clutches open independently in the event of actuation failure. The “self-opening” design prevents an unintentional overloading of the drive train and thereby the risk of wheel-lock. This can be realised very simply by the use of so-called active clutches in conjunction with non self-locking actuators. In active clutches, the clamping force and therefore the transferable clutch torque is equal to zero, provided there is no or only a low force on the diaphragm spring fingers.

In comparison with a conventionally opened clutch, this results in new boundary conditions for the actuation system and mechanism of the double clutch, yielding a positive impact on the strain of the engagement bearing and the power consumption of the actuation mechanism. **Figure 3** shows the respective time distribution of the bearing loads over a representative driving cycle. An AMT system, such as those offered by LuK in series production, is used as an example for the standard clutch. In both systems, the clutch torque permanently tracks the engine torque in order to improve comfort and the dynamics of the system. In terms of efficiency, this difference in the clutch design can be disregarded as the mean power consumption of the complete clutch and transmission actuating mechanism, as shown in Section 2.6, is only approximately 20 to 25 W.

2.2 Thermal Robustness

As the steady-state cooling capacity of a dry double clutch is lower than that of a wet clutch, more thermal mass for temporary storage of the heat is required. Dissipation of the majority of the heat energy generated during high energy situations, such as launching on a grade, is primarily driven after the event by convection in the clutch housing.

The thermal masses are provided in the form of the pressure plates. It has been shown that the increased rotating inertia, resulting from the required heat capacity, is approximately equivalent to that required for isolation of excitations coming from the engine. In wet clutches, which seem to have the advantage of smaller rotating masses, added inertia or rotating mass must be installed in the dual mass flywheel.

To reduce power losses due to slip when launching, first gear in double

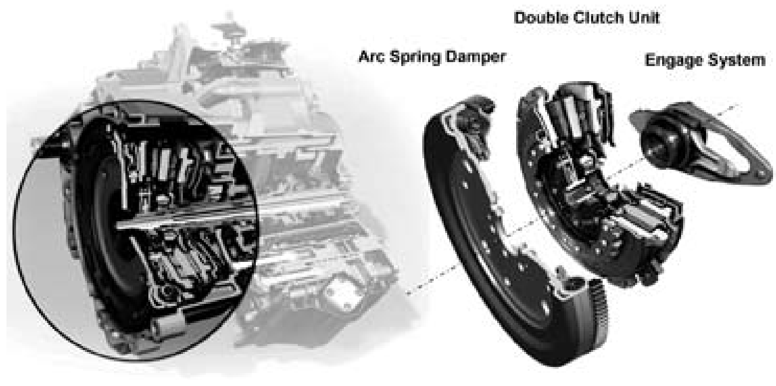

Figure 2: Dry double clutch system of the seven-speed DSG by Volkswagen (source: Volkswagen AG)

clutch systems with dry clutches is shorter. A positive side effect is the increased starting torque even at a low starting speed, similar to the behaviour of a torque converter, which is sometimes also used in transmissions with a wet double clutch [2]. With the corresponding spread and graduation of the gears, there is no negative result in terms of consumption, as shown by the seven-speed DSG by Volkswagen.

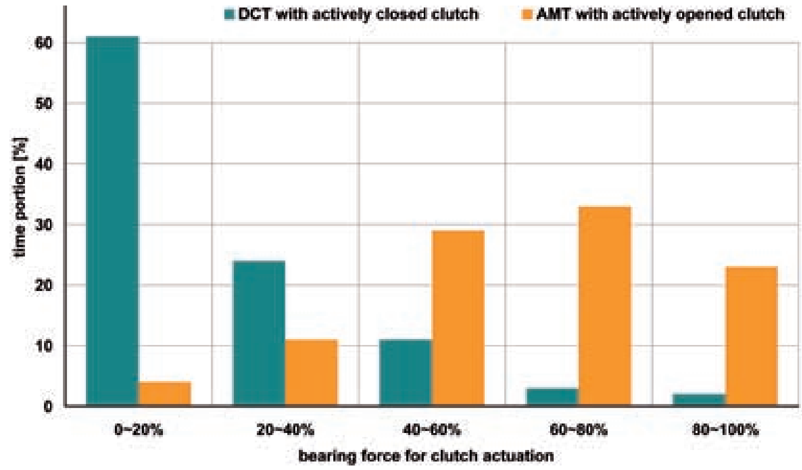

Figure 3: Distribution of the bearing forces for systems with torque tracking in a representative cycle

2.3 Wear Resistance and Characteristic Curve Stability

A dry double clutch is designed to be service-free over the entire service life of the transmission. In comparison with manual transmissions, the increased load caused by power shifts with simultaneously increased shifting frequency results in further exacting requirements on the clutch facing material. For this reason, special facings were developed, which exhibit greater thermal and mechanical robustness, yet maintain very good frictional characteristic stability.

In addition, when compared to a clutch in a manual transmission, the wear reserves per clutch are increased by around 20 – 50 %. To maintain a stable characteristic curve, a refined adjustment mechanism is required. Depending on the design of the clutch actuation, load adjusted and travel adjusted systems are available, **Figure 4**.

2.4 Compensation of Axial and Angular Offset

Clutches for manual transmissions are bolted onto the crankshaft via the flywheel. The release force required for actuation is supported directly via the flywheel on the crankshaft. As double clutches have a significantly longer axial design and the total actuation forces in the two clutches can be very high, direct connection and positioning on the crankshaft is not possible. Therefore, the dry double clutch is supported radially and fixed axially on the transmission's hollow input shaft with a support bearing. One of the resulting advantages is that the double clutch system can be tested as a complete system after installation in the gearbox.

To reduce potential NVH sources, the connection between the flywheel with arc spring damper and the double clutch is a pre-stressed spline. The connection of the double clutch to the floating flange of the arc spring damper ensures the axial and angular offsets can be compensated. When using a solid flywheel, the offset must be compensated by a corresponding device in the double clutch.

2.5 Torsional Vibration Isolation

Modern combustion engines, with increased torsional irregularity and rising demands for comfort, generally set high requirements for the vibration isolation of damper and clutch systems. The damping requirements for a double clutch transmission are further increased due to two primary factors. Firstly, the efficiency of the gearbox has been increased, leading to a decrease in gearbox damping. Secondly, one complete gear set is always unloaded. The result is that the unloaded gear set can be caused to vibrate via the active gear set.

To optimise isolation behaviour, simulation models, **Figure 5**, were developed, which take into account both the transmission and the connection to the engine and drive train suspension. As with uses in manual transmissions, an external arc spring damper has proven useful for drive train isolation. A torsional damper in one of the two clutch disks can also be useful for damping of vibration modes specific to double clutch systems. For applications with non turbocharged petrol engines, the use of damped clutch disks in combination with targeted adjustment of clutch slip instead may be sufficient.

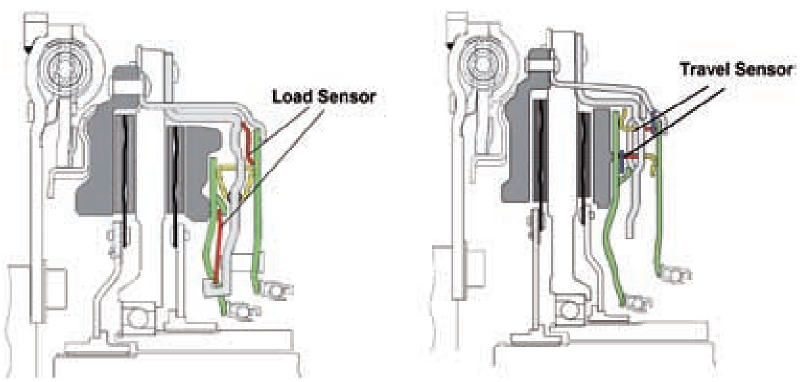

Figure 4: Cross-section of a double clutch with load adjusted clutch (LAC, left) and travel adjusted clutch (TAC, right)

2.6 Efficient Actuation

The requirements of an actuating mechanism to operate a dry double clutch are very demanding. Dynamics, accuracy, durability, efficiency, packaging space and weight are all high on the list of specifications.

2.6.1 The Lever Actuator

For its seven-speed DSG, Volkswagen developed a very compact and efficient hydraulic control, in which the actuation pressures are generated with an electric motor and are switched and regulated via corresponding control valves. An alternative to the electrohydraulic actuation is an electromechanical actuation mechanism, as developed by LuK, in the form of the lever actuator, illustrated in **Figure 6**. The actuator consists of electric motor, counter spring, ball screw drive, track roller and engagement lever.

With this actuating concept, the forces required to close the clutches are essentially generated by a spring accumulator in the actuation mechanism. The forces from the spring accumulator act against the outer end, or upper end, of the engagement lever. The lever ratio is determined by the position of a ball screw drive, which is driven by an electric motor fastened to the gearbox housing. Through the special design of the lever geometry, a variable ratio between electric motor and clutch can be realised so that the electric motor can be operated at as constant and low a power level as possible. This can significantly reduce the required electric motor size.

As standard production elements for translation of electric motor rotation into the linear displacement do not meet the requirements for power density and efficiency of a double clutch actuation system, a new ball screw drive was developed in cooperation with INA. A four-row design with an internal ball recirculation is used, maintaining a minimal packaging requirement. Further, special rollers were developed, which must be very smooth-running under a bearing force of up to 7000 N.

The electromechanical actuation system offers some advantages over an electro-hydraulic actuating mechanism. In addition to further improved efficiency, the lever actuator can almost be completely integrated in the clutch housing between the bearing lugs, where additional packaging space is not required. In addition, the modularity offers the possibility of separating the development responsibility for clutch actuation from that of gear selection. This allows a transmission manufacturer to purchase the clutch system including actuation mechanism from LuK and develop the gear selection mechanism internally.

2.6.2 The Electric Motor Gearbox Actuation Mechanism

The Active Interlock Actuator by LuK, as shown in **Figure 7**, is an example of an electromechanical gearbox actuation mechanism [3]. The special design of the shift finger allows the preselection and engagement of the gears in both partial transmissions in any combination. The shift finger unit with locking and releasing elements forms the interface to the inner shift system. The gears are engaged by using the shift finger, just as in a manual transmission.

The special feature of this actuator is the locking and releasing elements, which ensure all gears in the partial transmission are free before selecting a new gear in that partial transmission. This simple mechanical protection means eliminates the need for additional sensors for gear recognition and the associated monitoring and safety strategies. In combination with the cost-effective mechanical design this very efficient gearbox actuator together with the above-mentioned clutch actuation complete the entire actuation mechanisms for a dry double clutch transmission.

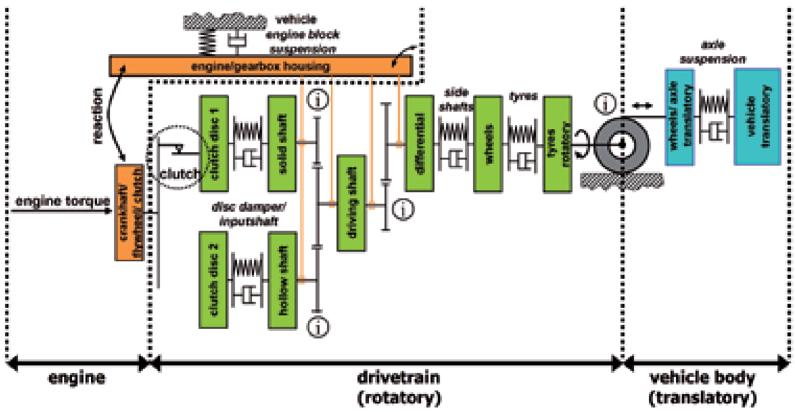

Figure 5: Model for vibration simulation of double clutch transmissions in vehicles

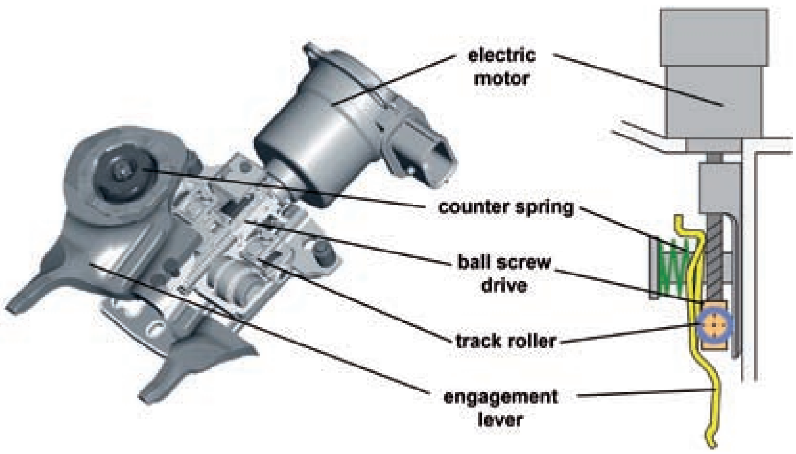

Figure 6: Lever actuator for clutch actuation

3 Summary and Outlook

The seven-speed DSG from Volkswagen has proven that the dry double clutch by LuK can meet all the requirements of a modern automatic transmission. Further applications with dry double clutch-

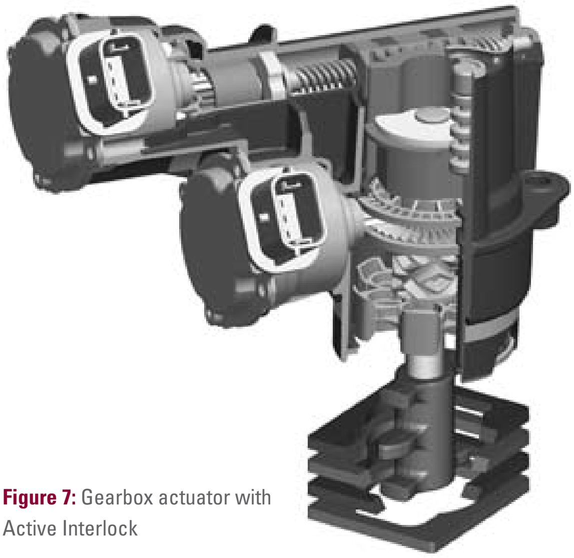

Figure 7: Gearbox actuator with Active Interlock

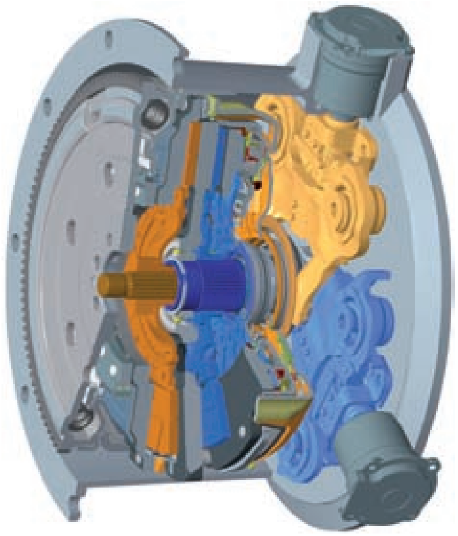

Figure 8: Dry double clutch system with lever actuators

es will soon enter series production. In combination with an efficient actuating mechanism, such as the lever actuator, the dry double clutch transmission is the benchmark in terms of consumption and meets the highest requirements of dynamics and service life, **Figure 8**.

As such a transmission can be actuated independently of the combustion engine due to the electric motor actuation mechanism, it is well suited for hybrid and start-stop operation. In practice, this has already been demonstrated in the „ESG“ demonstrator vehicle by LuK, with an axially parallel E-machine [4]. Such concepts will be used increasingly in future, as shown by the developments made by various transmission manufacturers [5].

In addition to the solutions described for dry double clutches, there will continue to be wet clutches – above all in connection with high vehicle weights and small radial packages. The aim is to minimize losses, in particular through cooling of the clutch. Concepts from dry clutch systems can also be used, such as actuation of wet clutches via engagement bearings [6]. Such a solution allows clutch actuation forces and oil cooling to be separated from each other and therefore carried out with less system energy, **Figure 9**.

The variety of transmission designs is unlikely to decline in future due to the different specifications of the vehicle manufacturers. For long-term success on the market, the benefit for the customer is what counts. The efficiency and therefore the consumption of the transmission in combination with the possibility of converting to hybrid systems will play a crucial role. The double clutch transmission with dry double clutch lays an excellent foundation for the future of automated transmissions in competition with this transmission with wet clutch, torque converter transmissions and continuously variable transmissions (CVT).

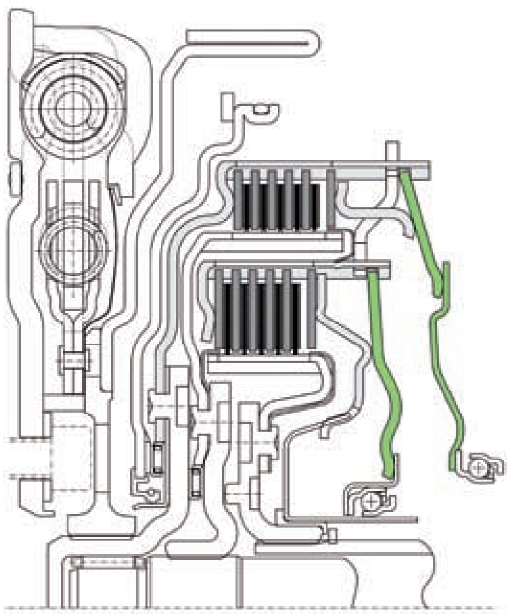

Figure 9: Wet double clutch with engagement bearings

References

[1] Schäfer, M.: Die Steuerung des neuen Doppelkupplungsgetriebes von Volkswagen. Vortrag, 6th International CTI Symposium, Berlin, 2007

[2] Lautenschlager, D. O.; Meffert, P.; Wankum, S.; Hauck, C.; Casper, T.: Innovatives Triebstrangkonzept mit Doppelkupplungstechnologie im neuen Porsche Panamera. VDI-Berichte Nr. 2071, Tagung „Getriebe in Fahrzeugen 2009“, Friedrichshafen, 2009

[3] Wagner, U.; Berger, R.; Friedmann, O.; Esly, N.: Elektromotorische Automatisierung für Doppelkupplungsgetriebe. VDI-Berichte Nr. 1827, Tagung „Getriebe in Fahrzeugen 2004“, Friedrichshafen, 2004

[4] Reitz, D.: ESG – Vom Parallelschaltgetriebe zum Minimalhybrid; VDI-Berichte Nr. 1852, Tagung „Innovative Fahrzeuggetriebe 2004“, Friedrichshafen, 2004

[5] Faust, H.: Contribution of Transmission to Fuel Efficiency and CO2 Emission Improvement. Getrag Drivetrain Forum, Cologne, October 2008

[6] Reik, W.: Die Kupplung, das Herz des Doppelkupplungsgetriebes – Ein Blick in die Zukunft. 5th International CTI Symposium, Berlin, 2006

Next-generation Ejector Cycle for Car Air Conditioning Systems

With increasing demand for energy-saving technologies, Denso develops highly efficient air conditioning systems. One of the newly developed technologies is an ejector cycle. The ejector is a fluid pump that converts expansion energy, which is lost in the conventional refrigeration cycle decompression expansion process, into pressure energy to help reduce compressor power. Denso introduced the first air conditioning system using this technology with an ejector-integrated evaporator.

1 Introduction

As reports of the accelerating pace of global warming grow, countries and regions around the world are focusing on ways to reduce CO_2 emissions and raise awareness of environmental issues, including tougher emission regulations. And it is working.

When consumers begin the process of purchasing a car, they are more seriously considering environmental performance, such as emissions and fuel economy, in addition to things like driving performance and safety. As a result, sales of vehicles with excellent environmental performance, such as fuel-efficient and cleaner-emission diesel engine vehicles, hybrid vehicles, and compact vehicles, have steadily risen. To comply with tougher regulations and meet market needs, automakers are accelerating the development of more environmentally friendly vehicles.

In Europe, a new regulation set by the European Union in 2007 will reduce the total amount of CO_2 emissions to 120 g/km or less for new vehicles introduced from 2012.

2 Ejector Cycle

For years, Denso has been committed to developing energy-saving air conditioning systems in anticipation of the growing need for higher efficiency. One of the products resulting from these efforts is an ejector cycle (Ejecs I), in which an ejector is used in the refrigeration cycle. In 2003, it has been introduced in a R404A truck-transport refrigerator, as well as in a hot-water system for household use, using CO_2 as the refrigerant.

2.1 What is an Ejector?

The ejector is a fluid pump that recovers expansion energy, which is lost in the conventional refrigeration cycle decompression expansion process, and converts the recovered expansion energy into pressure energy (pressure-rising effect). Accordingly, the ejector helps to reduce the compressor power, thereby improving the refrigeration cycle efficiency. The ejector is comprised of a nozzle, mixing section, and diffuser, **Figure 1**.

The high-pressure refrigerant flowing into the nozzle (drive flow) undergoes decompression and expansion by the nozzle. Specifically, in the nozzle, the fluid pressure energy including the conventionally lost expansion energy is converted into kinetic energy through the decompression expansion process and accordingly the refrigerant flow velocity increases while the refrigerant pressure decreases. The refrigerant pressure after the decompression expansion process is lower than that of an intake flow at an intake section, allowing the intake flow to be drawn into the mixing section. After that, in the mixing section, the drive flow and the intake flow are mixed to create a homogenous mixture, and in the diffuser having a gradually enlarging passage, the kinetic energy is reconverted into pressure energy so that the refrigerant flow velocity decreases and the refrigerant pressure increases. Thus, the ejector is designed to efficiently perform these conversion processes, and the fluid's velocity changes significantly in the ejector due to its design. During the velocity change, the fluid is accelerated from walking speed (1 m/s to 2 m/s) to the supersonic speed (100 m/s to 200 m/s), a level comparable to a jet plane in the nozzle, and then decelerated to the speed

The Authors

Naohisa Ishizaka
is Engineer, Thermal Systems R&D Dept. at Denso Corporation in Aichi (Japan).

Kohei Rokushima
is Group Leader, Thermal Systems R&D Dept. at Denso Corporation in Aichi (Japan).

Yoshiaki Takano
is Senior Manager, Thermal Systems R&D Dept. at Denso Corporation in Aichi (Japan).

Aung Thuya
is Engineer, Heat Exchanger R&D Dept. at Denso Corporation in Aichi (Japan).

Tomohiko Nakamura
is Group Leader, Heat Exchanger R&D Dept. at Denso Corporation in Aichi (Japan).

Dr. Hideaki Sato
is Chief Engineer, Heat Exchanger R&D Dept. at Denso Corporation in Aichi (Japan).

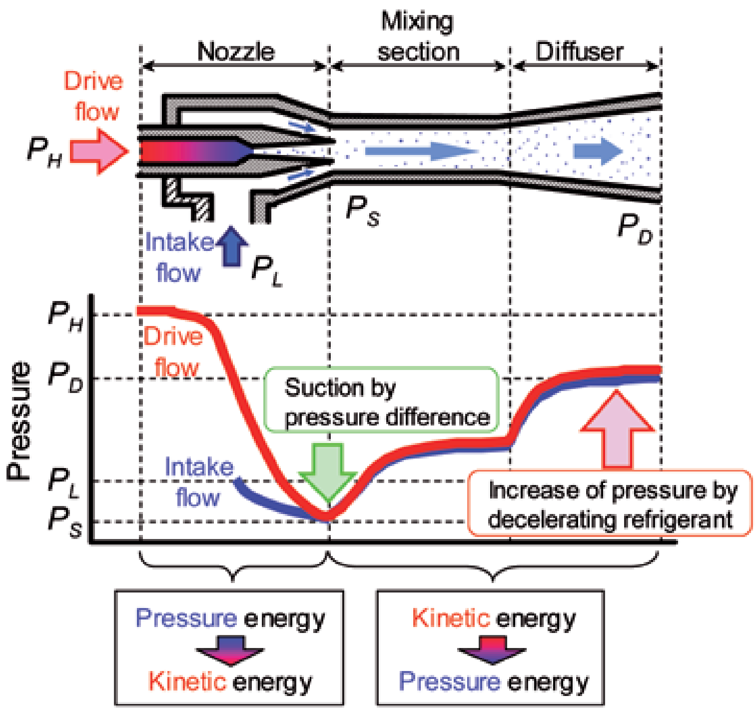

Figure 1: Ejector operating principle

of a vehicle (20 m/s to 30 m/s) in the diffuser.

2.2 What is Ejecs I?

Ejecs I is a refrigeration cycle comprised of a compressor, condenser, expansion valve (TXV), evaporator, ejector, and accumulator, **Figure 2**. The two-phase refrigerant discharged from the ejector is separated into gas and liquid refrigerant in the accumulator. The liquid refrigerant flows into the evaporator to evaporate, and then returns to the ejector, while the gas refrigerant flows into the compressor. Thus, the refrigeration cycle has two refrigerant circulation paths: a high-pressure path driven by the compressor power and a low-pressure path driven by the ejector's suction force.

3 Challenges and Breakthroughs

The biggest difficulty in applying the ejector cycle to a car air conditioning system was building it into a limited space of a vehicle. In the case of the truck-transport refrigerator, the functional components that comprise the refrigeration cycle are installed above the driver's cabin in the form of a single unit. The accumulator and the ejector are placed inside the package. The height of the accumulator and the length of the ejector are approximately 300 mm each. Because of installation space restrictions in passenger cars, the system had to be made much simpler and smaller. To solve this problem, the next-generation ejector cycle II (Ejecs II) and the ejector cycle system (ECS) evaporator that integrates an ejector and evaporator into one unit have been invented.

3.1 Invention of Next-generation Ejector Cycle

Figure 3 shows the schematic diagram of the refrigeration cycle of the second generation. In Ejecs II the two-phase refrigerant discharged from TXV is distributed into the ejector and a capillary tube. The refrigerant discharged from the capillary tube (intake flow) is evaporated in the downwind evaporator and then returns to the ejector. The refrigerant discharged from the ejector (drive flow) joins the intake flow in the mixing section, and then flows together into the upwind evaporator to evaporate.

3.1.1 Features and Focus

The ejector cycle of the second generation differs from the first generation in the following major aspects:

1. In Ejecs I, the accumulator, placed on the low-pressure side, serves two purposes: It acts as a liquid reservoir for the two-phase refrigerant from the ejector to stabilise the cycle, and it serves as a separator, separating gas and liquid refrigerant and distributing them to the compressor and evaporator. In Ejecs II, the accumulator is placed on the high-pressure side, allowing the modulator tank of the subcool condenser to serve as a liquid reservoir. The second generation is also designed so that the high-pressure two-phase refrigerant is distributed into the ejector and the capillary tube. These design modifications allowed elimination of the accumulator.

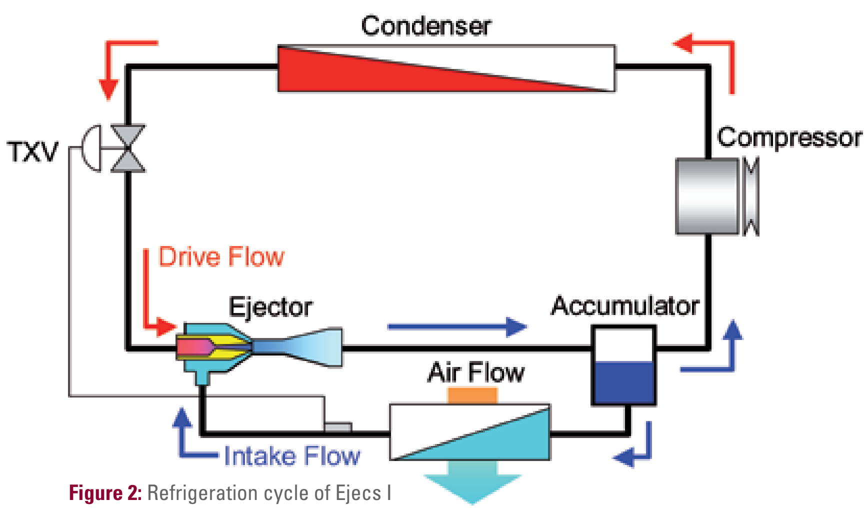

Figure 2: Refrigeration cycle of Ejecs I

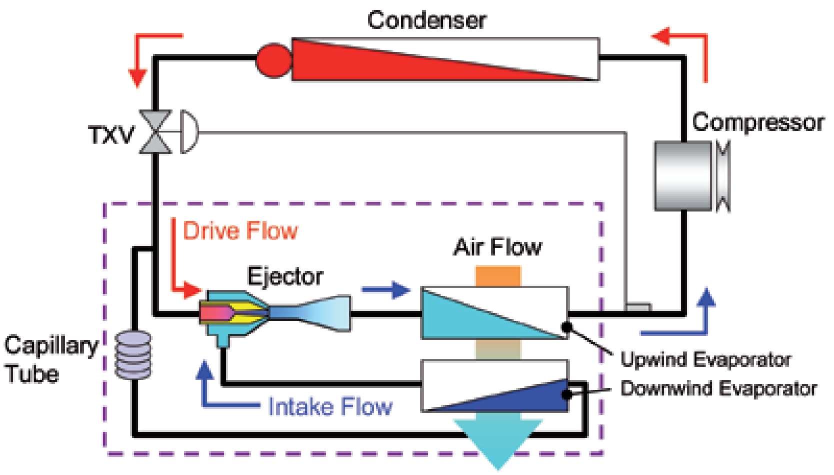

Figure 3: Refrigeration cycle of Ejecs II

2. Because the refrigerant from TXV is distributed to the ejector and the capillary tube, the refrigerant mass flow flowing through the nozzle can be reduced compared to that in the first generation, enabling a reduction in size of the ejector.

3.1.2 Performance Improvement Principle

As shown in **Figure 4**, the ejector cycle II improves the Coefficient Of Performance (COP) of the refrigeration cycle in the following major aspects:

1. The ejector pressure-rising effect (ΔP_{eje}) reduces the compressor power (Δh_{ir}).
2. The ejector pressure-rising effect (ΔP_{eje}) generates the additional cooling capacity (Δh_{ir}).
3. The refrigerant mass flow flowing through the downwind evaporator can be reduced, thereby decreasing the loss in pressure of the refrigerant (ΔPe).
4. The compressor efficiency increases due to the decrease in compression ratio.

3.2 Development of ECS Evaporator

The significant modification of the refrigeration cycle and improvement of the COP could have been achieved by developing the ejector cycle of the second generation using an installation package, in which the ejector and the capillary tube are located outside the evaporator and connected with pipes each other. However, this original package was difficult to be installed in a vehicle, because of additional parts including the ejector and the capillary tube. To solve this problem and help achieve mass-production, the ECS evaporator has been developed in which the evaporator, ejector, capillary tube, and connection pipes (components surrounded by dashed line in Figure 3) are integrated into one unit.

3.2.1 Exterior View and Size

The ECS evaporator looks almost identical to Denso's conventional evaporator, although it integrates all the modifications required for the ejector cycle II. This means that the ECS evaporator is perfectly compatible with the conventional evaporator, and the conventional air conditioning system can easily be modified into Ejecs II just by replacing the evaporator. To achieve this, a small, highly efficient ejector and a new structure for the evaporator have been developed.

3.2.2 Small, Highly Efficient Ejector

To integrate the ejector and the evaporator, the development engineers focused on a new concept placing the ejector inside the evaporator tank. Since the pressure applied to the ejector is smaller when placed inside the evaporator tank, compared to when located outside the evaporator, the ejector can have thinner walls and lighter weight. This significant size reduction and efficiency improvement of the ejector could have been achieved by thoroughly optimising the dimensions. As a result, the length of the new ejector for the ECS evaporator is reduced to approximately 150 mm, half the length of the ejector for the truck-transport refrigerator, and the volume is reduced by approximately 90 %.

Further, the suction inlet from the conventional single inlet suction configuration has been modified to a 360° inlet configuration to improve suction efficiency. Also a robust design for the noz-

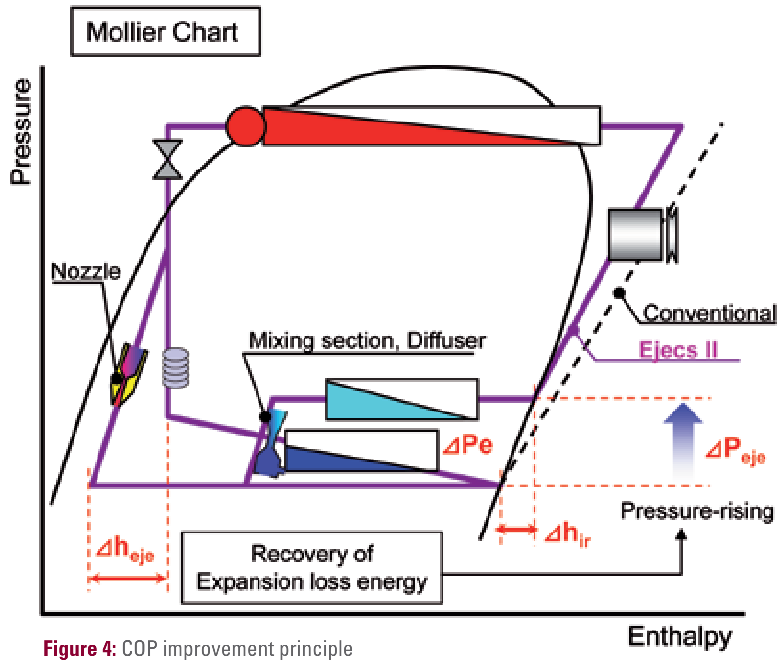

Figure 4: COP improvement principle

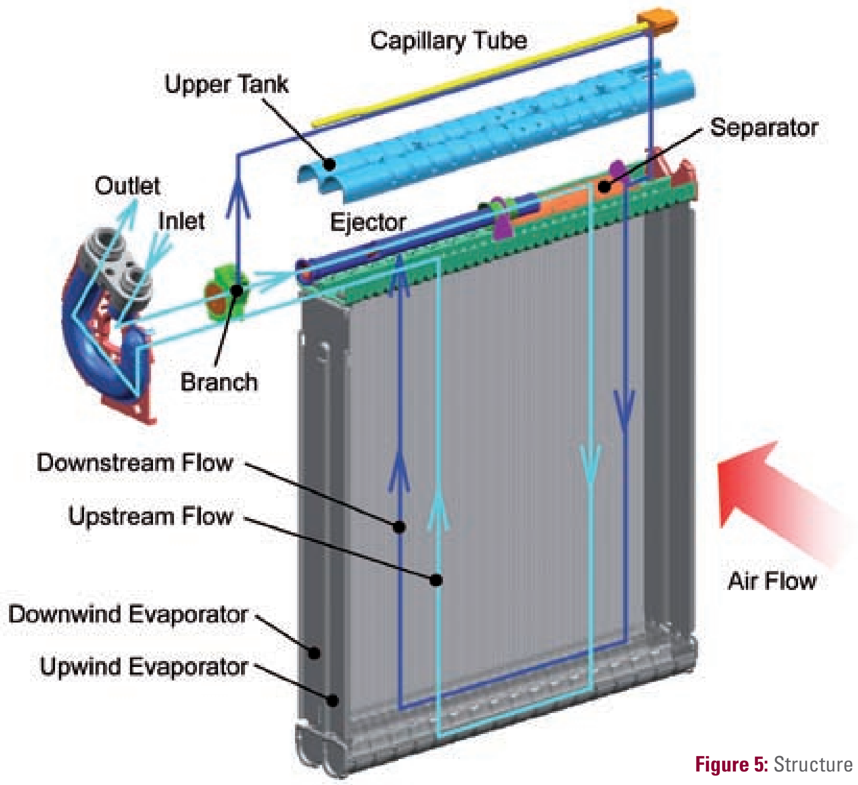

Figure 5: Structure and refrigerant paths of ECS evaporator

zle configuration has been employed in order to ensure the ejector's pressure-rising performance throughout the operating range of the air conditioning system.

3.2.3 Internal Structure and Refrigerant Paths

Figure 5 shows the internal structure and the refrigerant paths of the ECS evaporator. The newly developed ejector is placed inside the upper tank of the downwind evaporator, and the upper tank of the downwind evaporator at the ejector outlet side is partitioned into upper and lower spaces by a separator. With this two-level structure, the refrigerant from the ejector flows into the upper space of the upper tank and then into the upwind evaporator through communication holes. Meanwhile, the refrigerant from the capillary tube flows into the downwind evaporator through the lower space of the upper tank.

4 Effects in Saving Compressor Power and Reducing Fuel Consumption

Figure 6 shows the compressor power-saving and fuel consumption improvement effects when the ejector cycle of the second generation with the ECS evaporator is used in a car air conditioning system. When a car is stationary with an ambient temperature in the range of 25° C to 40° C, compressor power can be reduced by approximately 10 % to 25 %. The fuel consumption of a vehicle can be improved by 1.5 % at an ambient temperature of 30° C.

5 Conclusion

Ejecs II is an environmentally friendly technology that can improve fuel consumption by reducing compressor power. The ejector cycle II, using the ECS evaporator, has been installed on passenger cars since May 2009, and Denso will continue working to improve its efficiency in an effort to establish it as the de-facto standard for energy-efficient car air conditioning systems in the future.

Since the ejector can be adapted to all refrigeration cycle systems, it has great potential for a variety of refrigeration and air conditioning applications to help prevent global warming. ■

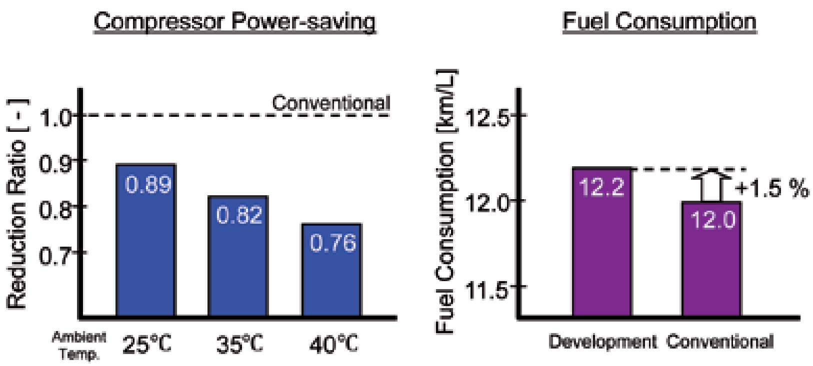

Figure 6: Effects of Ejecs II with ECS evaporator in vehicles

Special AVL

The Chassis Dynamometer as a Development Platform

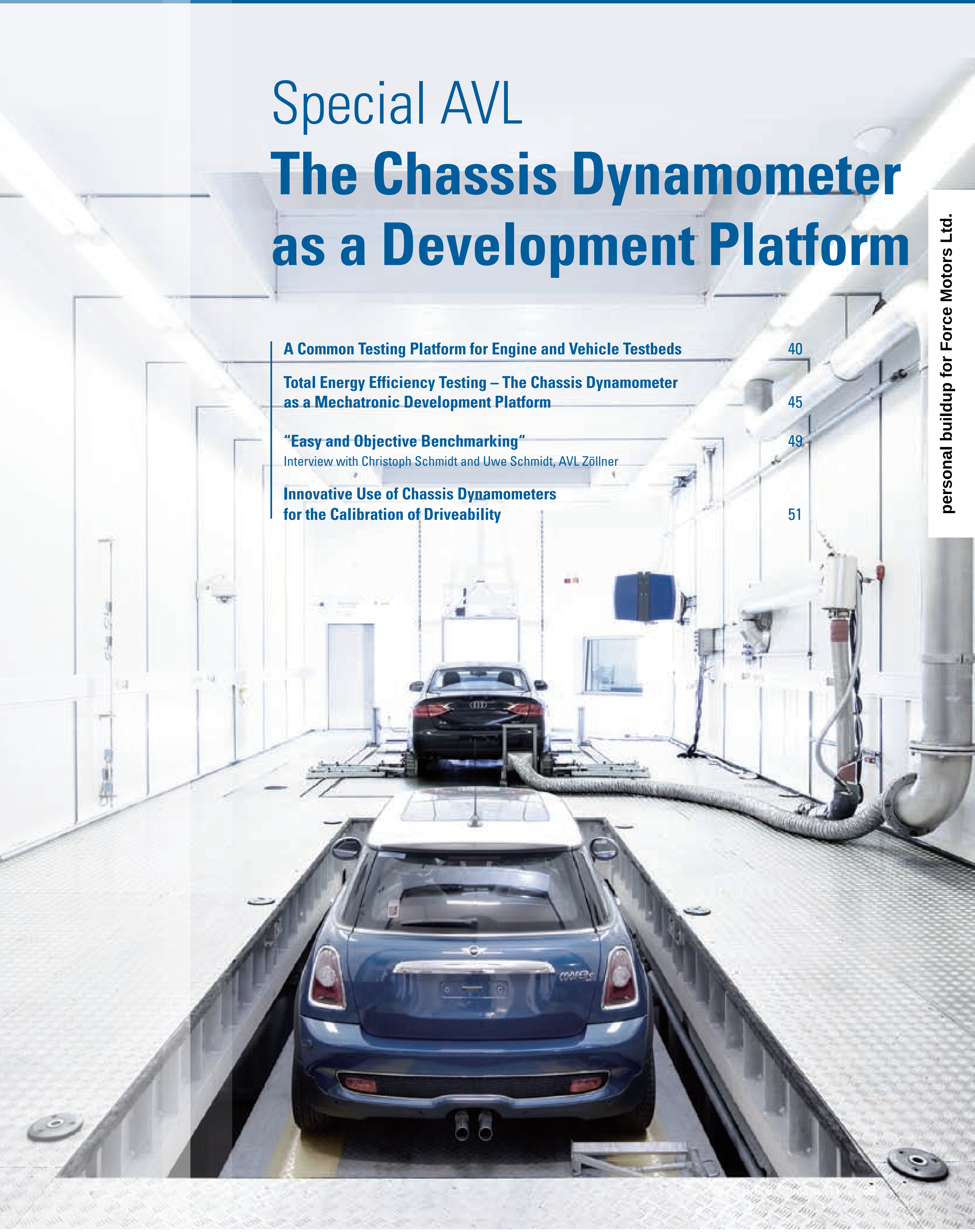

A Common Testing Platform for Engine and Vehicle Testbeds

In order to achieve time-savings during vehicle development, companies are increasingly looking to run the same tests on the engine test bed as on the chassis dynamometer. The aim is to correlate results in order to highlight differences and their influencing factors, as well as to verify the engine test bed results, and to achieve the additional benefit of reusing existing tests. A common test automation and data platform is required. The article describes an application in which this has been achieved for emissions certification testing and discusses the value of upgrading the chassis dynamometer to a higher level of automation.

1 The Synergies between Engine, Driveline and Vehicle Testbeds

The product development processes at OEMs and the component development process of tier 1 suppliers rely on extensive testing phases of the different powertrain components and of the complete vehicle. The testing is carried out using various types of test benches: hardware-in-the-loop benches, component testbeds, engine testbeds, driveline testbeds and vehicle testbeds. Finally, fleet testing of prototypes takes place on the test track or road for the final adjustments.

In each of these test environments, various testing tasks are carried out. For instance, an engine testbed is used during the development phase to verify the engine durability and its thermodynamics. It is also used to set up the base calibration of the ECU and predict the engine emission behavior using vehicle simulation.

The OEMs are coming under ever-increasing pressure to reduce the time to market of new vehicles while saving on development costs. This translates into a need for an efficient and shorter product development process. A key element in reducing development time is front-loading the testing of vehicle characteristics earlier in the process. Front-loading not only allows time-savings and a reduction in the number of vehicle prototypes needed; it also supports a reduction of development costs by addressing unplanned design changes much earlier in the process in a cost-efficient manner, as the later a component failure is detected the more expensive the fixing will be.

However, this requires a state-of-the-art development tool chain that fulfils the following requirements:

- the ability to accurately simulate the missing vehicle components on the testbed (e.g.: the vehicle powertrain on an engine testbed)
- the ability to reproduce environmental conditions realistically
- the ability to support iterative development loops efficiently between the different stages of the process.

This last point is the key for delivering the desired efficiency improvements since it must allow the correlation of similar testing tasks carried out at different stages in the process for the purpose of validating results obtained using simulation, or to comply with legislative requirements.

For example, emission tests are carried out on an engine testbed and repeated on the vehicle testbed for certification; drivability assessment and powertrain calibration optimization are carried out on engine, driveline and vehicle testbeds and verified later in the vehicle on the road; climatic testing takes place on the engine testbed and again later on the vehicle testbed; durability testing takes place on the transmission testbed and again later on the road or on the vehicle testbed, **Figure 1**.

One well-known way of facilitating the correlation is the use of a common simulation platform which also avoids the need to develop and maintain multiple models.

Another source of productivity gains is the use of a common automation platform across all types of testbeds.

2 The Common Automation Platform

The automation test system can be split into three different layers in terms of software functions, **Figure 2**:

The Authors

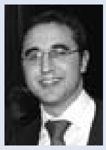

Charles Kammerer MSc. is Product Manager for Test System Automation at AVL List GmbH in Graz (Austria).

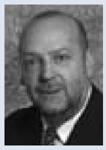

Roland Schmidt is Head of Application Development for Test Instruments and Systems at AVL Emission Test Systems GmbH in Gaggenau (Germany).

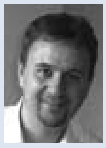

Ing. Gerald Hochmann is responsible for the Application of Engine Test Systems at AVL List GmbH in Graz (Austria).

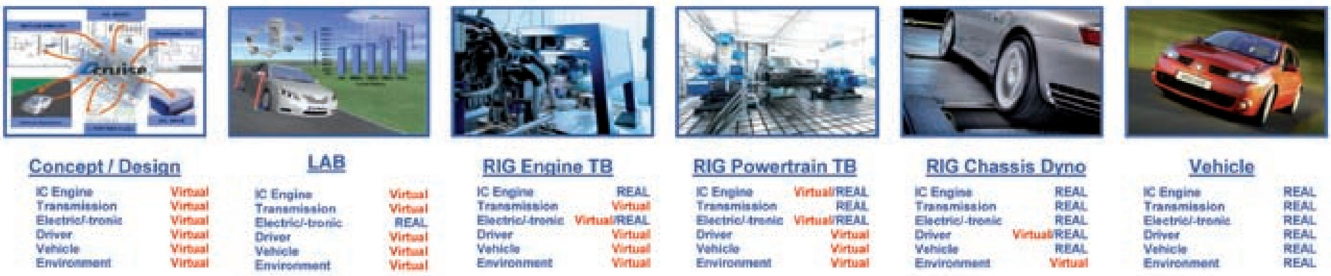

Figure 1: Simulation across the product development process

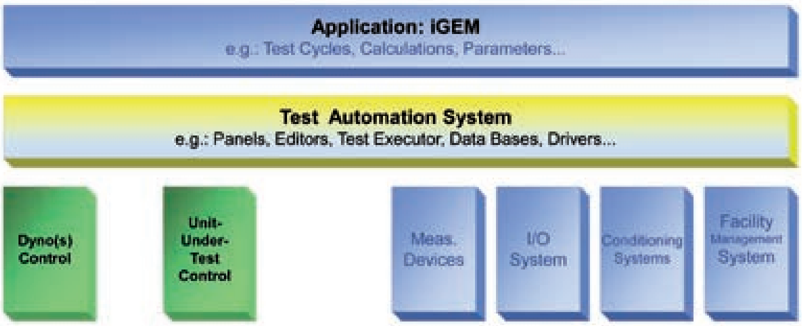

Figure 2: The architecture of a common automation platform

- the controller – for testbed and unit-under-test control
- the test automation system (TAS) – for data acquisition and test automation
- the application (e.g. an emission test run such as FTP 75).

If the controller is specific to the different types of testbed, the TAS is not. Therefore, provided consistent system architecture on engine, driveline and vehicle testbeds, the same TAS can be used on all types of testbeds and, if it successfully abstracts the application from the controller, the application is then portable from one type of testbed to another.

Being able to port the application from one testbed type to another allows the synergy potential between the different testing steps of the product development process to be efficiently leveraged. Result data can be correlated, test specifications can be reused (e.g.: shift quality and drivability assessment on a powertrain testbed and on a vehicle testbed). Parameters can also be reused (e.g.: vehicle parameters for the simulation on an engine testbeds and the parameters for the chassis dynamometer).

In addition, significant benefits can be derived from the effects of scale and standardization, which contribute to reducing the total cost of ownership of the TAS.

For instance, the "one window" approach reduces training needs and maintenance costs; a common data handling and IT infrastructure is used across the whole product development process; common process management tools are used across the whole product development process for scheduling, equipment management and supervising.

While the need for vehicle testbeds may have been challenged by front-loading many testing tasks, its use remains more crucial than ever for verifying the results obtained earlier in the process while also enabling the execution of traditional in-vehicle activities in a more deterministic manner in a testbed environment rather than on the road. One example is the shift quality and drivability assessment application. Being able to automate such an application on a vehicle testbed may bring significant productivity gains and address the increasing effort required for transmission calibration.

All this requires the vehicle testbed TAS to be able to: transfer testruns and correlate test results between the engine and the vehicle testbeds (e.g.: for emission testing); transfer testruns and correlate test results between the driveline and the vehicle testbeds (e.g.: for powertrain calibration optimization); transfer road profiles recorded in the vehicle and replicate them on the vehicle testbed (e.g.: for endurance testing); provide the frameworks and interfaces to the calibration tool chain (e.g.: automatic calibration software, direct access to the xCU and the application systems); provide the connectivity to the vehicle testbed subsystems (e.g.: dynamometer, emission benches, driver-robots, measurement devices, in-vehicle buses, facility and conditioning systems).

Up to now, automation of the chassis dynamometer was often limited to data acquisition while the testbed control was left to the chassis dynamometer controller and the human driver or robot system. However, to fulfill the above requirements, one requires a TAS for the vehicle testbed which is able to fully automate the testbed and provide the required compatibility with the TAS of other testbed types in terms of architecture and data formats.

3 The AVL Solution

AVL's solution is to use PUMA Open as the automation platform for rig testing: from the component testbed to the engine, powertrain and vehicle testbed. While PUMA Open is well-known and well-established as the TAS for component, driveline and engine testbeds, its extension to vehicle testbeds was required to fulfill the requirements of a common automation platform.

Thanks to its modular design and its scalability, PUMA Open can be tailored for a wide range of vehicle testing applications, from simple data logger to ad-

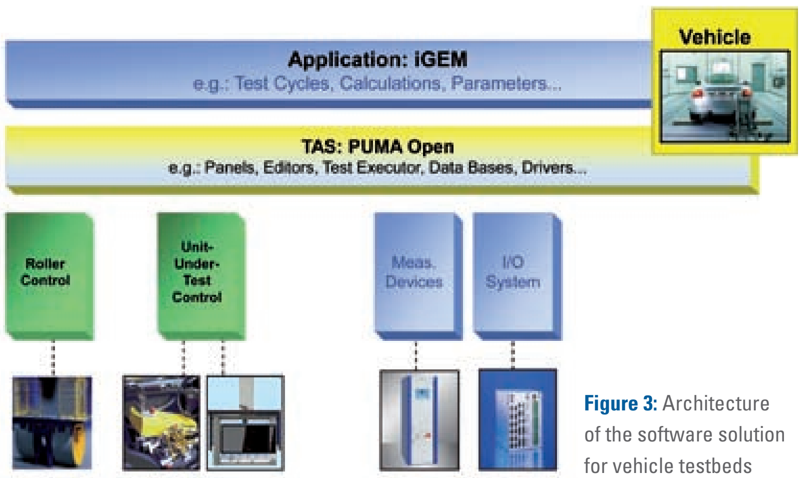

Figure 3: Architecture of the software solution for vehicle testbeds

Table: Automation of the vehicle test bed with PUMA Open

Data acquisition	PUMA Open supports industry-standard bus technology such as CAN, Profibus or FireWire and state-of-the-art ASAM compliant interfaces for ECU/TCU application and diagnostic systems (MCD3MC and MCD3D) or for automatic calibration tools (ACI).
Real-time execution	The parameterization of a test run is made easy through a graphical block sequence editor, thus avoiding the need for programming skills. Even complete road profiles can be directly imported in the test run enabling a real-time replication of road data. The real-time platform makes it also possible to carry out residual bus simulation, very much needed for development activities.
Real-time monitoring	Not only limited to channel monitoring with user-definable reactions, PUMA Open also features advanced monitoring functions such as reference cycle monitoring or online classification which makes it easy to analyze the behavior of a particular vehicle along its entire testing life.
Integration	Due to the availability of numerous device drivers, standard measurement devices, such as fuel meter or emission benches, can be easily connected to the TAS and their control and operation synchronized with the test run execution. Also, PUMA Open features a Configurable Device Handler which allows the user to connect any AK-based device using a wizard to create a dedicated driver. In addition, through a state-machine based real-time Test Cell Controller, conditioning systems such as fuel filling devices, environmental control systems and other PLCs can be closely integrated and controlled by the application, thus guaranteeing an accurate control of the test conditions.
Result evaluation	Using ASAM-ODS as a data backbone results can be centralized on a data HOST shared between different testbeds or test fields making the results available not only on the testbed but also in the office for evaluation and automatic report generation.
Data integration	The PUMA HOST system provides a central data repository for all parameters: vehicle parameters, robot vehicle specific configurations, test runs and test profiles, etc. The key benefit of centralization is the ability to start a test on one vehicle testbed and finish it on another one, transferring automatically all the necessary information and appending the results as appropriate.

vanced powertrain calibration optimization, while bringing its demonstrated performance and high level of automation on to the vehicle testbed.

3.1 Integration with the Chassis Dynamometer Controller

Depending on the application and the level of automation required, a close integration of the chassis dynamometer controller with the TAS may be required. For applications such as emission certification, where the chassis dynamometer is mostly used in road-load simulation mode, the AK interface provided by PUMA Open allows it to be connected to chassis dynamometers from various manufacturers without the need for complex integration.

However, for applications where a number of different control modes must be used and a dynamic switch between them is required, a closer integration of the chassis dynamometer controller with the TAS is needed. This is achieved through a high performance interface between the AVL Zoellner chassis dynamometer controller, VECON, and PUMA Open, **Figure 3**.

VECON is the latest version of AVL Zoellner's controller software. It leverages the same technologies used by other AVL software, in particular running all its advanced control algorithms under the AVL Real-Time Environment (ARTE) thus providing stunning control performance in terms of speed, accuracy and stability. Combining VECON with PUMA Open through a real-time interface allows the same degree of automation and dynamic control performance to be achieved on a vehicle testbed as on an engine or driveline testbed – especially raising the repeatability and reproducibility of tests on the vehicle testbed. These performance gains are a must for new innovative applications on the vehicle testbed: drivability assessment, TCU calibration optimization or maneuver based testing using advanced road & driver simulation. Thanks to a generic dynamometer interface via hybrid or Profibus DP to the cabinet, the combination of VECON and PUMA Open can also be used to modernize existing chassis dynamometers while keeping the required investment low.

3.2 Control of the Vehicle

Here again, various set-ups are possible depending on the application. In case of a human driver, like for emission certification, PUMA Open transfers the profile to be executed to the drivers-aid and synchronizes its execution with the data acquisition and the device control tasks. Having the TAS as the master for the profile execution guarantees a perfect synchronization between profile execution, data acquisition and control & commands sent to devices and subsystems.

If the vehicle testbed is fully automated like on a mileage accumulator, PUMA Open integrates a vehicle controller, EMCON, which replaces the human driver, taking care of throttle, brake and gear selection actuation. The controller is abstracted from the actuation itself which can be realized either through mechanical actuators or using drive-by-wire.

As mentioned above, if the controller layer is testbed specific, the common automation platform demonstrates the exact same automation capability at the TAS level on all types of testbeds. Therefore, PUMA Open on a vehicle testbed provides advanced automation and integration capability, **Table**.

The availability of high level automation functions on the vehicle testbed not only provides the benefits of a common platform from a product development process perspective but also supports the trend towards one-man operation of several vehicle testbeds.

The use of PUMA Open as the integration platform for AVL's chassis dynamometer controller VECON and the robot system centralizes the automation tasks, thus simplifying the overall system architecture and its operation and maintenance. For example, today, the same test profile can be defined in multiple places using different formats and editors: on the driver's aid, the chassis dynamometer controller, the robot driver or the emission automation system. By having one automation system centrally controlling all the other subsystems, the test profile like all other parameters are defined once and stored centrally. This also provides the ability to cover multiple applications with one vehicle testbed: a mileage accumulator, sharing parameters with the costly emission certification testbeds, can be used to carry out so-called prep cycles or, a highly automated NVH vehicle testbed can be used for shift quality optimization.

4 Emission Testing on Chassis and Engine Test Beds

The new emission and test bed automation technology AVL iGEM, **Figure 4**, is used in engine and vehicle development to carry out automated emissions tests and can be used for both light and heavy duty engines, following a common automation platform and seamless data exchange approach.

The iGEM emission automation software comes on top of the common automation platform PUMA Open. The engine test bed automation system as well as the emission equipment fulfils the new US legislation EPA CFR Part 1065.

Thanks to an innovative architecture which enables a complete abstraction of the application from the testbed, the iGEM application packages are fully independent of the testbed type and configuration. The software solution built around PUMA Open consists of the following components:

- iGEM Vehicle on the vehicle testbed
- iGEM Engine on the engine testbed
- graphical editors for test cycles and testruns
- PUMA HOST system: for data centralization
- iGEM Offline for offline emission calculation
- CONCERTO for report generation
- Emission Bench Handler for intelligent emission bench control
- iGeneration Emission Equipment Controller.

On the vehicle testbed, iGEM Vehicle communicates with the chassis dynamometer via the AK interface of PUMA Open. iGEM Vehicle prepares the chassis dynamometer for the test run by setting the chassis test bed parameters such as inertia and road load coefficients retrieved from a central database.

To ensure accurate emission data iGEM Vehicle communicates in 10Hz with the chassis dynamometer controller during the test run. For certification testing by the end of the test run the chassis dynamometer performs a coast down test confirming the right parameter setting.

5 Conclusion

The common automation platform strategy efficiently supports the need for shorter development processes. By bringing the vehicle testbeds closer to the engine and driveline testbeds, it enables significant savings by reusing test specifications, correlating test results and standardizing testing tools and methodologies. But it also significantly increases the capability of vehicle testbeds, making them suitable for relatively new applications, such as shift quality and drivability assessment or powertrain calibration optimization. ■

Figure 4: The PUMA Open automation system with iGEM Vehicle for vehicle emission certification

Total Energy Efficiency Testing

The Chassis Dynamometer as a Mechatronic Development Platform

Individual mobility today implies – in addition to comfort and safety – above all energy efficiency. An energy-efficient vehicle places high demands on automatic control systems because the functions are often divided up on to many controllers and the objectives defined in the requirements specification can only be achieved by means of optimized interplay between the controllers. So the further development of the classical chassis dynamometer into a powerful "vehicle-in-the-loop" test bed as pursued by AVL is a logical consequence. This article describes how a chassis dynamometer becomes a mechatronic development platform and helps automotive engineers to put "green" technology on the road in a cost-efficient and rapid manner.

The Authors

Dr.-Ing. Felix Pfister is responsible for Product Management and the Application "Hardware-in-the-loop" in the Business Segment Hybrid & Battery Testing Technology of AVL List GmbH in Graz (Austria).

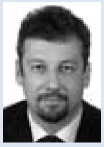

Dr.-Ing. Christian Schyr is Project Manager in the Business Segment Hybrid & Battery Testing Technology of AVL List GmbH in Graz (Austria).

Dipl.-Ing. Franck Le Rhun is Application Engineer in the Business Segment Hybrid & Battery Testing Technology of AVL List GmbH in Graz (Austria).

1 Introduction

The objective of "total energy efficiency testing" is the realistic measurement, assessment and optimization of energy consumption in real-world use by means of development carried out on the test bed. A wide variety of operating and ambient conditions for the following tasks have to be considered here:

- What is the real consumption of the vehicle in comparison with the statutory cycle?
- What consumption is measured in the tests by the popular press and the technical press? What measures enable a good rating here? For tests carried out by automotive journalists, such as the consumption group of "auto motor und sport", great importance is attached to real consumption, and therefore it is an important criterion for deciding what vehicle to buy [1].
- What are the effects of different friction contact conditions (tires/roadway), tire versions (summer/winter) and side wind behavior on fuel consumption?
- What are the effects of driver behavior? What design results in a high "fuel economy robustness" with regard to the driver behavior?
- What are the effects of different loads and their distribution (front/rear axle load)? Here, the driving maneuver catalogs differentiate between different tare weights due to equipment and types of construction, the test weight, the number of passengers as well as roof loads and towed loads.
- How can Advanced Driver Assistance Systems (ADAS) such as Adaptive Cruise Control (ACC) be used for reduced fuel consumption?
- How can fuel consumption be optimized with a view to "space and time", meaning optimized for a certain route which is often used by certain drivers at certain times of day, week and year, often regularly recurring as in a commute? In other words: Is it possible to realize a route memory? What will the future contribution of digital maps and GPS be with a view to a farsighted operating strategy?

The objective of the development and testing environment described in this article is to operate the vehicle under realistic conditions in the entire driving maneuver parametric space (as far as possible) by means of driving tests on a chassis dynamometer in order to cover the consumption-relevant situations that occur during everyday real-world use. The determination of an "energy fingerprint" is, against the backdrop of early determination of CO_2 emission and fuel consumption, a main concern of this test method developed by AVL. Furthermore the method makes a significant contribution towards the shortening of the development period. For one thing is clear: vehicle development engineers may have achieved a lot today, but as demands keep increasing, development tools and techniques have to keep improving as well.

2 Maneuver- and Event-based Testing

The method for implementing test cases on the AVL chassis dynamometer with AVL InMotion is called "maneuver- and event-based testing". This method is essentially based on the following idea: driving a vehicle, the ultimate driver of vehicle development, is a sequence of events and maneuvers. For this reason, such a maneuver- and event-based test description should be a highly efficient "lingua franca" for the vehicle development process. In the end, a maneuver- and event-based development environment also enables the merging of traditionally separate fields of development (chassis/drive train), which enables the exploitation of additional cross-linking potentials. The unique integration of the four test environments office, laboratory, test bed and road in a common user interface and data management system also enables a new level of quality within the development process.

Over the past ten years, there has been much talk about "synergies" – too much talk. But as a result of the combination of technological maturity (for example, of assistance systems, electrical horizon) and today's economic necessity of sustainable mobility, we know that CO_2 optimization has to be achieved across all functions and fields of work. With appropriate modifications, the AVL chassis dynamometer enables efficient testing of the interaction of the highly cross-linked individual systems within the complete system.

3 Absinth Control Strategy

According to the current state of the art, the rolling resistance on chassis dynamometers is computed by means of a polynomial formula

$$F_x = F_{x0} + C_0 \cdot v + C_2 + v^2 \quad (1)$$

Figure 1. This approach is insufficient to comprehensively evaluate the energy balance and the tasks described in the introduction [3]. What is the contribution of the walk resistance of tires, for example? What are the effects of ambient conditions (e.g. tire temperature and tire inflation pressure)? How significant is the impact of unevenness of the road and the dynamic wheel loads? How great is the influence of a wet- or snow-covered road (resistance due to water displacement, increased slippage) or bad road conditions? How large is the loss due to the axle geometry – in particular toe-in and camber – when driving straight ahead too? How great is the power loss when curves are negotiated (combined rotational slip and side slip, restoring torques, etc.) and during transient tire response? What contribution can the chassis development (suspension design) make towards CO_2 reduction? To date, it has not been possible to answer these and many other questions that are pivotal in the determination of the "energy fingerprint" and therefore the comprehensive and realistic assessment of the power loss and, as a result, the fuel consumption, of a vehicle on a chassis dynamometer.

AVL chassis dynamometers in combination with the "Absinth control strategy", for which the authors have applied for a patent, can be used to take remedial action here. The basic idea behind this is to move the frictional connection (power bond) from the tire-road contact zone to the axle shafts or even before the axle drive (differential gear). By definition, the real world and the virtual world exchange the performance quantities on the test bed via defined interfaces (so-called power bonds). For this purpose, the driving torques and speeds in the power bond are determined either from the tractive force measurement on the test bed or by means of torque measuring wheels. By doing so, the tire is no longer part of the unit under test, but becomes a part of the test bed. If the power bond is moved to the input side of the axle differential, axle shafts and the axle differential are also part of the test bed and not part of the unit under test. As far as simulation goes, the tire losses are simulated on the AVL chassis dynamometer with AVL InMotion by means of powerful, real-time tire models, **Figure 2**. As a result of the large number of active parameters (wheel load, slip angle, camber, rotational slip, inflation pressure, tire temperature, road conditions, friction coefficient etc.) and the distinct non-linearity and dynamics of the physical tire properties, very detailed tire models are used, such as TaMeTire, a thermo-mechanical tire model developed by Michelin [4]. Other standard formats such as TYDEX, Pacejka MagicFormula, or customer-specific tire models are integrated in the tire model library via standard interfaces.

Several additional 3D mechanical coupling effects between the real drive train (unit under test) and the whole vehicle (simulated) are also considered by AVL InMotion: restraining torques (unit bearing, bogie bearing), time-variant bending of the cardan shafts (including the effects of wheel travel) as well as gyroscopic effects which act, for example, on a yawing vehicle during steering operations in particular [5].

Furthermore the control strategy has the advantage that the tire is eliminated as a disturbing quantity (variation of the measurement results due to heating-up and tread wear). Tires have to be changed less often in test operation because their behavior has no influence on the test results any more – which saves you money and time. If a wheel-force measuring hub is not used, the tire model is operated in the "Absinth mixed mode": the force FX is really measured (in the vehicle longitudinal axis), and the other force/torque components of the tire are simulated. If tractive force measurement is also not available, and only the torque of the drum, it is not possible to differentiate between FX and rolling resistance torque in the wheel contact point (My) with measurement techniques. In this case, My is separated by means of suitable estimation methods. Then Fx and My are taken from the measurement, and the four other forces/torques come from the simulation. If the tire is operated within the limits of the power transmission potential and especially in combined slip-

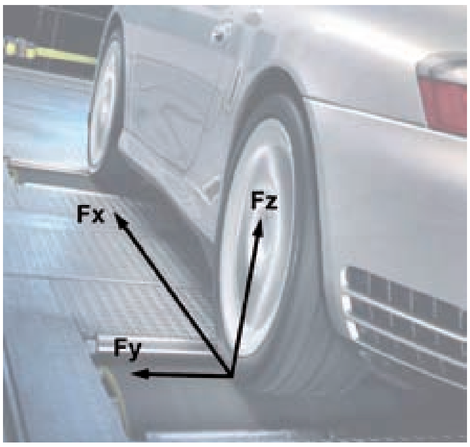

Figure 1: Forces acting on tires

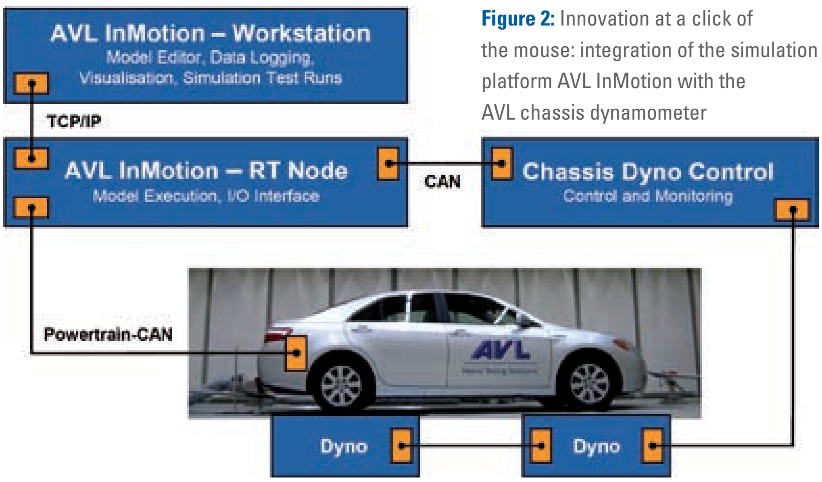

Figure 2: Innovation at a click of the mouse: integration of the simulation platform AVL InMotion with the AVL chassis dynamometer

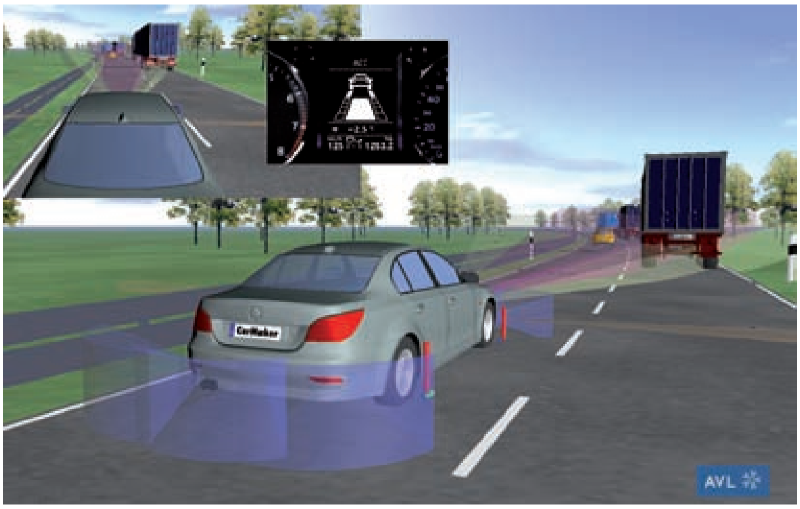

Figure 3: Traffic simulation on the chassis dynamometer: The integration of driving assistance systems and drive train control enables reduced fuel consumption

page during the maneuver, it is highly recommended to use a wheel-force measuring hub.

4 Simulation and Test Bed Dynamics

In general, it can be said that chassis dynamometers are operated in a manner similar to drive train test beds with a focus on control engineering. The power bond is identical in both cases. On drive train test beds, the power coupling between the unit under test and the test bed is of the positive-action type, while on chassis dynamometers, it is of the power-grip type. This is the main difference. This creates different test bed dynamics. Another variable between the two types of test beds is the different inertias of the load units. For many application tasks – especially for the optimization of fuel consumption – the dynamics of modern chassis dynamometers are sufficient, **Figure 3**. Tire sidewall stiffness and damping as well as the first normal vibration modes of a tire (tire / belt rigid body mode [6]) are simulated in a sufficiently realistic manner "in the first order" for most testing tasks.

Here a widespread misunderstanding has to be cleared up: a simulation-based development and testing environment does not necessarily require a highly dynamic test bed. For example, the speed/torque set points of a highway cruise at constant speed may originate from a powerful, realistic 3D real-time vehicle simulation. However, a highly dynamic test bed is not necessary for the physical simulation of this maneuver.

At the other end of the spectrum, there are dynamic driving maneuvers such as shock loads or jump starts. These can only be reproduced in a realistic manner on highly dynamic drive train test beds [7]. In the virtual universe, any speed/torque gradients can be generated, even those that will only rarely occur in the later area of application of the vehicle or not at all. The conclusion drawn from this is that not every test bed can cover the entire driving maneuver range (which the proving ground test site cannot do either), but that quasi-stationary, transient as well as highly dynamic test beds can be operated on the basis of the maneuvers and events it can properly simulate.

5 Operating Modes in the Simulation Mode

An operating mode during which the unit under test is operated in a closed-loop control system via the power bonds with the virtual vehicle and environment model is referred to as "free mode". However, no test bed can – as already discussed above – obtain any bandwidth, so it cannot implement any gradients and frequency characteristics requested by the simulation environment with a view to control engineering. In part, the speed and torque are also intentionally limited in order to protect the unit under test. However, in most cases the test bed dynamics are very well known in advance. So the requested speeds can be checked for feasibility of the test bed by means of suitable online test bed models. These considerations have resulted in a strategy for which a patent has been applied for by AVL that aims at influencing the simulation in such a way that the simulation and the test bed are "synchronous" and do not diverge. The simulation is carried out in the so-called "servo mode" in this case.

This is realized either by applying suitable servo torques or by means of rheonomic speed control (as defined by classical mechanics) with constraining torques. The term "servo mode" is derived from the "servo constraints" introduced by H. Beghin [8]. Switching between the "servo mode" and the "free mode" is realized smoothly between two integration steps. The virtual additional torques impressed on the model in the servo mode are recorded and made available to the user. The simplest example of "servo mode" operation is a limitation of speed.

Figure 4: Interfaces of the chassis dynamometer to the environment

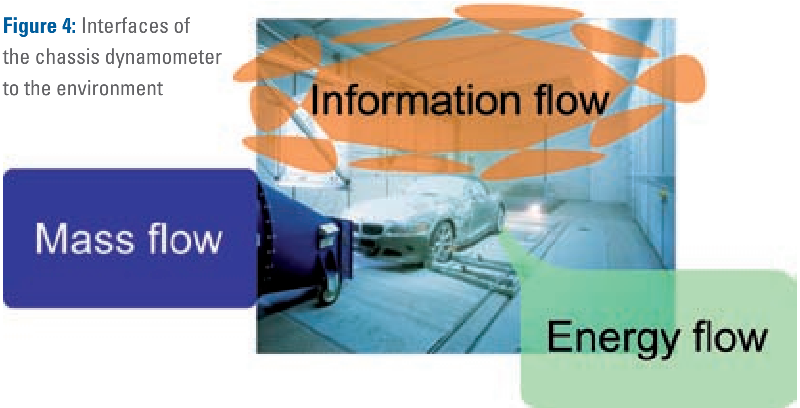

„Easy and Objective Benchmarking"

Interview with Dr.-Ing. Christoph Schmidt and Dipl.-Ing. Uwe Schmidt,
both Business Managers of AVL Zöllner GmbH in Bensheim (Germany) and AVL-Moravia s.r.o. in Hranice (Czech Republic)

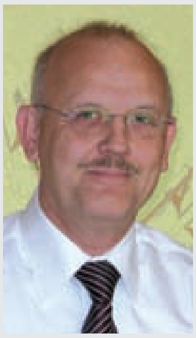

Christoph Schmidt

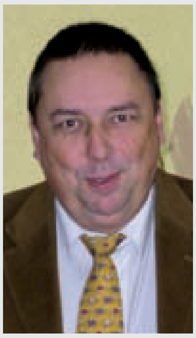

Uwe Schmidt

Will we still really need chassis dynamometers if we can test components and systems „in the loop" with much less effort?

Modern development processes are characterised by the intensive use of simulation, replacing many tests particularly at the beginning of the process. Yet at the same time tests are being transferred from the road into the chassis dyno lab, which means that the vehicle test bed is increasingly being used for additional and new development and validation tasks. The advantage of the chassis dyno in these cases is that results are objective – reproducible environmental conditions that can be simulated at any time and guarantee efficient testing and measurement. Tests are no longer limited due to bad weather, travelling time or working hours. Replacing road tests by a chassis dyno that is situated very close to where the development is taking place enables complex measurement equipment to be used „on the road". The increasing complexity and interrelated nature of components and systems in the complete vehicle also put a limit on how far components can be developed purely „in the loop". Both methods are valid, their use depending on the development phase. An additional benefit of the chassis dyno is that it can be used for easy and objective benchmarking of variants, further developments and competitive products, as the vehicle is tested as a closed system.

How high are the gains in productivity when you can control all test beds in the same manner and guarantee consistent data availability?

Merely introducing a consistent development platform for engine and vehicle tests does not lead to an increase in efficiency. In addition, processes need to be adapted and implemented in order to leverage the potential that the platform offers. We believe that development times, which have been significantly reduced over the last few years, will be shortened further, or at the very least kept at their current level, in spite of increasing complexity – in hybrid development for example. AVL provides customers with the necessary environment to enable a consistent development process. AVL can also support the customer in designing and rolling out processes so that the tools will be used to the optimum.

Will driveability assessment on the chassis dyno ever completely replace the test driver's subjective rating?

No, but it does spare some of the routine work and provides a rational test result. The test driver is freed up for more challenging tasks such as validation. But it won't replace the CEO's test drive.

What role does the chassis dyno play in configuring new powertrain concepts – such as partial electrification, for example?

After the road itself, the chassis dyno provides the most realistic environment, as it is where the least is simulated. Vehicles with any kind of powertrain system – whether conventional, hybrid or electric – can be tested there, making it a universal development environment. And as powertrains become more diversified the chassis dyno will become even more important.

AVL Zöllner enjoys an excellent reputation as test bed supplier. How important are the close links to other areas of AVL such as simulation or application development?

AVL Zöllner develops and provides reliable and modern vehicle test bed technology for applications such as NVH, EMC, MACD, Emission development and calibration of vehicles of any kind or size. Being an integral part of AVL, with its modern instrumentation and application tools, allows us access to new ideas that can be built into the test bed and provide the customer with additional benefits.

6 Application as a Mechatronic Development Platform

6.1 Interfaces

In hybrid and increasingly also in conventional vehicle models, interlinked control units take over the functions that are relevant to energy in a consistent and powerful integrated system. For testing, this implies the need for powerful interfaces used by the unit under test to communicate with the test bed. As everybody knows, the three central mechatronic interfaces are "matter", "energy" and "information" [9], **Figure 4**. Control over the interface "matter" is ensured on AVL performance test beds by means of a powerful oil, water and fuel conditioning systems as well as climatic chambers and altitude chambers.

Control over the interface "energy" is realized by means of dynamometric brakes with the respective measurement and control equipment and, for hybrid and electric vehicles, by means of battery simulators. It is astonishing that the realistic simulation of the interface "information" is not yet paid the attention that it deserves considering its importance as an innovation carrier and market driver. The "vehicle-in-the-loop" approach that is consistently pursued by AVL fills this gap. So the classical chassis dynamometer further develops into an integrated mechatronic development and testing platform in an evolutionary manner. Such a platform should be regarded as the master plan for the optimization of product development.

In the following, selected examples are used to show the application possibilities of a "vehicle-in-the-loop" chassis dynamometer.

6.2 Examples of Application

In one-axle chassis dynamometers, the wheels that are not driven by the vehicle powertrain do not turn. As a result, the wheel speed of the stationary wheels is not consistent with real driving operation. Any wheel braking torque of the axle that is not driven is not considered either. Realistic wheel speeds are generated from the simulation. AVL enables the simulation of inductive, magneto-resistive or "intelligent" wheel speed signals via IO-modules. If there are braking operations during the requested maneuver, the forces and pressures are directly measured in the brake body piston and played back to the model online. The use of plug connectors from series production and of mass-produced instrumented brake discs results in short setup times. The result is that, for example, it is now possible to simulate the "rock cycle" (rocking out of a depression in the snow) or driving away uphill from rolling backwards with very smooth braking and controlling interventions on the chassis dynamometer. It is important for an energy-efficient design that the instrumented brake discs also determine the residual braking torques that remain after the brake pedal has been released and make them available to the simulation. Residual braking torques are up to 50% of the rolling resistance torque and so are relevant for consumption development.

Especially in city traffic, but also in single-lane traffic with changing speeds, ACC systems (Adaptive Cruise Control) offer a significant potential for reduction of fuel consumption, and not nearly enough attention is paid to that at the moment. The wide variety of possible scenarios that result from the interactions between the driver, the vehicle, the traffic situation and the environment constitute a special challenge here. The most important scenarios have to be identified as test cases and implemented in the simulation in a reproducible manner.

With AVL InMotion, ACC can now be tested on the AVL chassis dynamometer under realistic conditions. Freely configurable traffic situations with any number of movable objects are created. The sensor information from the radar is created by the test system and transmitted to the real vehicle. Superordinate driving dynamics controllers coordinate the interventions in the engine control and also actively modulate the hydraulic brakes if necessary.

Map and GPS information are not yet used in any applications that reduce fuel consumption, but they offer great potential. Future navigation systems ("electrical horizon") will provide information about gradients, curve radii, speed limits, other traffic restrictions and even information about the smoothness of the road. Furthermore they calculate the route that the vehicle will probably follow. Forward-looking systems adapt the drive management to the course of the expected route. Learning systems record and recognize constantly recurring "paths of usage" of the vehicle (traffic density, driving style) and so reduce the average and the variance of the cycle for which the estimation is carried out. Especially for hybrid and electric vehicles, this technology offers the potential of significantly reduced fuel consumption.

In order to enable the practical application of such developments on the road in a faster and more cost-efficient way, AVL will equip future chassis dynamometers with additional functions: simulation of the "GPS antenna", Road-Importer (importing and mapping of the GPS route in the test system), preconfigured ADASIS interface and preview sensor.

7 Summary

The examples given show that the continued development of the classical chassis dynamometer into a mechatronic development and testing platform pursued by AVL enables cost- and time-efficient development methods. The complete vehicle becomes an "embedded system" of the virtual environment in which it is tested. The continuously expanding possibilities in sensor technology, mechatronics, data processing and communication will enable the simulation of a wide variety of functions in the future. The increased system integration in the vehicle brings about synergy effects, but it also results in a major increase in complexity at the same time. In the real vehicle, the individual systems are integrated and can so be tested in combination. So the ViL (Vehicle-in-the-Loop) test bed is a key to complexity control and the protection of the entire functional integrated system; undesired system interactions and conflicts between the individual systems with effects that often overlap are detected on the ViL test bed early and in a cost-efficient manner and are eliminated by means of a suitable adaptation of the controller software in a targeted manner. The handling of the growing variety of versions is facilitated as well.

References

[1] Bangemann, C.: Rollenspiele. In: auto motor und sport (2007) 22, S. 180-182
[2] Düser, T.; Albers, A.: Integration von Simulation und Test am Beispiel Vehicle-in-the-Loop auf dem Rollenprüfstand und im Fahrversuch. 3. Internationales Symposium für Entwicklungsmethodik, Wiesbaden, 2009
[3] Frey, M.; Gnadler, R.; Günter, F.: Untersuchung der Verlustleistung an Pkw-Reifen. VDI Berichte (1995), 1224, S. 101-128
[4] Février, P.; Fandard, G.: Thermische und mechanische Reifenmodellierung zur Simulation des Fahrverhaltens. In: ATZ 110 (2008) 5
[5] Pfister, F.; Reitze, C.: The motion equations of rotors, gyrostats and gyrodesics: application to powertrain-vehicle mechanical systems. In: Archive of Applied Mechanics 79 (2009) 1
[6] Gong, S: A Study of In-Plane Dynamics of Tires. Dissertation, Delft, U of Technology, 1993
[7] Brodbeck, P.; Pfeiffer, M.; Germann, S.; Schyr, C.; Ludemann, S.: Verbesserung der Simulationsgüte von Antriebsstrangprüfständen mittels Reifenschlupfsimulation. VDI-Tagung Getriebe in Fahrzeugen, Friedrichshafen, 2001
[8] Beghin, H.: Étude théorique des compas gyrostatiques Anschütz et Sperry. Paris imprimerie Nationale, 1921
[9] Albers, A.; Schyr, C.: Modellbasierte Produktvalidierung mittels Integration von funktionalen und physikalischen Beschreibungen. 4. Paderborner Workshop Entwurf mechatronischer Systeme, 2006

Innovative Use of Chassis Dynamometers for the Calibration of Driveability

One of the most time-intensive calibration tasks in vehicle development is the optimisation of driveability. In order to guarantee brand and variant specific driveability, a great number of parameters relevant to vehicle handling must be calibrated. AVL has developed a new approach to driveability calibration that makes an objective, robust and efficient calibration possible on the chassis dynamometer.

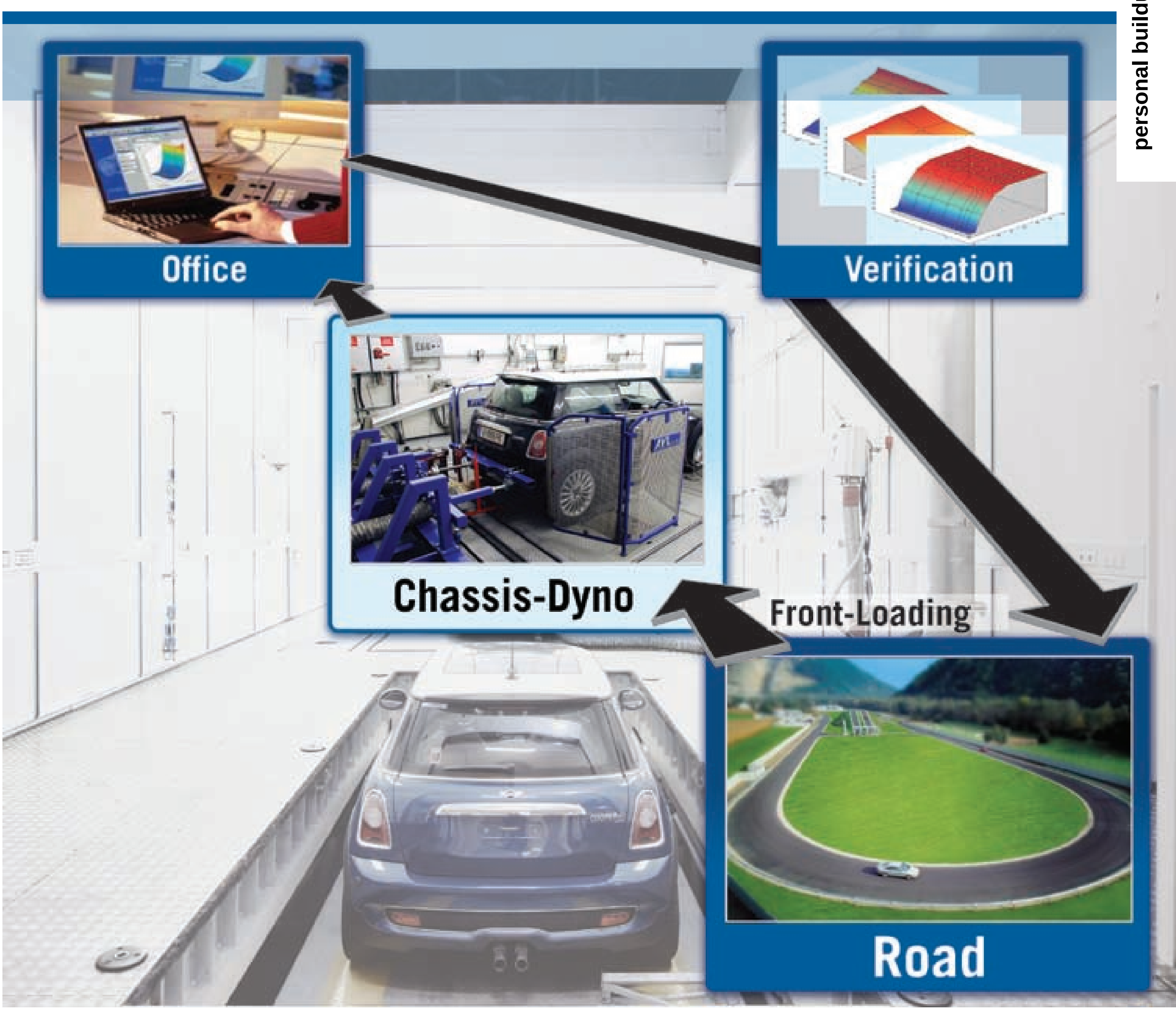

The Authors

Dipl.-Ing. (FH)
Rainer Vögl
is Lead Engineer for Vehicle and Testbed Methodology at AVL List GmbH in Graz (Austria).

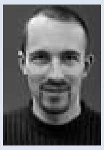

Dipl. Ing. Erik Bogner
leads the Group for Driveability and Simulation at AVL List GmbH in Graz (Austria).

Dr. Thomas Ebner
is responsible for CAMEO Customer Projects at AVL List GmbH in Graz (Austria).

Dipl.-Ing.
Tom Dein Dias Terra
is Development Engineer for Vehicle and Testbed Methodology at AVL List GmbH in Graz (Austria).

Dipl.-Ing.
Gianluca Vitale
is Product Manager for Vehicle Calibration in the Business Unit Instrumentation at AVL List GmbH in Graz (Austria).

1 Introduction

The continuing pressure to reduce costs is leading OEMs towards a growing focus on "front loading". The front loading process shifts tests that would traditionally be run on chassis dynos to engine or component test beds. Simultaneously, road testing, trials and recently quality testing are being transferred from the road to the chassis dyno. This is particularly true for calibration of engine and transmission control systems for the desired driveability. This paper will discuss an approach for such calibration tasks to be completed using chassis dynos.

2 Model-based Approach for the Calibration of Driveability

The classic manual calibration of driveability of the vehicle on the road is carried out by the application engineer using subjective evaluation criteria. These criteria consist of the perceived vehicle's longitudinal acceleration (absolute value, gradient, oscillations and consistency) and the analysis of the signals corresponding to the driveability functions in the control unit. The signals for load change manoeuvres are torque build-up, whereas for shift procedures in automatic transmissions the signals are engine torque and clutch pressure behaviour. The set values are filter parameters, with which the torque build-up or interventions are affected and other parameters such as fill time, fill pressure or clutch shift pressure. Using expert knowledge of the relationship between the set values and the evaluated signals, the application engineer is able to optimize driveability in terms of driving comfort and dynamic behaviour.

The manual approach is limited not only by the mainly subjective evaluation of data but also by additional difficulties such as: differing environmental conditions (road, weather, traffic) leading to low reproducibility of test conditions. Tests cannot be easily run overnight or over weekends: which combined with short development times leads inexorably to a higher number of prototypes. Due to the increasing complexity of the set values, the application engineer finds it more and more difficult to achieve an overview of the complete system.

An objective evaluation of driveability on a chassis dynamometer is both beneficial and pragmatic in order to obtain higher flexibility in terms of test environment, level of automation and efficient utilization of the test object. Since the vehicle longitudinal acceleration is not available due to the vehicle being locked in position on a chassis dyno, the acceleration signal must be derived from other sources, in this case, via the force applied by the vehicle on the restraint or via the tractive force applied by the vehicle's wheels on the rollers. These physical signals make it possible to judge subjective driveability based on objectively measured values.

AVL-DRIVE, used for the objective evaluation of driveability, contains more than 400 criteria for more than 80 different driving manoeuvres (such as „tip-in", tip-out, shift manoeuvre, full load and partial load acceleration, drive-away manoeuvre). These manoeuvres are automatically recognised during a test run and evaluated online. AVL-DRIVE calculates physical characteristics for each driving manoeuvre from pre-defined evaluation criteria such as kick, jerks or response delay for the "tip-in". These individual criteria are rated from 1 (no function) to 10 (excellent). An overall rating for a manoeuvre is calculated from the individual criteria (for example for full load acceleration out of motoring) and an overall vehicle rating is calculated from all the manoeuvre ratings. These calculations reduce the driveability relevant signals to scalar values, whereby a single manoeuvre corresponds to a single measurement point.

By running the test on a chassis dynamometer and employing tools to objectivise the driveability, the whole process can now be automated.

By doing so, pre-defined driving manoeuvres can be run more efficiently and reproducibly. Despite an increase in the reproducibility of the manoeuvres, there is still a spread in the evaluation of the driving events. This is dependent on many factors such as the current oscillatory state of the powertrain or the clutch due to the previous shift [1].

However, the spread of subjective evaluation is considerably higher than that of the objective evaluation as shown in **Figure 1**.

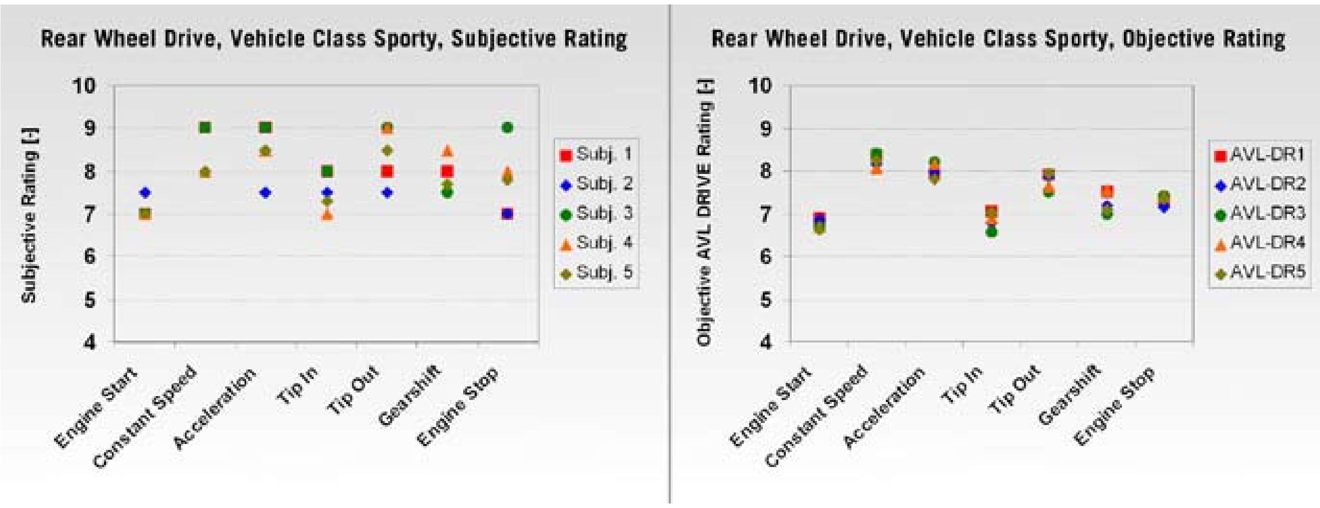

Figure 1: Comparison of subjective and objective driveability ratings from 5 tests with 5 different application engineers and AVL-DRIVE

A large population of tests is necessary in order to provide a statistically firm statement in view of the deviation. In order to be able to run a large number of tests in the shortest possible time, the chassis dyno is run in different control modes for the shift quality optimisation. An operating point, defined by speed, load and gear number is run via a fast speed ramp. The chassis dyno is only run in road load simulation during the actual driving manoeuvre. This requires that the chassis dyno is capable of a "bump less" transition between control modes and stable control after the transition has been completed. This then enables successive shift manoeuvres to be run every 12 seconds and load change cycles to be run every 15 seconds. This results in a total test time between 10 and 70 hours of unmanned operation, independent of the calibration task.

The general work process is shown in **Figure 2**. A DoE test plan is created then run in automatic mode on the chassis dyno. Global models are then generated in the office for drive comfort and dynamic behaviour. A manual calibration is performed in local operating points, whereas the automated process follows a global approach, which includes not only the measured signals, but also the set values. This global data set contains all pertinent information concerning driveability. This data set makes it possible to generate optimized calibrations for various driveability modi such as comfort, sport or super-sport modes, without the necessity of further data gathering loops. Today, where individual brand definition means that each OEM currently has up to seven such driveability programmes, the effort required to calibrate these programmes is considerably reduced – as is the number of prototype vehicles required for the calibration work. The completed data sets are then verified conventionally in the vehicle on the road.

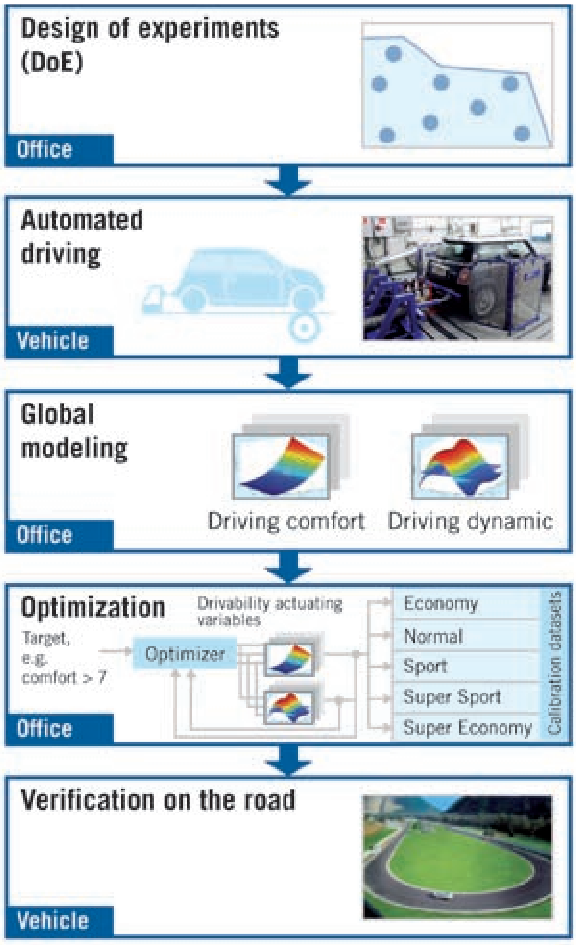

Figure 2: General work process of the model-based calibration of driveability

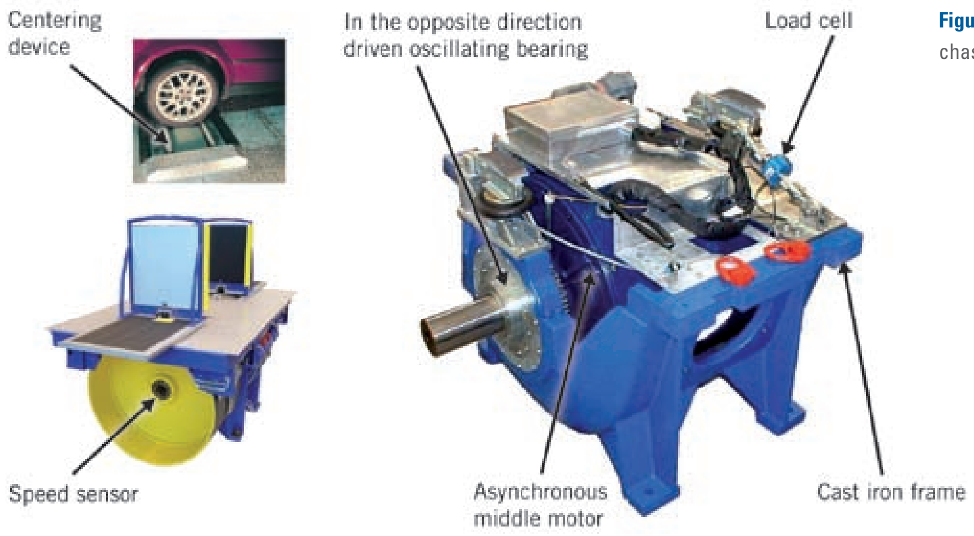

Figure 3: Hardware components of the chassis dynamometer

3 System Configuration

The vehicle is fixed on the chassis dyno via a load cell with a very stiff clamp, since the longitudinal forces can only be measured by the load cell. This upgrade variation was used for the tests in this article. The possibility of using the acceleration signal directly from the chassis controller on the AVL-Zöllner chassis dyno avoids extra mechanical systems and promises high dynamic response and measurement repeatability. This signal is transmitted to the AVL-DRIVE system, other necessary signals, such as vehicle speed, engaged gear, accelerator pedal position are taken from the vehicle's CAN bus.

The layout and control of the chassis dyno are of paramount importance for the application. A chassis dyno with high dynamic response is necessary for the reproduction of driveability test manoeuvres. In addition, if the requirements for emissions specification C100081T1 are fulfilled, then the chassis dyno offers a wide field of application beyond driveability calibration: amongst other things emissions calibration, endurance testing or fuel consumption reduction testing, and at the same time cost efficient.

Two 48" rollers with centering device, coupled directly to an asynchronous centrally mounted motor, form the roller assembly for an axle (simulation unit), **Figure 3**. The active centering device guarantees that tyre contact with the roller is horizontal during vehicle installation.

Multiple axle test beds use two of these devices mechanically connected via a frame construction, whereby one is adjustable in the vehicle longitudinal direction. A torsionally rigid cast frame is used to mount the asynchronous motor and

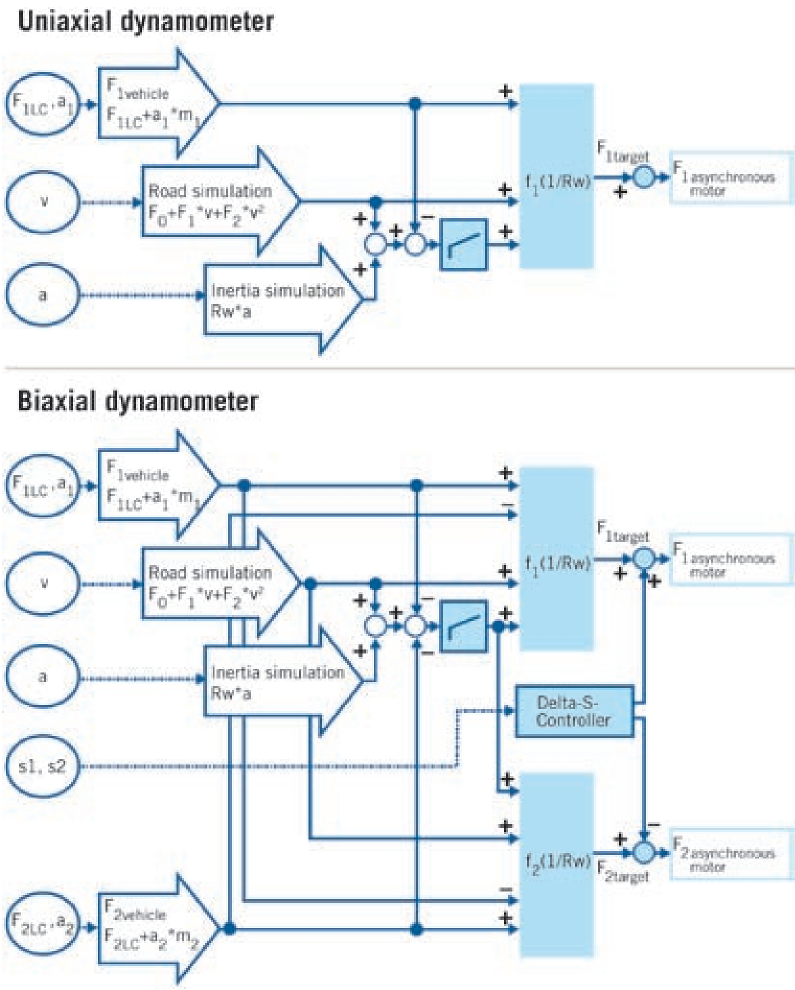

Figure 4: Controller configuration for single and twin axle test beds

provides exact and fast reaction torque even when subjected to dynamic conditions. The cradle bearings, located within the torque measurement system, are motorized to avoid pressure points and the related breakaway torque. This also means that temperature dependent bearing losses are automatically compensated for and do not influence the accuracy of the torque measurement. The precise measurement of the torque itself is done via a temperature-compensated load cell. The load cell and pivot arm are rigidly mounted leading to a high natural frequency.

This then permits the full dynamic response of the fast current control of the motor and converter to be exploited. Control times of below 10 ms are possible.

The calculation and control of the road load applied to the vehicle is done in realtime. Deterministic and fast reaction time is guaranteed by the deployment of an ARTE environment (AVL Real Time Environment), which provides the pre-requisite for stable control, **Figure 4**. The simulation takes into account stiction, kinetic friction and the aerodynamic resistance in the form of coefficients F0, F1 and F2 of the road load equation. The missing mass inertia of the fixed vehicle is reproduced by the rotating mass of the rollers. The difference between the vehicle mass and the roller mass is compensated for by mass simulation. The force of the vehicle applied to the road surface (FxVehicle), the force of the road load simulation and the force derived from the mass simulation are calculated using the measured vehicle speed (v), acceleration (a) and force signals (Fx-LC) of the test bed motor. Using feed forward control of the forces from the road load simulation and the vehicle FXVehicle in combination with the control of all forces that act additively on the feed forward loop, it is possible to apply the necessary force FXDemand to the wheels via the AC motor within milliseconds. This type of control guarantees a fast and deterministic reaction by the test bed. For vehicles driven by two axles, symmetrical controllers on both axles maintain the calculated total force and identical speed of both rollers.

In order to compensate for inaccuracies of the simulation model and to reduce the angular difference between the rollers to below 0.2°, the system uses an overlying delta-s controller to reduce differences between the roller speeds and positions (s1, s2). This guarantees a high synchronicity between the rollers for an arbitrary force distribution by the vehicle.

In addition to the controllers described here, the AVL Zöllner chassis dyno supports "bumpless" transition between controller modes speed control and road load simulation providing a major pre-requisite for an effective automation of the system.

Figure 5 shows the complete system layout with the roller controller AVL-VECON, the automation system AVL-Dricon/PUMA-Vehicle, the evaluation system AVL-DRIVE, the optimisation system AVL-CAMEO, the applications systems and the fixed vehicle. Using either AVL-Dricon or PUMA-Vehicle, the vehicle's accelerator pedal and the shift lever for automatic or DCT transmissions can be controlled purely electronically.

The advantages of the electronic control are:

- can be used in both development vehicles and those in series production
- lower cost, shorter setup times and the required faster conversion of control signals than a robot
- identical layout for both road and chassis dyno.

The AVL DriCon/PUMA Vehicle receives the commands for the current driving manoeuvre from the AVL-CAMEO optimisation system via an Ethernet UDP interface. These commands are converted into ramps for the accelerator pedal and the roller speed and then sent together with the control mode and road gradient to the vehicle and the roller controller.

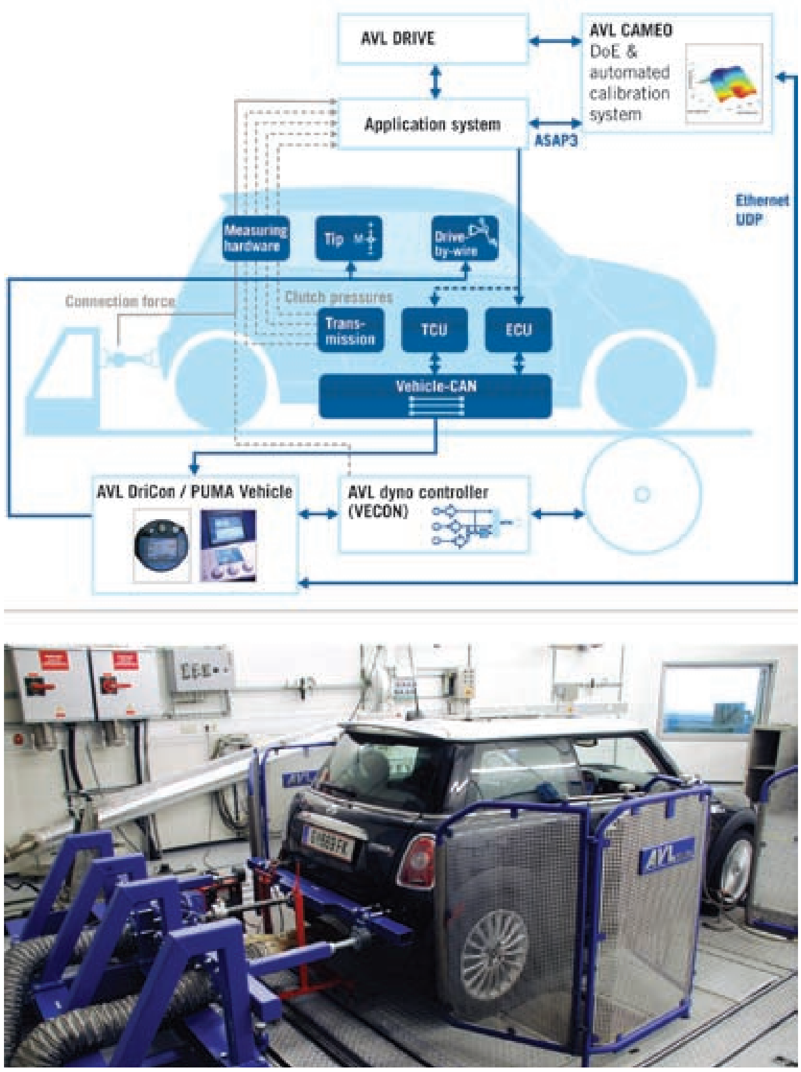

Figure 5: System layout, test vehicle on the high dynamic chassis dyno

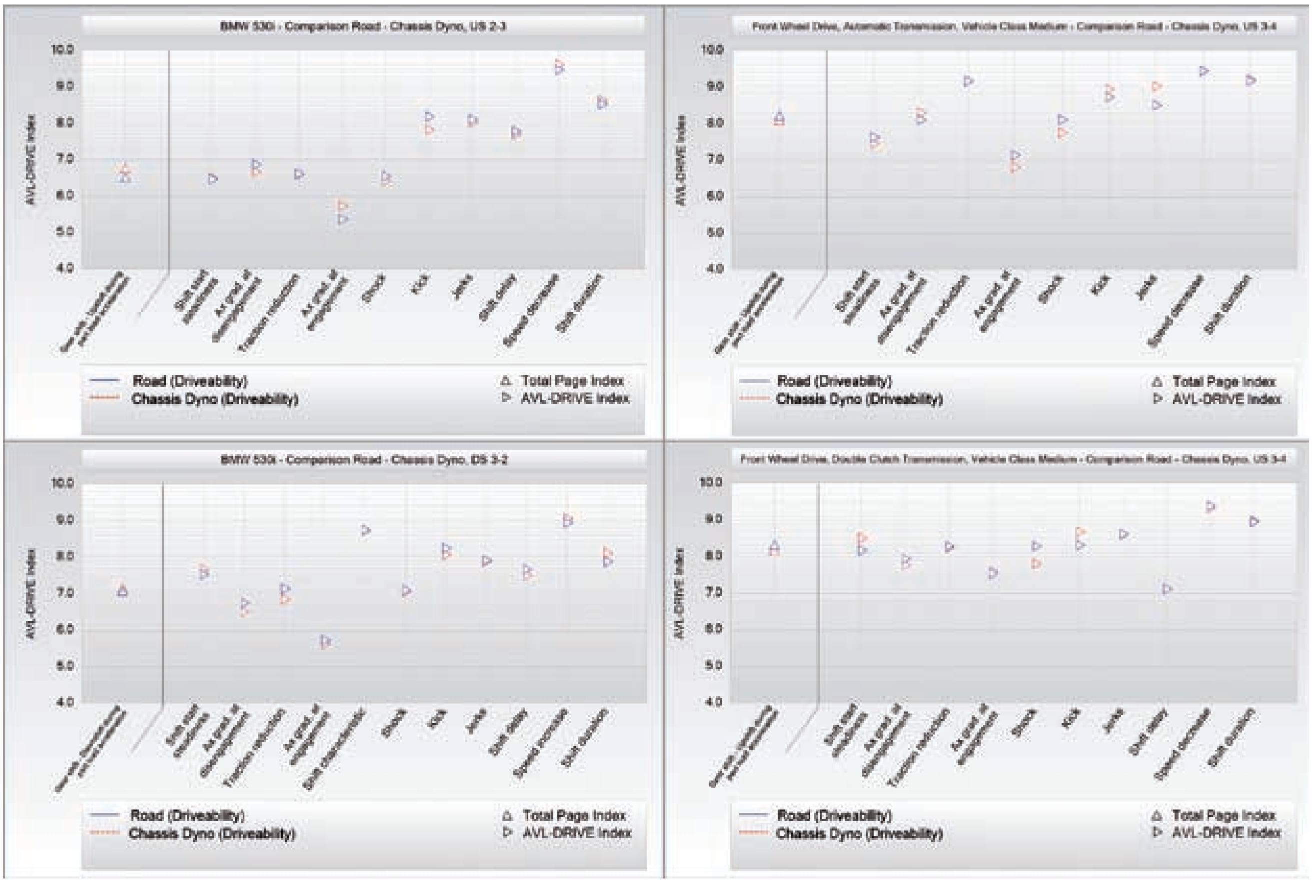

Figure 6: Comparison of driveability ratings for shift quality between road and chassis dyno

AVL-CAMEO is used not only for the overall control of the test sequence but also for the test plan, data modelling and control map generation. The system uploads all relevant ECU/TCU demand values via an ASAP-3 interface to the application system. The ratings and physical characteristics of the driving manoeuvre as calculated by AVL-DRIVE are transmitted online to AVL-CAMEO and stored together with the demand values in a database.

The complete measurement log with tractive force and other signals such as clutch pressures, emissions and fuel consumption values is generated by the applications system using appropriate hardware.

In order to run continuously unmanned, it is necessary to monitor relevant vehicle CAN bus signals and to prevent damage by fire and overheating by the engine and transmission, by overspeed or overtorque conditions, tyre damage and excessive vehicle movement, diagnostic errors or fuel leakages. Automated refuelling systems must also be implemented. Detailed correlation tests were carried out with this system configuration in order to be able to guarantee the portability of the test results from the chassis dyno to true road conditions.

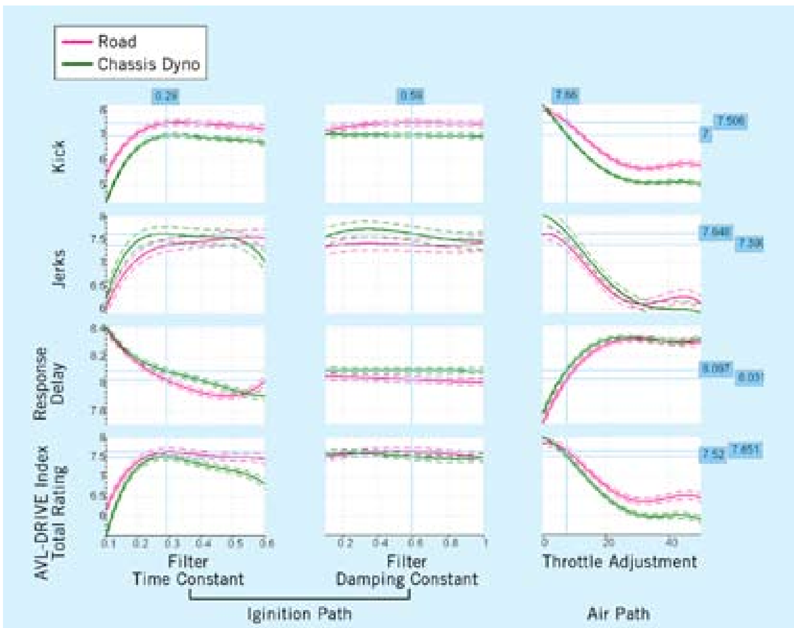

Figure 7: Comparison of the driveability rating models for „tip-in" between road and chassis dyno

4 Correlations Test between Road and Chassis Dynamometer

A BMW 530i with automatic transmission (AT), a front-wheel drive vehicle with automatic transmission and a FWD vehicle with DCT transmission were selected for the comparison tests of gear shift quality measurements. The measurement plan consisted of sets of 10 operating points defined by turbine speed against turbine torque (AT) and engine speed against engine torque (DCT), applied to gear shifts from 2nd to 3rd and from 3rd to 4th gear. A downshift from 3rd to 2nd was also analysed. Each operating point was run with series production calibration and repeated 5 times. The measurements were run on the road and on a high dynamic AVL Zöllner chassis dynamometer.

The comparison values for each driveability criteria for the shifts are shown in **Figure 6**.

The difference in the ratings is 0.5 [-] at the most and is firmly within the scatter band of the AVL-DRIVE evaluation, Figure 1. The „tip-in“ comparison uses variations in driveability relevant set values with a grid-test plan (343 variations) in the road and on the chassis dyno:

Table: Operating ranges and set values for „tip-in“

Load	Pedal steps: 0 – 20, -30, -50, -75, -100 %
Engine speed	1000 – 3000 rpm in steps of 250 or 500rpm
Gear	1st, 2nd, 3rd, 4th
Set value 1	gain factor anti-jerk function
Set value 2	filter damping constant for torque demand (ignition path)
Set value 3	filter time constant for the torque demand (ignition path)
Set value 4	pedal position for the torque demand (air path)

- operating point 1500 rpm (engine), pedal step from 0-50 % in 2nd gear
- set point variation: pedal, filter constants for torque rise.

The set values for the „tip-in“ are split into those for the fast torque demand via spark advance (ignition path) in the form of filter constants and the slow torque demand via the accelerator pedal (air path). The model shape in **Figure 7** is qualitatively very similar for both road and chassis dyno. The optimisation leads to equivalent demand values and the difference in ratings is in the range of 0.5[-]. The pre-requisite for portability of optimisation results from the chassis dyno to the road environment is thus fulfilled.

5 Usage in Driveability Calibration

The following example for the application of a model based methodology for driveability calibration will limit itself to a „tip-in“ for a gasoline engine (results for shift quality calibration have

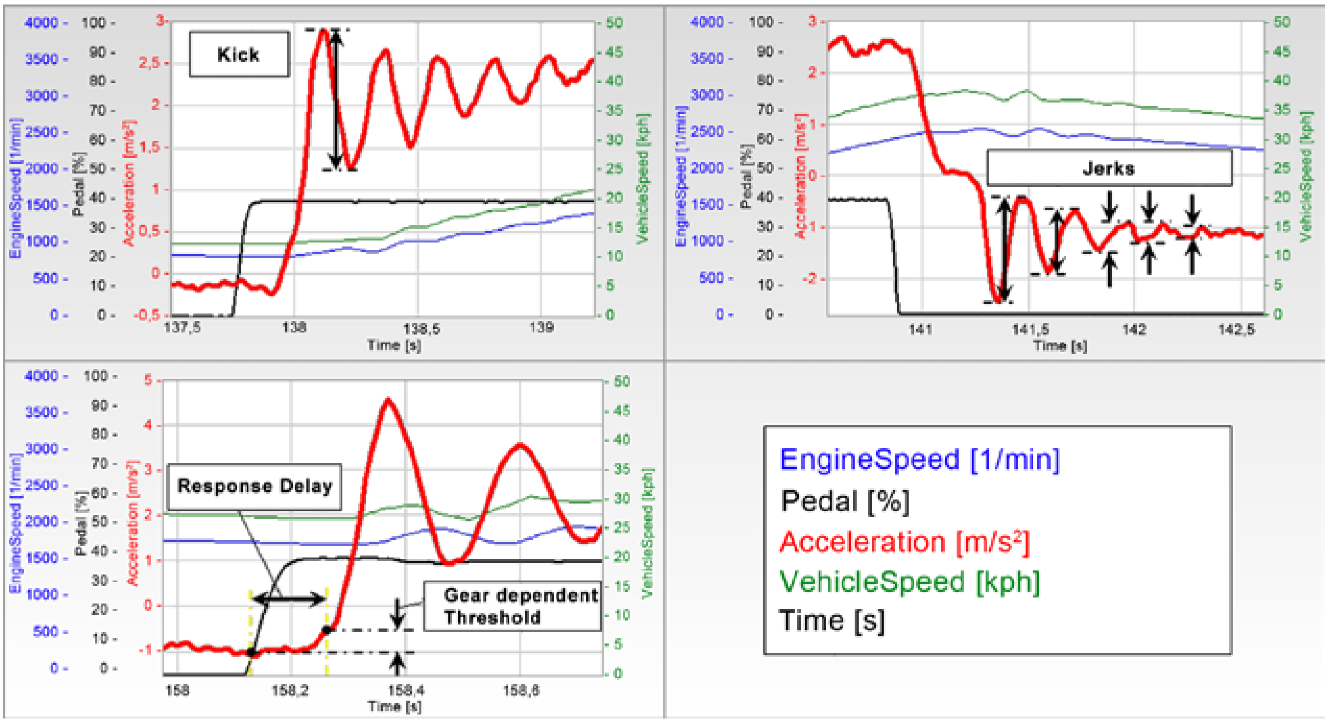

Figure 8: Significant factors for the “tip-in” rating: multiple oscillations, single jerk event, delay

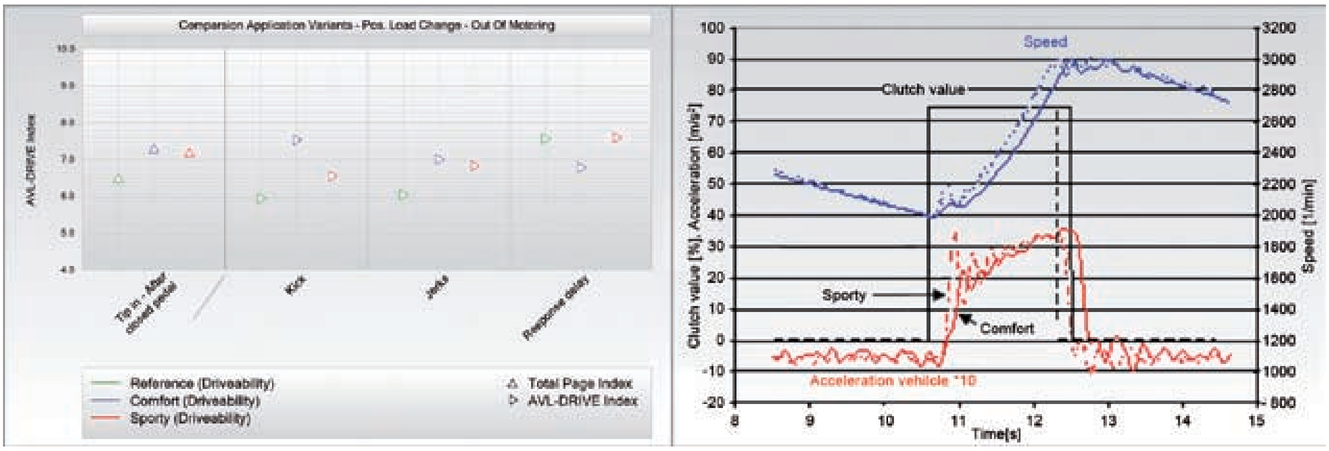

Figure 9: Comparison of calibration variants, effect of limiting physical signals
(the signal traces correspond to a "tip-in" of 0-75 % pedal position in 2nd gear at a speed of 2000 rpm)

already been published in [3]. In addition to the set values mentioned for the „tip-in" for the correlation tests, the gain factor for the anti-jerk function was varied. The anti-jerk function in the ECU is used to recognise and dampen undesirable oscillations in speed in the powertrain. The **Table** shows the operating ranges and the set values.

After the automated test had gathered the data, AVL-DRIVE built global models for the most relevant AVL-DRIVE detail evaluations and the overall rating for the „tip-in", refer to **Figure 8**.

The overall rating for a „tip-in" results from the weighting of the detail ratings: jerks are weighted at 25 %, a kick 20 % and the response delay 15 %. A high overall rating is achieved above all by low jerks and a low kick, which, from a driver's perspective, corresponds to high driving comfort. Other detail ratings contributed only 5-10 % to the overall rating and were considered insignificant and therefore not modelled.

Two different driveability variations were optimised in AVL-CAMEO. A "sport" calibration was generated by maximising the overall driveability rating while limiting the maximum delay (the smaller the response delay, the better the rating). Optimising the overall rating with no further limitations generated a "comfort" calibration.

After optimisation and data set generation, the first validation test was performed on the test track. **Figure 9** shows the AVL-DRIVE ratings for the evaluated reference calibrations and example signal traces for a "comfort" and "sport" calibration.

As expected, the rating for the delay with a "comfort" calibration is the lowest. The gentle and harmonic torque rise leads to better ratings for jerks and kick compared to the reference. The "sport" calibration shows improved ratings for kick and jerks with simultaneous response delay.

6 Summary

AVL has responded to the increasingly demanding market requirements in the domain of vehicle calibration by developing a new method for driveability calibration. The main focus of the methodology lies in the automated data gathering process on a chassis dynamometer, the model-based approach and the inherent avoidance of multiple calibration loops.

Since data is gathered at night and at weekends, a significant increase in chassis dyno productivity is achieved. The subsequent data evaluation and generation of all driveability calibration variants in the office environment makes it possible to simultaneously use vehicle prototypes for other calibration tasks. The sum of these factors leads to considerable savings in time and costs. This approach is a significant step in being able to cope with the future demands of driveability calibration.

References

[1] Koegeler, H. M.; Schantl, R.; Schuch, N.; Pfragner,S.; Pfister, F.; Beidl, Ch.: Optimisation of driveability using vehicle simulation on a HiL test bed with AVL-DRIVE and AVL-CAMEO. VDI-Tagung 2005, Würzburg

[2] Altenstrasser, H.; Vitale, G.; Winsel, Th.; Keuth, N.; Pflügl, H.: Multi-level global DoE for the automated optimisation of shift quality of automatic transmissions. 5. Konferenz „Design of Experiments in der Motorenentwicklung", Berlin, 2009

[3] Bagot, B.; Schmidt, A.; Ebner, Th.; Altenstrasser, H.: Model-based methodology for the automated optimisation of shift quality of automatic transmissions. In: ATZ 05 (2008), S. 404-411

Peer Review ATZ|MTZ

Peer Review Process for Research Articles in ATZ and MTZ

Steering Committee

Prof. Dr.-Ing. Stefan Gies	RWTH Aachen	Institut für Kraftfahrwesen Aachen
Prof. Dipl.-Des. Wolfgang Kraus	HAW Hamburg	Department Fahrzeugtechnik und Flugzeugbau
Prof. Dr.-Ing. Ferit Küçükay	Technische Universität Braunschweig	Institut für Fahrzeugtechnik
Prof. Dr.-Ing. Stefan Pischinger	RWTH Aachen	Lehrstuhl für Verbrennungskraftmaschinen
Prof. Dr.-Ing. Hans-Christian Reuss	Universität Stuttgart	Institut für Verbrennungsmotoren und Kraftfahrwesen
Prof. Dr.-Ing. Ulrich Spicher	Universität Karlsruhe	Institut für Kolbenmaschinen
Prof. Dr.-Ing. Hans Zellbeck	Technische Universität Dresden	Lehrstuhl für Verbrennungsmotoren

Advisory Board

Prof. Dr.-Ing. Klaus Augsburg	**Dr.-Ing. Markus Lienkamp**
Prof. Dr.-Ing. Bernard Bäker	**Prof. Dr. rer. nat. habil. Ulrich Maas**
Prof. Dr.-Ing. Michael Bargende	**Prof. Dr.-Ing. Martin Meywerk**
Dr.-Ing. Christoph Bollig	**Prof. Dr.-Ing. Klaus D. Müller-Glaser**
Prof. Dr. sc. techn. Konstantinos Boulouchos	**Dr. techn. Reinhard Mundl**
Prof. Dr.-Ing. Ralph Bruder	**Prof. Dr. rer. nat. Cornelius Neumann**
Dr. Gerhard Bruner	**Dr.-Ing. Lothar Patberg**
Prof. Dr. rer. nat. Heiner Bubb	**Prof. Dr.-Ing. Peter Pelz**
Prof. Dr. rer. nat. habil. Olaf Deutschmann	**Prof. Dr. techn. Ernst Pucher**
Dr. techn. Arno Eichberger	**Dr. Jochen Rauh**
Prof. Dr. techn. Helmut Eichlseder	**Prof. Dr.-Ing. Konrad Reif**
Dr.-Ing. Gerald Eifler	**Dr.-Ing. Swen Schaub**
Prof. Dr.-Ing. Wolfgang Eifler	**Prof. Dr. sc. nat. Christoph Schierz**
Prof. Dr. rer. nat. Frank Gauterin	**Prof. Dr. rer. nat. Christof Schulz**
Prof. Dr. techn. Bernhard Geringer	**Prof. Dr. rer. nat. Andy Schürr**
Prof. Dr.-Ing. Uwe Grebe	**Prof. Dr.-Ing. Ulrich Seiffert**
Prof. Dr.-Ing. Horst Harndorf	**Prof. Dr.-Ing. Hermann J. Stadtfeld**
Prof. Dr. techn. Wolfgang Hirschberg	**Prof. Dr. techn. Hermann Steffan**
Univ.-Doz. Dr. techn. Peter Hofmann	**Dr.-Ing. Wolfgang Steiger**
Prof. Dr.-Ing. Günter Hohenberg	**Prof. Dr.-Ing. Peter Steinberg**
Prof. Dr.-Ing. Bernd-Robert Höhn	**Prof. Dr.-Ing. Christoph Stiller**
Prof. Dr. rer. nat. Peter Holstein	**Dr.-Ing. Peter Stommel**
Prof. Dr.-Ing. habil. Werner Hufenbach	**Prof. Dr.-Ing. Wolfgang Thiemann**
Prof. Dr.-Ing. Roland Kasper	**Prof. Dr.-Ing. Helmut Tschöke**
Prof. Dr.-Ing. Tran Quoc Khanh	**Dr.-Ing. Pim van der Jagt**
Dr. Philip Köhn	**Prof. Dr.-Ing. Georg Wachtmeister**
Prof. Dr.-Ing. Ulrich Konigorski	**Prof. Dr.-Ing. Jochen Wiedemann**
Dr. Oliver Kröcher	**Prof. Dr. techn. Andreas Wimmer**
Dr. Christian Krüger	**Prof Dr. rer. nat. Hermann Winner**
Univ.-Ass. Dr. techn. Thomas Lauer	**Prof. Dr. med. habil. Hartmut Witte**
Prof. Dr. rer. nat. Uli Lemmer	**Dr. rer. nat. Bodo Wolf**
Dr. Malte Lewerenz	

Scientific articles in ATZ Automobiltechnische Zeitschrift and MTZ Motortechnische Zeitschrift are subject to a proofing method, the so-called peer review process. Articles accepted by the editors are reviewed by experts from research and industry before publication. For the reader, the peer review process further enhances the quality of ATZ and MTZ as leading scientific journals in the field of vehicle and engine technology on a national and international level. For authors, it provides a scientifically recognised publication platform.

Therefore, since the second quarter of 2008, ATZ and MTZ have the status of refereed publications. The German association "WKM Wissenschaftliche Gesellschaft für Kraftfahrzeug- und Motorentechnik" supports the magazines in the introduction and execution of the peer review process. The WKM has also applied to the German Research Foundation (DFG) for the magazines to be included in the "Impact Factor" (IF) list.

In the ATZ|MTZ Peer Review Process, once the editorial staff has received an article, it is reviewed by two experts from the Advisory Board. If these experts do not reach a unanimous agreement, a member of the Steering Committee acts as an arbitrator. Following the experts' recommended corrections and subsequent editing by the author, the article is accepted. *rei*

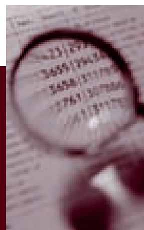

ATZ Peer Review
The Seal of Approval
for scientific articles
in ATZ.
Reviewed by experts from research and industry.

Received ....
Reviewed ....
Accepted ....

Seal of Approval – this seal is awarded to articles in ATZ and MTZ that have successfully completed the peer review process

Computer-aided Simulation of Instationary Wind Noise

In addition to classic stationary wind noise optimisation in the wind tunnel, the increasing demand for a high comfort standard will make it necessary for instationary wind noise to be included as well in the vehicle development process. Noise synthesis offers an efficient, novel approach to this end. The Research Institute of Automotive Engineering and Vehicle Engines Stuttgart (FKFS) has successfully developed and tested such a method.

1 Introduction

With passenger vehicles on low-noise tyre-road combinations the contribution of wind noise to the overall noise becomes dominant from approximately 130 km/h onward [1]. The complex air flow around the vehicle is responsible for the development of wind noise, with the acoustic effect of the changing pressures exerted on the vehicle surface playing an important role. Relevant aeroacoustic noise sources are for example leaks in the insulation system, add-ons such as wing mirrors, windshield wipers and the antenna, as well as special geometries such as the A-pillar, wheel houses and the underbody.

In aeroacoustic wind tunnels wind noise excitation can be measured and subjectively assessed under defined flow conditions. The noise generated under these flow conditions (so-called smooth flow conditions) leave a steady auditory impression on the passenger. On the road, however, the flow conditions change constantly in intensity and direction in dependence on time and place as a result of meteorologic and local conditions (such as vehicles driving ahead, road side obstacles) [2]. This turbulent flow produces wind noise varying constantly in noise level and frequency composition over time [3]. Human hearing has a high sensitivity towards time-related structures in noise [4]. These leave a disagreeable auditory impression on the passenger.

Hence, a detailed knowledge of the turbulent flow field and its impact on the instationary wind noise is essential. Acoustic effects of changing flow conditions, however, have so far been largely neglected in the vehicle development process. In order to provide a high level of noise comfort, it should be possible to examine the acoustic behaviour of a vehicle under these conditions as well.

In a first solution approach to examine the influence of turbulent flows, special vortex generators have already been used in different wind tunnels. **Figure 1** shows an example of such an installation in the nozzle of the model wind tunnel of the University of Stuttgart.

Such systems, however, are suitable for the simulation of instationary wind noise in the wind tunnel only to a certain extent, as the large turbulent length scales occurring under atmospheric conditions cannot be reproduced by this method [6].

The Research Institute of Automotive Engineering and Vehicle Engines Stutt-

Figure 1: Vortex generators in the model wind tunnel of the University of Stuttgart [5]

The Authors

Dipl.-Ing.
Susanne Krampol
is Research Assistant in the Acoustic Measurement and Analysis Technology Group in the Vehicle Acoustics and Vibrations Department of the FKFS in Stuttgart (Germany).

Dipl.-Ing.
Matthias Riegel
is Leader of the Acoustic Measurement and Analysis Technology Group in the Vehicle Acoustics and Vibrations Department of the FKFS in Stuttgart (Germany).

Prof. Dr.-Ing.
Jochen Wiedemann
is Member of the Executive Board of the FKFS and Full Professor for Automotive Engineering at the Institute of Internal Combustion Engines and Automotive Engineering at the University of Stuttgart (Germany).

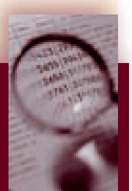

ATZ Peer Review
The Seal of Approval for scientific articles in ATZ.
Reviewed by experts from research and industry.

Received .... July 2, 2009
Reviewed .... July 13, 2009
Accepted .... July 18, 2009

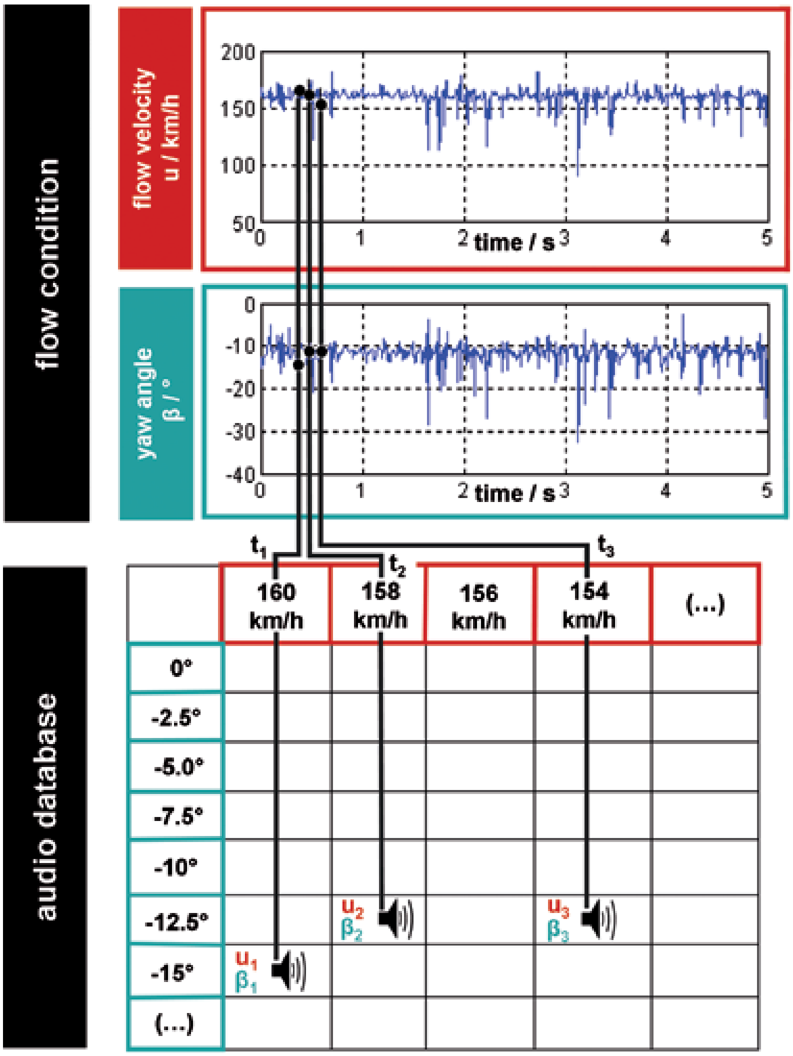

Figure 2: Diagram of noise synthesis

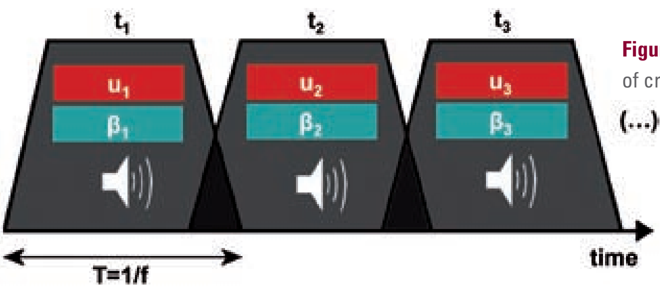

Figure 3: The procedure of crossfading

gart (FKFS) has, therefore, developed a method for the computer-aided simulation of instationary wind noise. The noise synthesis used here represents an efficient, innovative approach for the integration of instationary wind noise into noise assessment, without having to carry out extensive modifications to the wind tunnel hardware or time-intensive road measurements.

2 Basics of Noise Synthesis

The computer-aided synthesis of instationary noise is based on vehicle-specific wind noise measurements carried out in the wind tunnel under smooth flow conditions at varying flow velocities and yaw angles (angle between longitudinal vehicle axis and flow vector). Different noise sequences taken from the stationary measurements are then combined to form the corresponding instationary wind noise in each case. **Figure 2** illustrates this method schematically.

The input data required to carry out noise synthesis consists of a randomly selected flow situation, by which the noise sequences to be combined can be determined and the audio database, where the stationary wind noise measured in the wind tunnel is stored. The flow situation for which the instationary wind noise is to be synthesised must be available as a time signal and must contain the spatial flow components (u-, v- and w-component) so that yaw angle and flow velocity in the longitudinal direction (u-component) of the vehicle can be determined. Here the flow's time signal can be available as an actually measured signal or it can be computer-generated.

The basic principle of noise synthesis is reading the values of the flow velocity and yaw angle from the flow condition at a discrete point in time as well as loading the pertinent stationary noise file from the audio database. By sampling the time signal of the flow condition, as shown in Figure 2 the sequential order and length of the individual noise sequences from the noise database are determined. Within a second, ten stationary noise files – by using for example a sample rate of f = 10 Hz of the flow condition – are combined consecutively to form synthesised wind noise. Each noise sequence taken from the stationary measurement has a length of $T = 1/f$ s. The combination of stationary noise files is realised by crossfading, **Figure 3**. By using a crossfader one stationary noise file is faded out and the next one is faded in. In this way synthesised noise files of any length and for selected flow conditions can be generated and assessed for any vehicle measured in the wind tunnel.

3 Detailed Procedure

In order to keep the expenditure in time and work for the generation of synthesised noise to a minimum and to guarantee that the results provide significant values, it is necessary to assess methods of measurement and analysis technology. An automated run of instationary noise syn-

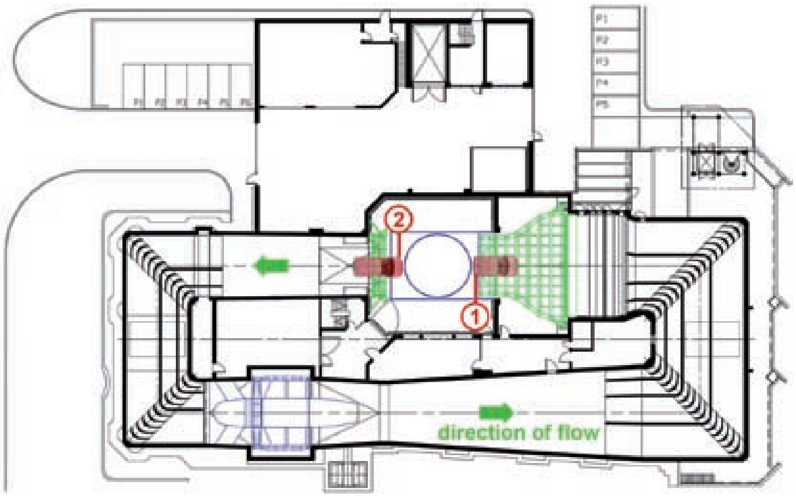

Figure 4: Plan view of the full-scale aeroacoustic wind tunnel of the University of Stuttgart including the measurement set-up for the validation of noise synthesis (1: turbulence generating vehicle in the nozzle; 2: test vehicle in the centreline of the collector)

thesis ensures a fast comparison of synthesised sound samples. Among others, the following points must be clarified:

- Which measuring position near the vehicle is most suitable for measuring the local flow conditions? At which measuring positions do vortices occur which have the highest influence on the instationary wind noise?
- Which factors must be considered when compiling the audio database? Which range of flow velocity and yaw angle occurs in the time signal, this means which ranges are important for recording the stationary measurements?
- What sampling frequency of the flow provides optimum results? How can the sampling frequency be selected optimally on the basis of the flow spectrum?
- How should the stationary noise files be combined? What fade-over time is best?

4 Validating the Procedure

In order to find answers to the above questions a method for validating noise synthesis must be found. Due to interference caused by other noise sources, road measurements are of only limited use. Validation examinations were thus carried out in the full-scale aeroacoustic wind tunnel of the University of Stuttgart.

Figure 4 illustrates the turbulent flow situation in the full-scale aeroacoustic wind tunnel for the case of a vehicle driving ahead. The measurement set-up consists of a turbulence generating vehicle in the nozzle exit with the vehicle to be measured positioned in the centreline of the collector downstream. Here, test vehicles of varying vehicle classes were used consecutively, **Figure 5**: a vehicle of the compact-size category (test vehicle 1), an

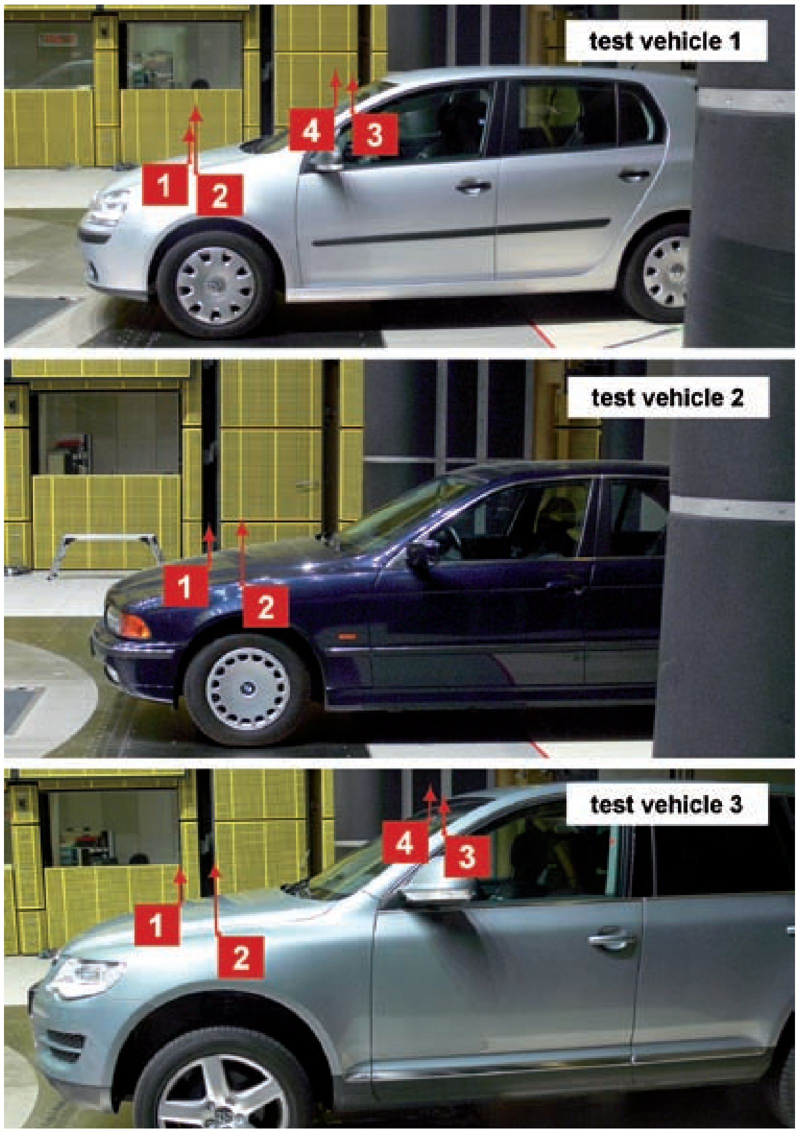

Figure 5: Positions for measuring the local flow with the four-hole probe on test vehicles of different vehicle classes (measuring position 1: hood; measuring position 2: fender; measuring position 3: A-pillar; measuring position 4: windshield)

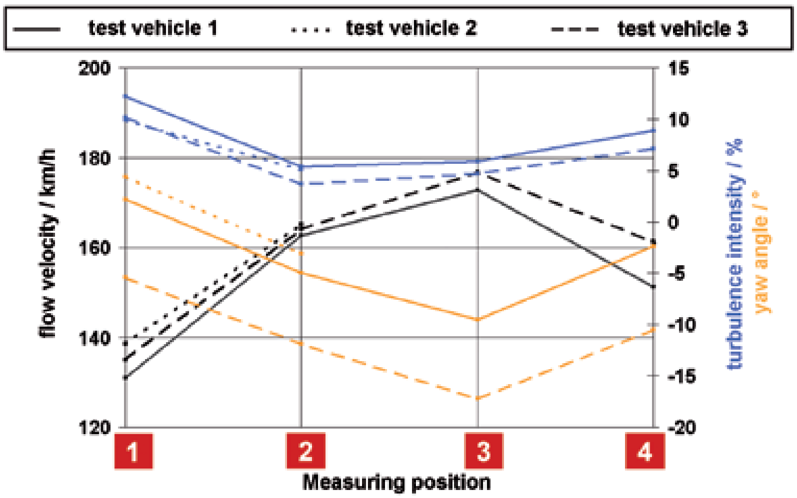

Figure 6: Averaged flow properties of measuring position 1 to 4 for the different test vehicles

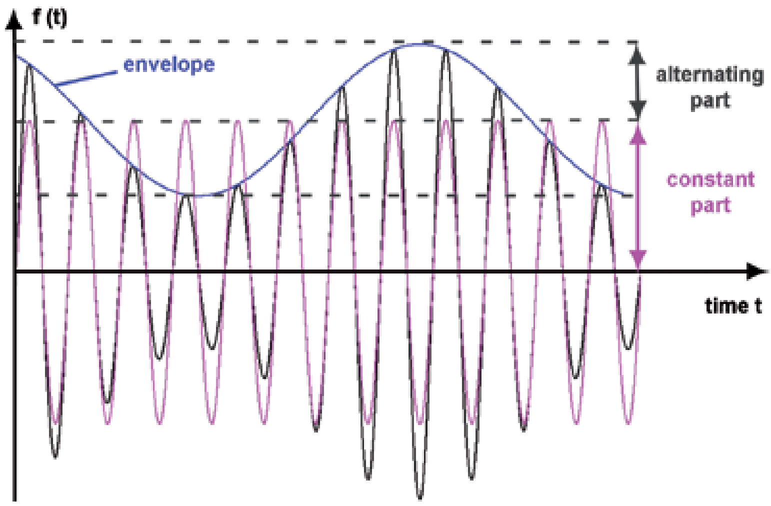

Figure 7: Plot of an amplitude-modulated sine signal

upper-middle class car (test vehicle 2) and a SUV (test vehicle 3). Acoustic time signals were recorded at a flow velocity of 160 km/h by means of an artificial head which was placed on the driver's seat of the vehicle for which readings were to be taken. The instationary wind noise generated under this turbulent flow condition was used as a reference signal. The reference signal and the generated synthesised noise files were compared during validation later.

Furthermore, it was necessary to determine the local flow approaching the vehicle, as it is one of the input quantities for noise synthesis. A Turbulent Flow Instrumentation four-hole probe was selected for measuring the local flow components at different measuring positions close to the vehicle. Closer details of the probe can be found for example in [7] and [8]. Selecting a suitable measuring position is of great importance. The flow situation in the area of the front vehicle has a particular effect on the generation of aerodynamic noise and can be influenced to a great extent by the shape in this area of the vehicle [9]. Hence, the flow measuring positions were primarily positioned there. Among others, they were in the centre of the hood, over the fender, above the A-pillar and above the windshield, Figure 5.

In addition to providing the instationary flow data, an audio database must be compiled. For this purpose, the wind noises of each test vehicle were measured and stored in an audio database using various flow speeds and yaw angles for smooth flow conditions in the wind tunnel.

The basic preconditions for noise synthesis are fulfilled with the time history of the flow and the audio database. Now, the measured data can be loaded with the noise synthesis-audio mixer developed on the basis of Matlab and the synthesised noise can be subsequently calculated. Noise synthesis is then carried out including the measuring positions and different sampling frequencies of the time history of the flow.

5 Findings

Stationary noise files with velocity increments of 2 km/h and yaw angles with increments of 2.5° proved to be optimal for compiling the audio database. In order to avoid unnecessary cost and in order to reduce the time needed, the noise files were recorded at the respective yaw angles (range from -20° to +20°) by means of speed ramps (from 60 to 200 km/h).

It is found that the flow measured with the four-hole probe strongly depends on the measuring position and on the shape of the test vehicle, **Figure 6**. As the composition of the stationary noise files is based on the flow condition, the measuring position thus significantly affects the synthesised noise.

Assessments of the synthesised noises were carried out in hearing comparisons. A group of 25 persons had to compare different synthesised noises with the corresponding reference noise. The results revealed the highest similarity of reference noise and synthesised noise for the measuring position 2 and sampling frequencies for the flow condition at 10 or 15 Hz.

For an objective examination and the visualisation of the instationary auditory impression, the modulation spectrum of the acoustic signal over time is an appropriate tool. In this context, it is important to know that human hearing reacts with particularly high sensitivity to amplitude modulations of f_m = 4 Hz. This may be due to the normal speaking rate which is four syllables per second [10].

The modulation analysis is primarily based on the calculation of the envelope of a bandpass filtered noise signal by using the Hilbert transform. Finally, a frequency spectrum of the envelope is calculated.

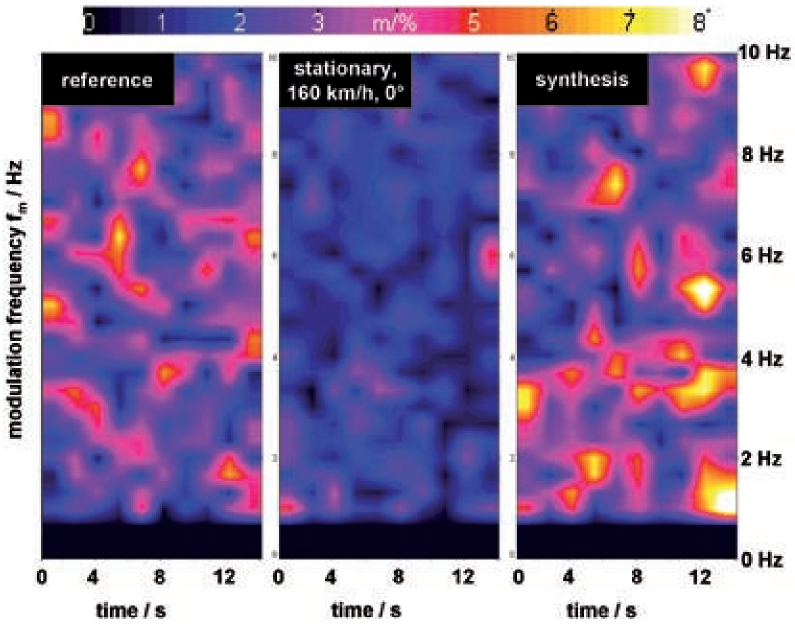

Figure 8: Modulation spectra in the 5.6-kHz octave band for the compact class car (test vehicle 1, driver's seat, left ear)

The strength of modulation is given by the degree of modulation m and is generally defined as the ratio of an alternating part to a constant part of an amplitude modulated signal. A schematic representation of an amplitude-modulated sine signal is presented in **Figure 7**.

Figure 8 shows the modulation spectra of the recorded noises measured under smooth and turbulent flow conditions as well as the modulation spectrum of the synthesised noise for the compact class car (test vehicle 1). The result of the synthesised noise is shown for a sampling frequency of 15 Hz and the flow condition measured above the fender. The degree of modulation *m* is colour-coded. The flow and the acoustic measurements were not recorded simultaneously, this means that the time history of the modulations differs for all three noise samples. Relevant, however, is that synthesised noise and reference noise have similar degrees of modulation at different modulation frequencies, see Figure 8. As expected, the stationary noise measured under a yaw angle of 0° (frontal approaching flow) has the lowest modulation degrees.

The similarity of the modulation spectra and the results from the hearing comparisons prove the basic applicability of noise synthesis for analysing instationary noise caused by turbulent flows.

6 Conclusion

In order to be able to meet the increasing demand for higher acoustic comfort in the future, it will be crucial to include – apart from classic wind noise optimisation – the optimisation of instationary wind noise in the vehicle development process. One approach to this end is the application of noise synthesis processes for simulating the acoustic behaviour of vehicles in turbulent flows. The method developed at the Research Institute of Automotive Engineering and Vehicle Engines Stuttgart (FKFS) for this purpose shows promising initial results. The noise synthesis-audio mixer developed on the basis of Matlab permits an optimised procedure in the generation of synthesised noise as well as a flexible implementation of parameters.

Using this method for acoustic development can avoid time-intensive road measurements and complex turbulence generation mechanisms in aeroacoustic wind tunnels. Before noise synthesis can be integrated into the vehicle development process on a regular basis, however, more extensive optimisation of the method is required, above all the determination and validation of other relevant flow situations. Additional effort should go into determining an index for describing a vehicle's proneness to interior noise with respect to turbulent flows. This would permit the fast and easy comparison of various vehicles in benchmark studies.

References

[1] Helfer, M.; Blumrich, R.; Riegel, M.: Aeroakustik in der Fahrzeugentwicklung. In: Bargende, M.; Reuss, H.-C.; Wiedemann, J. (Hrsg.): Kraftfahrwesen und Verbrennungs-motoren: 6. Internationales Stuttgarter Symposium. Renningen: Expert-Verlag, 2005
[2] Cogotti, A.: Unsteady Aerodynamics at Pininfarina. Road Turbulence Simulation and Time-Dependent Techniques. In: Bargende, M.; Wiedemann, J. (Hrsg.): Kraftfahrwesen und Verbrennungsmotoren: 5. Internationales Stuttgarter Symposium. Renningen: Expert-Verlag, 2003
[3] Riegel, M.; Helfer, M.; Wiedemann, J.: The Effect of Turbulence on In-cabin Wind Noise – a Comparison of Road and Wind Tunnel Results. In: 6th Mira International Vehicle Aerodynamics Conference, Warwick, October 25-26, 2006
[4] Miehling, H.; Lindener, N.; Cogotti, A.; Cogotti, F.; Maffei, M.: Aeroakustik in turbulenter Anströmung- und Windkanal und Straßenmessungen. In: Fortschritte der Akustik, DAGA, Tagungsband, 2007
[5] Schröck, D.; Widdecke, N.; Wiedemann, J.: The Effect of High Turbulence Intensities on Surface Pressure Fluctuations and Wake Structures of a Vehicle Model. SAE Paper 2009-01-0001, Detroit, USA, 2009
[6] Cooper, K.; Watkins, S.: The Unsteady Wind Environment of Road Vehicles. Part Two: Effects on Vehicle Development and Simulation of Turbulence. SAE Paper No. 2007-01-1237, Detroit, USA, 2007
[7] Mousley, P.D.; Watkins, S.: A Method of Flow Measurement About Full-Scale and Model-Scale Vehicles. SAE Paper No. 2000-01-0871, Detroit, USA, 2000
[8] Watkins, S.; Riegel, M.; Wiedemann, J.: The Effect of Turbulence on Wind Noise: A Road and Wind-Tunnel Study. In: Bargende, M.; Wiedemann, J. (Hrsg.): 4. Internationales Stuttgarter Symposium, Expert-Verlag, Stuttgart, 2001
[9] Burgade, L.: Mise au Point Aéroacoustique des Véhicules chez PSA. In: Interactions Mécaniques entre Fluides et Structures. Tagungsband, Colloques 6-2000, S. 16-21; ISSN 0018-6368, 2000
[10] Zwicker, E.; Fastl, H.: Psychoacoustics – Facts and Models. 2nd Edition, ISBN 3-540 65063-6, Springer, Berlin, 1999